

# RECLAMATION

*Managing Water in the West*

Technical Report No. SRH-2012-15

## Hydraulic Studies for Fish Habitat Analysis

San Joaquin River Restoration Project  
Mid-Pacific Region



U.S. Department of the Interior  
Bureau of Reclamation

December 2012

## **Mission Statements**

The U.S. Department of the Interior protects America's natural resources and heritage, honors our cultures and tribal communities, and supplies the energy to power our future.

The mission of the Bureau of Reclamation is to manage, develop, and protect water and related resources in an environmentally and economically sound manner in the interest of the American public.

**Technical Report No. SRH-2012-15**

# **Hydraulic Studies for Fish Habitat Analysis**

## **San Joaquin River Restoration Project Mid-Pacific Region**

Report Prepared by:

Daniel Dombroski, Ph.D., Hydraulic Engineer  
Sedimentation and River Hydraulics Group, Technical Service Center, Bureau of Reclamation

Blair P. Greimann, P.E., Ph.D., Hydraulic Engineer  
Sedimentation and River Hydraulics Group, Technical Service Center, Bureau of Reclamation

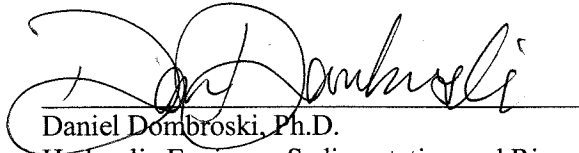
Elaina Gordon, P.E., M.S., Hydraulic Engineer  
Sedimentation and River Hydraulics Group, Technical Service Center, Bureau of Reclamation

Citation:

Reclamation (2012). *Hydraulic Studies for Fish Habitat Analysis*, Technical Report No. SRH-2012-15. Prepared for San Joaquin River Restoration Project, Mid-Pacific Region, US Bureau of Reclamation, Technical Service Center, Denver, CO.

Peer Review Certification: This document has been peer reviewed per guidelines established by the Technical Service Center and is believed to be in accordance with the service agreement and standards of the profession. Questions concerning this report should be addressed to Timothy Randle, Group Manager of the Sedimentation and River Hydraulics Group (86-68240) at 303-445-2557.

PREPARED BY:



Daniel Dombroski, Ph.D.

Hydraulic Engineer, Sedimentation and River Hydraulics Group (86-68240)

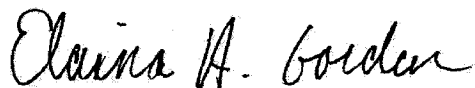
DATE: 12-21-12



Blair Greimann, Ph.D., R.E.

Hydraulic Engineer, Sedimentation and River Hydraulics Group (86-68240)

DATE: 12-21-12



Elaina Gordon, M.S., P.E.

Hydraulic Engineer, Sedimentation and River Hydraulics Group (86-68240)

DATE: 12/21/12

PEER REVIEWED BY:



Robert Hildale, M.S., P.E.

Hydraulic Engineer, Sedimentation and River Hydraulics Group (86-68240)

DATE: 12/21/12

## Contents

1	Introduction.....	1
2	Methodology.....	3
2.1	Geometry.....	3
2.2	Boundary Conditions.....	6
3	Calibration and Boundary Conditions .....	8
3.1	Reach 1B .....	8
3.1.1	Boundary Conditions .....	8
3.1.2	Calibration.....	10
3.2	Reach 2A .....	19
3.2.1	Boundary Conditions .....	19
3.2.2	Calibration.....	22
3.3	Reach 2b.....	26
3.3.1	Boundary Conditions .....	26
3.3.2	Calibration.....	26
3.3.3	Alternative Levee Alignment Models.....	28
3.4	Reach 3.....	32
3.4.1	Boundary Conditions .....	32
3.4.2	Calibration.....	32
3.5	Reach 4A .....	37
3.5.1	Boundary Conditions .....	37
3.5.2	Calibration.....	38
3.6	Reach 4B1 .....	41
3.6.1	Calibration.....	41
3.6.2	Alternative Levee Alignments .....	41
3.7	Reach 4B2 .....	49
3.7.1	Boundary Conditions .....	49
3.7.2	Calibration.....	49
3.8	Reach 5.....	53
4	Habitat Analysis.....	55
4.1	Hydraulic Suitability .....	55
4.2	Cover Suitability .....	57
4.2.1	Vegetation Mapping.....	57
4.2.2	Edge Habitat Classification.....	64
4.3	Habitat Modeling.....	68
5	Results.....	71
5.1	Available Suitable Habitat .....	71
5.2	Sensitivity Tests .....	81
5.2.1	Grid Sensitivity.....	81
5.2.2	Sensitivity to Method of Total HSI Calculation .....	83
6	References.....	84

## Index of Tables

Table 2-1. Characteristic length scale $L_{E4Q}$ of the average quadrilateral element for each computational mesh, organized according to river reach. The Reach 2A simulations were performed at two different model resolutions, as discussed in Section 5.2.1.....	4
Table 2-2. Hydraulic roughness values from the MEI (2008) study. Actual roughness values used in the simulations vary somewhat from reach to reach as a result of the calibration process. ....	6
Table 3-1. Downstream boundary conditions applied for all simulated flows in Reach 1B. Shown in the table are simulated flow rate (left) through the reach and water surface elevation (right) at the exit boundary. ....	9
Table 3-2. Measured discharge and simulated flow used in model calibration. All flows are in cubic feet per second (cfs). ....	10
Table 3-3. Land use designations and Manning's $n$ values modeled. ....	12
Table 3-4. Summary of boundary conditions applied for each Reach 2A SRH-2D simulation. Orthometric height $H$ is specified in the NAVD 88 datum.....	22
Table 3-5. Measured flows and calibration data for Reach 2A model. Also shown are the average difference and calculated standard deviation of the variation between measured and simulated water surface elevation after calibration. The columns labeled CBCS and CDS contain the boundary conditions applied at the CBS structures, respectively. Consistent with the CBS operational model, only differential flows above 1500 cfs are routed through the CBCS. ....	24
Table 3-6. Calibrated Manning's $n$ values for land use type in the Reach 2A SRH-2D model.....	25
Table 3-7. Combinations of roughness values used in model calibration. The 2008 model used 2005 highwater marks and 1997-99 topography. ....	27
Table 3-8. Manning's $n$ values applied in the alternative levee alignment IAFP2 and IAFP4 hydraulic models. ....	28
Table 3-9. Downstream Boundary Conditions used in the Reach 2B models to evaluate effects of alternative levee alignments. ....	28
Table 3-10. Summary of flows simulated in Reach 3 with corresponding water surface elevation boundary condition applied at Sack Dam. An additional outflow boundary condition of 57 cfs to Arroyo Canal was applied for all simulations. ..	32
Table 3-11. Summary of surveyed flows in Reach 3 used for model calibration. ....	33
Table 3-12. Calibrated Manning's $n$ values for land use type in the Reach 3 SRH-2D model.....	35
Table 3-13. Summary of flows simulated in Reach 4A with corresponding water surface elevation boundary condition applied in the vicinity of SSCS. Flows into Reach 4B1 were assumed negligible. ....	38
Table 3-14. Summary of surveyed flows in Reach 4A used for model calibration .....	39
Table 3-15. Calibrated Manning's $n$ values for land use type in the Reach 4A SRH-2D model.....	40
Table 3-16. Area enclosed by Levee Alignments A, B, C, and D. ....	42

Table 3-17. Hydraulic Roughness Values used in Reach 4B2. ....	49
Table 3-18. Comparison between Measured and Simulated Water Surface Elevations for the data collected on April 7, 2011 in Reach 4B2. ....	50
Table 3-19. Flows used in Reach 5 corresponding to Friant Release. ....	54
Table 4-1. Cover habitat categories considered in development of cover methodology. ....	58
Table 4-2. Cover HSI scores from literature and those assumed for this study. ....	58
Table 5-1. Maximum two-week Restoration flows in Settlement for various year types used in the analysis. ....	71
Table 5-2. Summary of habitat analysis results for “dry” water year type. The columns from left to right indicate the river reach, total inundated area ( <i>TIA</i> ), and available area of suitable habitat ( <i>ASH</i> ). Available <i>ASH</i> is given as fraction of <i>TIA</i> and as acres; the standard deviation of the available <i>ASH</i> calculation is also given. Habitat computations were not performed for Reaches 2B and 4B1 because future vegetative conditions are unknown. ....	78
Table 5-3. Summary of habitat analysis results for “normal” water year type. The columns from left to right indicate the river reach, total inundated area ( <i>TIA</i> ), and available area of suitable habitat ( <i>ASH</i> ). Available <i>ASH</i> is given as fraction of <i>TIA</i> and as acres; the standard deviation of the available <i>ASH</i> calculation is also given. Habitat computations were not performed for Reaches 2B and 4B1 because future vegetative conditions are unknown. ....	78
Table 5-4. Summary of habitat analysis results for “wet” water year type. The columns from left to right indicate the river reach, total inundated area ( <i>TIA</i> ), and available area of suitable habitat ( <i>ASH</i> ). Available <i>ASH</i> is given as fraction of <i>TIA</i> and as acres; the standard deviation of the available <i>ASH</i> calculation is also given. Habitat computations were not performed for Reaches 2B and 4B1 because future vegetative conditions are unknown. ....	79
Table 5-5. Summary of total inundated area ( <i>TIA</i> ) calculations for the levee .....	79
Table 5-6. Available <i>ASH</i> (acres) organized by reach and water year type. Also shown is the average <i>ASH</i> for each Reach, weighted by the estimated time percentage of each water type. ....	80
Table 5-7. Summary of results from sensitivity test of habitat analysis to change in resolution of the SRH-2D computational mesh. ....	82

## Index of Figures

Figure 1-1. Project Overview Map (From SJRRP 2011d).....	2
Figure 2-1. Example of the computational mesh in the vicinity of the Chowchilla Bifurcation Structure in Reach 2A. The color scale is mapped to the assigned elevation (NAVD88, ft) at each nodal point. Roughness .....	5
Figure 2-2. Example vegetation density classification in Reach 3. ....	6
Figure 3-1. Downstream boundary condition rating curves for Reach 1B. Water surface elevation at the boundary is plotted as a function of simulated discharge. ....	9
Figure 3-2. Measured and simulated water surface elevations for 570 cfs. The measured water surface elevation and simulated water surface elevation for three in-channel Manning’s <i>n</i> values are plotted as a function of distance from the Gravelly Ford station. ....	14
Figure 3-3. Measured and simulated water surface elevations for 1,100 cfs. The measured water surface elevation and simulated water surface elevation for three in-channel Manning’s <i>n</i> values are plotted as a function of distance from the Gravelly Ford station. ....	15
Figure 3-4. Measured and simulated water surface elevations for 2,500 cfs. The measured water surface elevation and simulated water surface elevation for three in-channel Manning’s <i>n</i> values are plotted as a function of distance from the Gravelly Ford station. ....	16
Figure 3-5. Measured and simulated water surface elevations for 4,000 cfs. The measured water surface elevation and simulated water surface elevation for three in-channel Manning’s <i>n</i> values are plotted as a function of distance from the Gravelly Ford station. ....	17
Figure 3-6. Measured and simulated water surface elevations for 7,100 to 7,500 cfs. The measured water surface elevation and simulated water surface elevation for three in-channel Manning’s <i>n</i> values are plotted as a function of distance from the Gravelly Ford station. Note that the low floodplain <i>n</i> values were only used at the 7,100 cfs flow.....	18
Figure 3-7. Aerial view of the Chowchilla Bifurcation Structure (CBS). ....	20
Figure 3-8. Rating curve for the CBS calculated from results of 1D HEC-RAS modeling. Water surface elevation (y-axis) is plotted as a function of discharge (x-axis). Two 1D models were developed: The first model included flow only through the CDS (Existing SJR), and the second model included flow only through the CBCS (Existing Bypass). The CBCS creates a greater backwater influence and therefore is assumed to determine the water surface elevation for total flows greater than 1500 cfs (SJR1500).....	21
Figure 3-9. Model calibration for 7400 cfs simulated flow. Water surface elevation is plotted from survey data (gray) and simulation results (black) as a function of distance upstream from the Chowchilla Bifurcation Structure (CBS). Also shown for reference is the location of Gravelly Ford. Nonphysical measurement anomalies are apparent at a few locations and are due to survey error.....	23



Figure 3-10. Model calibration 1000 cfs simulated flow. Water surface elevation is plotted from survey data (gray) and simulation results (black) as a function of distance upstream from the Chowchilla Bifurcation Structure (CBS). Also shown for reference is the location of Gravelly Ford.....	24
Figure 3-11. Measured and modeled results for 161cfs. No floodplain areas are accessed at this discharge and therefore these results illustrate the differences in the channel roughness values of 0.035, 0.03 and 0.025 applied.....	29
Figure 3-12. Measured and modeled results at 1,130 cfs showing variation in floodplain roughness combinations in Table 3-5 with all in-channel roughness values constant at 0.035. ....	30
Figure 3-13. Measured and modeled results showing variation in channel roughness combinations at 1,130 cfs. The floodplain roughness values for each run were held constant while the channel roughness values were varied at 0.035, 0.03, and 0.025.....	31
Figure 3-14. Water surface elevation plotted as a function of distance upstream from Sack Dam for 875 cfs simulated flow. Survey data (light gray) are plotted in comparison to simulation results before (gray) and after (black) calibration. ....	33
Figure 3-15. Water surface elevation plotted as a function of distance upstream from Sack Dam for 3500 cfs simulated flow. Survey data (light gray) are plotted in comparison to simulation results before (gray) and after (black) calibration...	34
Figure 3-16. Water surface elevation plotted as a function of distance upstream from Sack Dam for 1800 cfs simulated flow. Survey data (gray) are plotted in comparison to simulation results (black). ....	35
Figure 3-17. Rating curve developed from simulation calibration data for Reach 3. Water surface elevation (downstream boundary condition, NAVD88 ft) at Sack Dam is plotted as a function of flow through the reach. ....	36
Figure 3-18. Rating curve for Reach 4A model developed from HEC-RAS modeling. Water surface elevation (NAVD 88, ft) is plotted as a function of simulated flow (cfs). ....	37
Figure 3-19. Water surface elevation as a function of distance upstream from SSCS. Shown is survey data (gray) and the model calibration result (black) for a simulated flow of 730 cfs.....	39
Figure 3-20. Water surface elevation as a function of distance upstream from SSCS. Shown is survey data (gray) and the model calibration result (black) for a simulated flow of 3300 cfs.....	40
Figure 3-21. Levee options for Reach 4B1. ....	43
Figure 3-22. Design Features in Example Area 1 in Reach 4B1. Cross sections A and B are shown in.....	44
Figure 3-23. Design Features in Example Area 2 in Reach 4B1. Cross sections C and D are shown in Figure 3-25.....	46
Figure 3-24. Existing and modified cross sections A and B for Levee Option D.	47
Figure 3-25. Existing and modified cross sections C and D for Levee Option D.	48
Figure 3-26. Rating curve used for Reach 4B2 downstream boundary condition at XC 55382, which is just downstream of Eastside Bypass Control Structure. ....	51
Figure 3-27. Comparison between calibrated and measured water surface elevations for the flow occurring on April 7, 2011 in Reach 4B2.....	52

Figure 4-1. Habitat Suitability Index values as a function of depth and velocity from Stanislaus River (Aceituno, 1990). .....	56
Figure 4-2. Percentage within each vegetation category for Reach 1B from Moise and Hendrickson (2002). .....	59
Figure 4-3. Percentage within each vegetation category for Reach 2 from Moise and Hendrickson (2002). .....	60
Figure 4-4. Percentage within each vegetation category for Reach 3 from Moise and Hendrickson (2002). .....	61
Figure 4-5. Percentage within each vegetation category for Reach 4A from Moise and Hendrickson (2002). .....	62
Figure 4-6. Percentage within each vegetation category for Reach 4B from Moise and Hendrickson (2002). .....	63
Figure 4-7. Percentage within each vegetation category for Reach 5 from Moise and Hendrickson (2002). .....	64
Figure 4-8. Example high (left) and low (right) heterogeneity habitats. Green and brown areas represent cover. Blue areas represent open water. Juvenile salmonids generally station themselves on the edges of cover features, so a greater number of smaller cover features generally provides more suitable “edge” habitat than a limited number of larger cover features even though the larger cover features may provide more overall cover area. ....	65
Figure 4-9. Representative cover habitat areas used to determine cover habitat available in each reach. ....	67
Figure 4-10. Example of the vegetation types overlaid with the Edge Habitat in Reach 1B. ....	68
Figure 4-11. Graphical representation of an example HSI and suitable area calculation. ....	70
Figure 5-1. Combined HSI for portion of Reach 1B for normal year conditions.	73
Figure 5-2. Combined HSI for portion of Reach 2A for normal year conditions.	74
Figure 5-3. Combined HSI for portion of Reach 3 for normal year conditions....	75
Figure 5-4. Combined HSI for portion of Reach 4A for normal year conditions.	76
Figure 5-5. Combined HSI for portion of Reach 4B2 for normal year conditions. ....	77

# 1 Introduction

The San Joaquin River Restoration Project Office of Reclamation has requested the Technical Service Center to analyze the hydraulic conditions of the San Joaquin River in Reaches 1B through Reach 5 (Figure 1-1) using hydraulic models. This analysis is a component of the San Joaquin River Restoration Program (SJRRP). The SJRRP was established in late 2006 to implement the Stipulation of Settlement (Settlement) in *Natural Resources Defense Council, et al., v. Kirk Rodgers, et al.* This report contains preliminary analyses subject to further refinement and evaluation as the requirements for fish habitat are better understood.

The hydraulics in Reaches 1B through 4B2 were modeled using the Sedimentation and River Hydraulics- Two Dimensional (SRH-2D) software package (Lai, 2008), while Reach 5 was modeled using HEC-RAS (USACE, 2010). Results from the simulations were used to predict and compare potential Salmonid habitat area given prescribed river restoration flows. This report documents the model development, simulations, and habitat analysis calculations performed for Reaches 1B through Reach 5 of the San Joaquin River.

Sections 2 and 3 document the hydraulic modeling methodology and calibration. Section 4 describes how the hydraulic modeling results were used to inform estimates of available suitable habitat within the SJRRP.

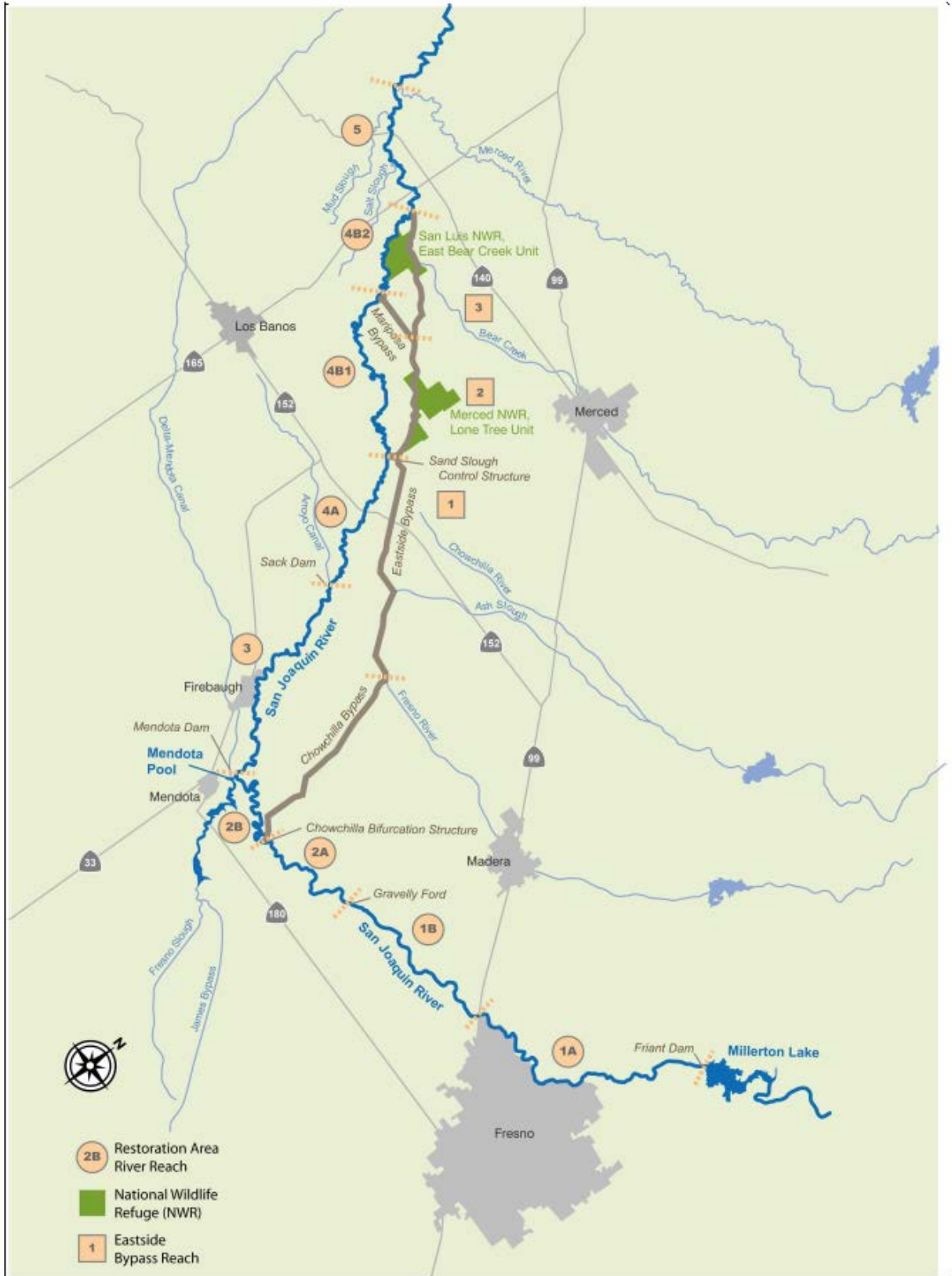


Figure 1-1. Project Overview Map (From SJRRP 2011d).

## 2 Methodology

Hydraulic conditions in Reaches 1B through 4B were simulated using the two-dimensional hydraulic model SRH-2D (Lai, 2008). Hydraulic conditions in Reach 5 were simulated using the one-dimensional model HEC-RAS (USACE, 2010).

There are three basic informational components needed to construct a hydraulic model: river geometry, hydraulic roughness, and boundary conditions. Each of these components are described in the following sections.

### 2.1 Geometry

Terrestrial geometry is comprised of the above water and below water ground elevations in the vicinity of the river, floodplain and levees. For this study, we used 2008 aerial LiDAR to define the topography over the study reach, acquired by the California Department of Water Resources (CDWR). Horizontal and vertical datums of the LiDAR data are NAD83 and NAVD88, respectively. The geographical coordinates are in the California State Plane system, Zone III, in units of US Survey Feet. Several separate boat surveys using SONAR were performed between 2009 and 2011 to obtain the below water geometry of the stream channel. The projection and datums of the bathymetric surveys match those of the 2008 airborne LiDAR.

The one-dimensional (1D) HEC-RAS model used for simulating Reach 5 hydraulics has been described by Mussetter Engineering Inc. (2008). Two-dimensional (2D) SRH-2D models were developed for simulating hydraulics in each of the other SJRRP reaches. The development of the 2D numerical model begins with construction of the computational mesh, and is dependent on a model surface built from geographically-referenced ground elevations. The topographic model surface was developed in a Geographic Information System by combining filtered LiDAR with a rasterized channel surface based upon SONAR data. The computational mesh was constructed using the Surface-water Modeling System (SMS), version 10.1 ([www.aquaveo.com/sms](http://www.aquaveo.com/sms)). Elevations from the model surface were imposed onto the computational mesh. The design extent and resolution of the mesh was based on the objective of capturing an appropriate level of topographic and hydraulic detail while considering the practical limits imposed by the computational time to run the simulations. Figure 2-1 shows a representative portion of a computational mesh and a color scale representing the surface elevation.

Quadrilateral elements in the mesh were generally used along the primary flow path within the channel and tetrahedral elements generally used outside the channel and in the floodplain. In practice, several computational meshes for each reach may be developed with varying spatial extent and resolution; the magnitude of the flows being considered and the desired level of resolution determine an appropriate mesh for a given simulation. The computational mesh is a hybrid

unstructured grid, which means that the resolution varies with element shape and size throughout the domain (Figure 2-1). It is useful to have a quantitative metric for the resolution of a computational mesh; therefore, a characteristic length scale  $L_{E4Q}$  of the average quadrilateral element is defined as:

$$L_{E4Q} = \left( \frac{1}{N_{E4Q}} \sum_i^{N_{E4Q}} A_i \right)^{\frac{1}{2}}, \quad (1)$$

where  $A_i$  is the area of quadrilateral element  $i$  and  $N_{E4Q}$  is the number of quadrilateral elements in the computational mesh. The metric  $L_{E4Q}$  is used to quantify the resolution of computational meshes discussed in this report. Distinct 2D hydraulic models were constructed for each of the Reaches 1B, 2A, 3, 4A, 4B1, and 4B2. This approach is beneficial because (a) the large overall simulation task is divided into smaller portions and (b) analysis on a reach-by-reach basis is more consistent with the settlement stipulations. Table 2-1 contains the values  $L_{E4Q}$  for each 2D model computational mesh. The Reach 2A simulations were performed at two different  $L_{E4Q}$  values in order to test the sensitivity of the results to mesh resolution (discussed in Section 5.2.1).

Table 2-1. Characteristic length scale  $L_{E4Q}$  of the average quadrilateral element for each computational mesh, organized according to river reach. The Reach 2A simulations were performed at two different model resolutions, as discussed in Section 5.2.1.

SJRRP River Reach	Mesh $L_{E4Q}$ (ft)
1B	31
2A	16, 8
2B	30
3	14.5
4A	16
4B1	30
4B2	19

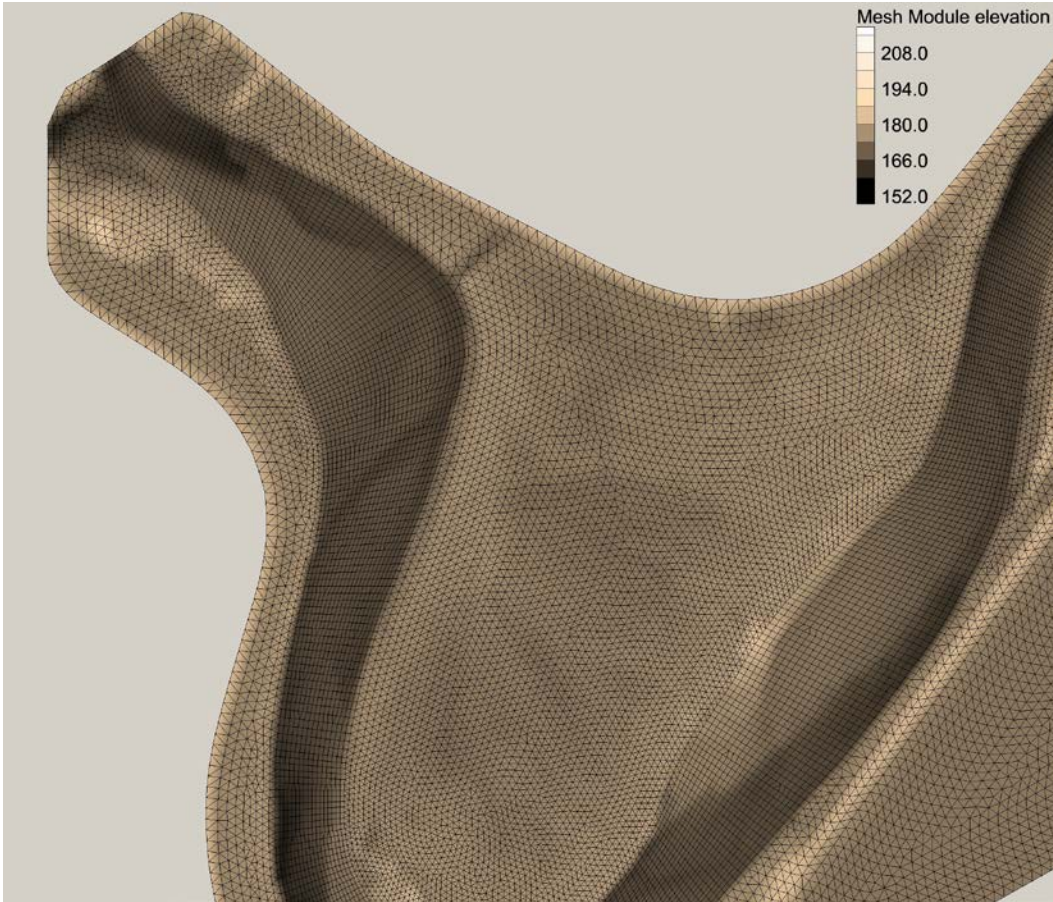


Figure 2-1. Example computational mesh in the vicinity of the Chowchilla Bifurcation Structure in Reach 2A. The color scale is mapped to the assigned elevation (NAVD88, ft) at each nodal point.

Hydraulic roughness represents the resistance to flow provided by the channel and floodplain boundary. The hydraulic roughness accounts for flow resistance provided by the bed material, bed forms, vegetation, and channel planform. It is often used as a calibration parameter to match modeled and observed hydraulic conditions. This study uses Manning's  $n$  to quantify hydraulic roughness.

The initial channel and floodplain hydraulic roughness (Manning's  $n$ ) values were taken from the MEI (2008) study that mapped hydraulic roughness to vegetation density in the floodplain. Table 2-1 presents vegetative surface classification and roughness values from the MEI (2008) study. Figure 2-2 shows a representative classification draped over aerial imagery of a small subsection of Reach 3. The initial hydraulic roughness values from the MEI (2008) study were systematically adjusted within each reach during the model calibration process to bring the model-predicted water surface elevation into closer agreement with the measured water surface elevation under a given set of hydro-geomorphic conditions. Because the river reach models were calibrated independently, the final roughness values used in the simulations varied somewhat from reach to reach.

Table 2-2. Hydraulic roughness values from the MEI (2008) study. Actual roughness values used in the simulations vary somewhat from reach to reach as a result of the calibration process.

Land Use Type	MEI (2008) Manning's <i>n</i>
Channel	0.035
Bare soil	0.045
Scattered Trees and Light Brush	0.060
Medium Density Trees and Brush	0.080
Dense Trees and Brush	0.100

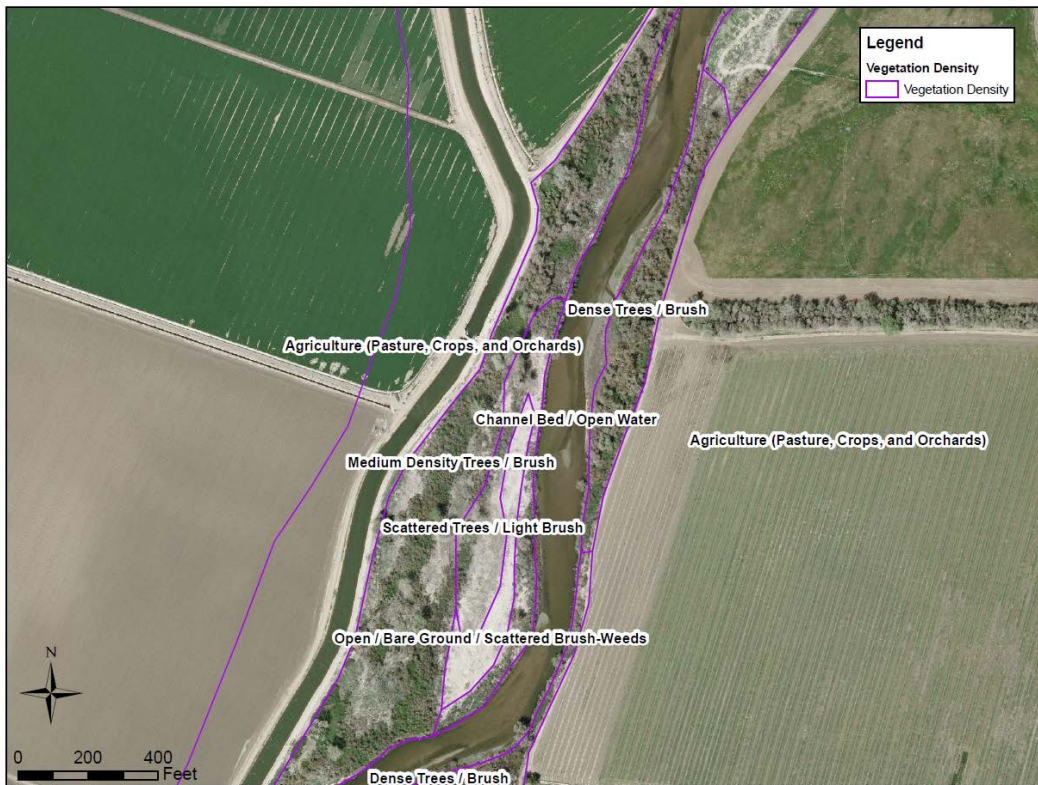


Figure 2-2. Example vegetation density classification in Reach 3.

## 2.2 Boundary Conditions

Boundary conditions for the hydraulic models are specified at the upstream and downstream extent of each model reach. Additional boundary conditions are defined for each input or output to a model reach (e.g., tributaries, inlets, outlets, diversions, etc).

The downstream boundary condition of each reach was specified with a water surface elevation for each simulated flow. These elevations were developed from measured water surfaces when possible, or from simulated conditions (HEC-RAS model) when sufficient measurements were not available.



The upstream boundary condition of each reach was specified as an input volumetric flow rate. The flow rates simulated were based upon the high spring release flows outlined in the Settlement, ranging from approximately 700 cubic feet per second (cfs) to 8000 cfs, depending upon the reach.

## **3 Calibration and Boundary Conditions**

The boundary conditions and calibration procedure used for each reach are described in the following sections. SRH-2D was used to simulate the hydraulics in the reaches with the exception of reach 5, where HEC-RAS was used to simulate inundation.

### **3.1 Reach 1B**

#### **3.1.1 Boundary Conditions**

The downstream boundary condition for Reach 1B was defined using a combination of simulation results from the Reach 2A SRH-2D hydraulic model and measured water surface elevations collected by DWR between April 2010 and October 2011 (Figure 3-1). The former was possible because the Reach 2A and Reach 1B computational meshes were constructed with sufficient spatial overlap. Measured water surface elevations were available for flows between 570 cfs and 7,500 cfs. For Reach 1B simulated flows between 570 and 7500 cfs, linear interpolation along the DWR measured rating curve was applied to define the downstream boundary. For Reach 1B simulated flows below 570 cfs, the Reach 2A simulated rating curve was applied to define the downstream boundary. The downstream boundary condition used for each simulated flow rate is shown in Table 3-1.

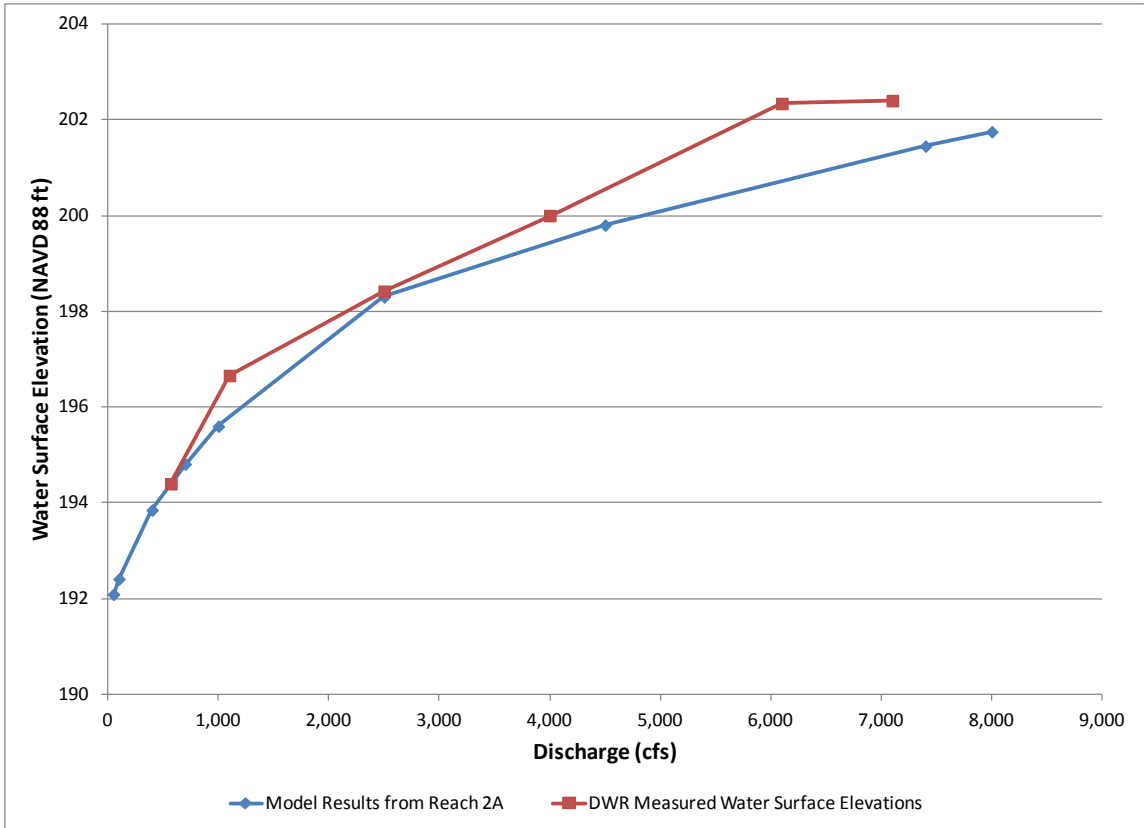


Figure 3-1. Downstream boundary condition rating curves for Reach 1B. Water surface elevation at the boundary is plotted as a function of simulated discharge.

Table 3-1. Downstream boundary conditions applied for all simulated flows in Reach 1B. Shown in the table are simulated flow rate (left) through the reach and water surface elevation (right) at the exit boundary.

Reach 1B Flow (cfs)	H (NAVD 88, ft)
100	192.41
200	192.89
350	193.61
500	194.17
570	194.40
700	194.95
1100	196.66
1500	197.16
2000	197.79
2500	198.42
4000	200.00
7500	202.40

### 3.1.2 Calibration

Water surface profiles and discharge measurements were collected by DWR in Reach 1B between April 2010 and October 2011 for flows ranging between 570 cfs and 7500 cfs (SJRRP 2010, 2011b). Measured discharges were compared with upstream and downstream gage measurements to determine the most suitable flow to simulate for calibration purposes. The measured discharge, gage data, and calibration flows are shown in Table 3-2.

Table 3-2. Measured discharge and simulated flow used in model calibration. All flows are in cubic feet per second (cfs).

	Dates of Discharge Data Collection				
	4/22/2010	3/31/2011	5/5/2011	6/9/2011	10/18/2011
<b>Measured by ADCP</b>					
DWR transect D18 (RM 237.5)	1130	7090	3950	2430	571
DWR transect D19 (RM 232.5)	1050	7120	4110	2640	562
<b>Measured by gages</b>					
GRF (Gravelly Ford)	1160	7300-7450	3780	2375	575
DNB (Donny Bridge)	1085	NA	NA	2350	695
SJF (below Friant)	1255	7530-8500	4450	2775	685
<b>Simulated for calibration</b>	1100	7100-7500	4000	2500	570

Reach 1B extends from HW 99 (MP 243) to Gravelly Ford (MP 229). However, the downstream extent of the Reach 1B model is approximately 2.5 miles upstream from Gravelly Ford. The lower 2.5 mile-portion of Reach 1B was incorporated into the Reach 2A model. Calibration results are illustrated for Reach 1B approximately 2.5 miles upstream of Gravelly Ford to HW 99. However, only results downstream from Skaggs Bridge will be used for evaluation of rearing habitat because potential spawning habitat is found in Reach 1B from HW 99 to Skaggs Bridge (Paul Bergman, Cramer Fish Sciences, Personal Communication, 4/12/2012). Therefore, the focus of this calibration was to match the modeled results with the measured water surface profile as closely as possible downstream from Skaggs Bridge.

#### 3.1.2.1 In-channel Roughness Calibration

Flows below 1,100 cfs generally remain within the channel. Therefore, the 570 cfs and 1,100 cfs measured water surface profiles were used to determine the in-channel Manning's *n* roughness values that result in the best match between the measured water surface elevations and the model results. In-channel *n* values of 0.030, 0.035, and 0.040 were evaluated. A sensitivity analysis of floodplain

Manning's  $n$  at these flows resulted in insignificant differences in the water surface profiles.

For flows that remained within the channel, a Manning's  $n$  value of 0.035 was selected to best represent the in-channel portion of the model (Figure 3-2 and Figure 3-3). However, at 570 cfs, the modeled water surface profile was consistently about 0.5-1 ft above the measured water surface profile. For the 1,100 cfs simulated flow, a Manning's  $n$  value of 0.035 resulted in good correspondence between the measured and simulated profile below Skaggs Bridge; this value was also consistent with values used to represent in-channel roughness within Reach 1 in other studies.

For the 570 cfs flow, several factors may be responsible for the lack of agreement in the measured versus modeled results using a Manning's  $n$  value between 0.030 and 0.040. These include: (1) a general limited definition of the channel from the survey data, (2) possible changes in localized channel controls and in-channel vegetation between the bed elevation survey (2009) and the water surface profile survey (2011), and (3) possible divergence in the actual and measured flow in the reach. The channel geometry collected in the reach may not provide sufficient channel definition in some areas, particularly compared with the detailed LiDAR surveys of the floodplain. The channel was rasterized using a spline with barriers technique within ArcGIS, which may not adequately represent the bed surface for in-channel flows. In addition, flood releases from Friant Dam were experienced in 2011, with flows of over 7,000 cfs released in three distinct peaks between January and July. Flow releases remained above 2,000 cfs for 3 consecutive months in 2011, after which the water surface profile survey at 570 cfs occurred. These substantial flows may have resulted in changes to the in-channel vegetation, gravel pit entrance and exit configurations, and other local controls, such as sediment deposits, which caused discrepancies between the measured and simulated values. Although the differences in the measured and simulated profiles are noteworthy at 570 cfs, floodplain rearing habitat within the reach generally does not get accessed at flows below 1,000 cfs.

### **3.1.2.2 Floodplain Roughness Calibration**

Land use designations used to represent the floodplain in Reach 1B were primarily derived from previous polygon mapping performed by TetraTech (formerly MEI) based upon aerial photography from 2007. TetraTech mapping did not cover the entire reach modeled for this effort. Therefore, near the upstream boundary of the model (near HW 99), additional hydraulic roughness areas were delineated based on the 2007 aerial photography due to TetraTech mapping limits. Modeled floodplain roughness values for each land use designation are shown in Table 3-3. The "low" floodplain  $n$  values shown in Table 3-3 correspond with the initial TetraTech values in Table 2-2. Following evaluation of initial model results for flows accessing significant portions of the floodplain, it was apparent that the low floodplain  $n$  values were too low in the overbank areas. Subsequently, overbank Manning's  $n$  values were increased 25%

and 50% for flows accessing the floodplain to improve the correlation between the model results and measured water surface elevations.

Table 3-3. Land use designations and Manning's *n* values modeled.

<b>Land Use Type</b>	<b>Low Floodplain <i>n</i></b>	<b>Mid Floodplain <i>n</i></b>	<b>High Floodplain <i>n</i></b>
Channel Bed / Open Water*	0.035	0.035	0.035
Agriculture	0.045	0.056	0.068
Open / Bare Ground / Scattered Brush-Weeds	0.045	0.056	0.068
Scattered Trees / Light Brush	0.060	0.075	0.090
Medium Density Trees / Brush	0.080	0.100	0.120
Dense Trees / Brush	0.100	0.125	0.150
Urban / Industrial	0.080	0.100	0.120

\*Manning's *n* values to represent the channel were unchanged for calibration flows above 1,100 cfs.

Hydraulic simulation results were compared with measured water surface profiles for flows exceeding bankfull conditions at 2500 cfs, 4000 cfs, and 7500 cfs (Figure 3-4 to Figure 3-6).

At flows exceeding 1,100 cfs, the floodplain begins to inundate and the Manning's *n* values selected to best represent water surface elevations on the floodplain were the "mid" floodplain *n* values shown in Table 3-3. Calibration data indicate variation in model results at 2,500 cfs, 4,000 cfs, and 7,500cfs for the different combinations of floodplain roughness values. At 2,500 cfs, the set of Manning's *n* values corresponding to the best-fit profile changed throughout the reach. However, the mid floodplain *n* values clearly resulted in the best match with the measured water surface profile for 4,000 cfs and 7,500 cfs. The initial run of 7,100 cfs with the low floodplain Manning's *n* resulted in simulation results that were 1 to 2 feet lower than the measured profile. The flow was therefore increased to 7,500 cfs to more closely match the gage measurements.

Reach 1B contains numerous gravel pits, some of which are connected at all flows and others that are only connected during overbank flows. The gravel pits, combined with activities aimed at improving channel and floodplain conditions, make calibration of the reach challenging using topographic and water surface data sets collected across multiple years and flow conditions. To improve model calibration results, updated mapping of land use polygons and more detailed analyses of topography within the channel could be performed in the future.

Based on the results of the calibration analysis, all flows in Reach 1B were simulated using the mid floodplain  $n$  values and a channel  $n$  value of 0.035.

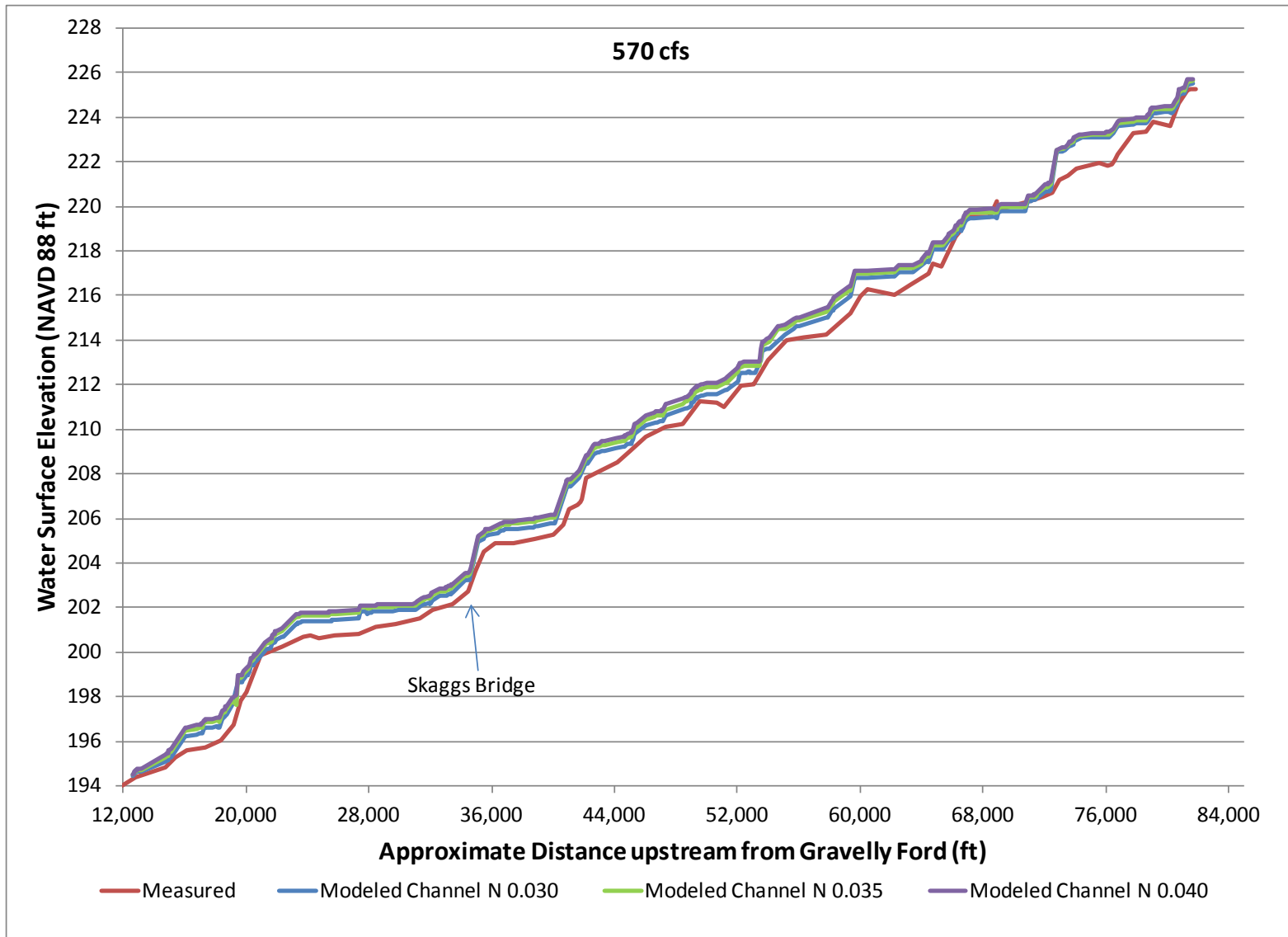


Figure 3-2. Measured and simulated water surface elevations for 570 cfs. The measured water surface elevation and simulated water surface elevation for three in-channel Manning's  $n$  values are plotted as a function of distance from the Gravelly Ford station.



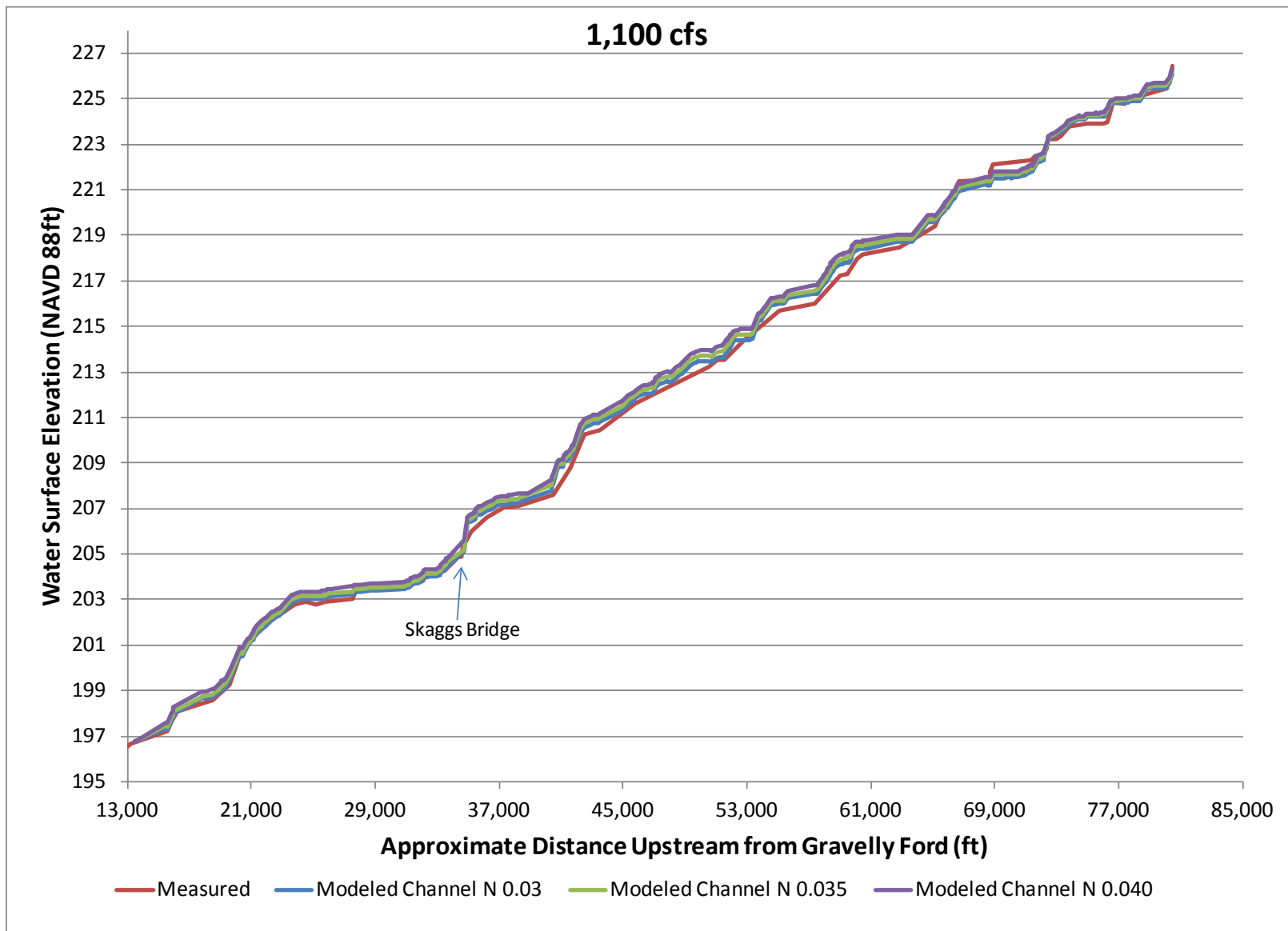


Figure 3-3. Measured and simulated water surface elevations for 1,100 cfs. The measured water surface elevation and simulated water surface elevation for three in-channel Manning's  $n$  values are plotted as a function of distance from the Gravelly Ford station.

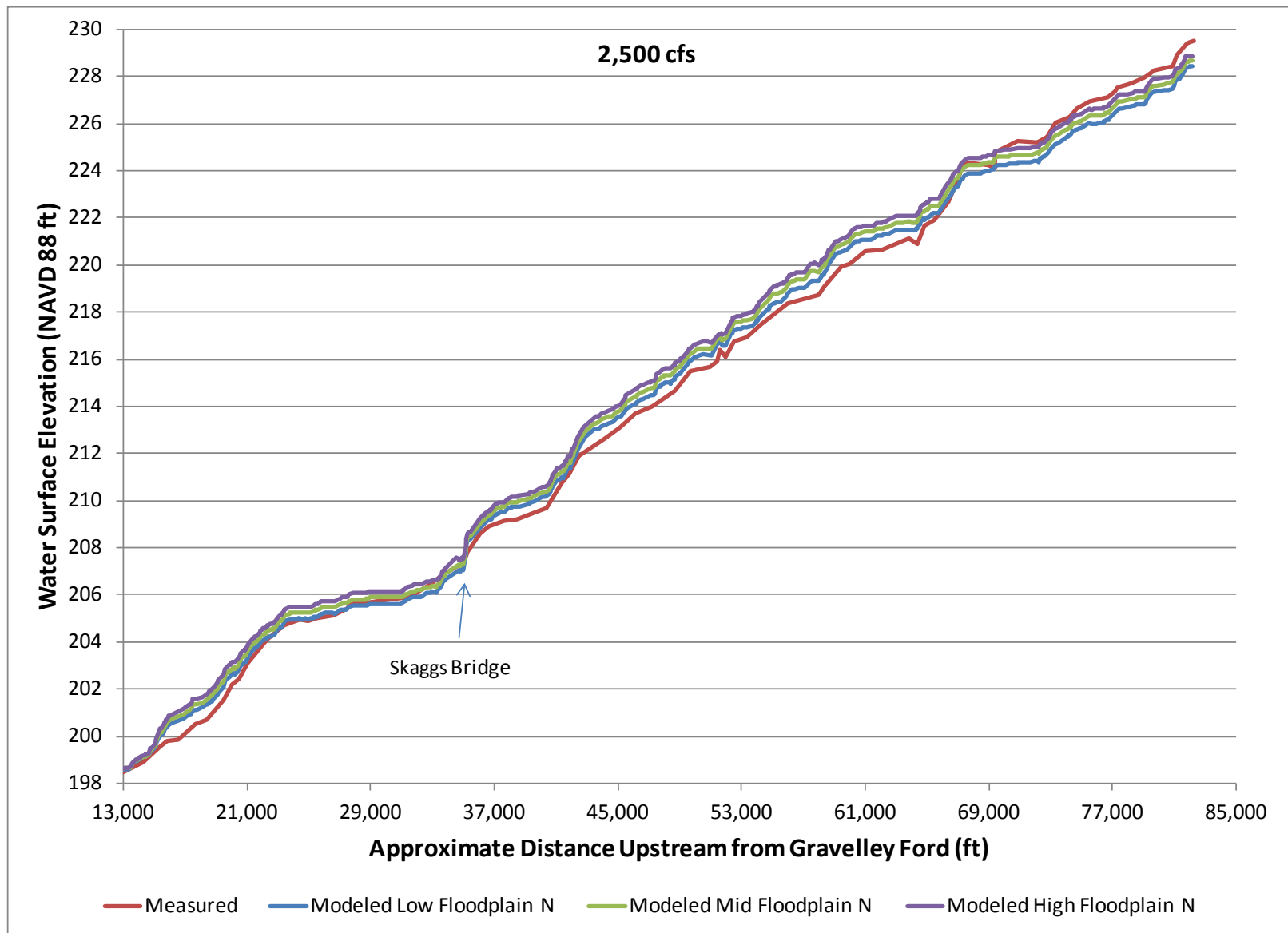


Figure 3-4. Measured and simulated water surface elevations for 2,500 cfs. The measured water surface elevation and simulated water surface elevation for three in-channel Manning's  $n$  values are plotted as a function of distance from the Gravelley Ford station.

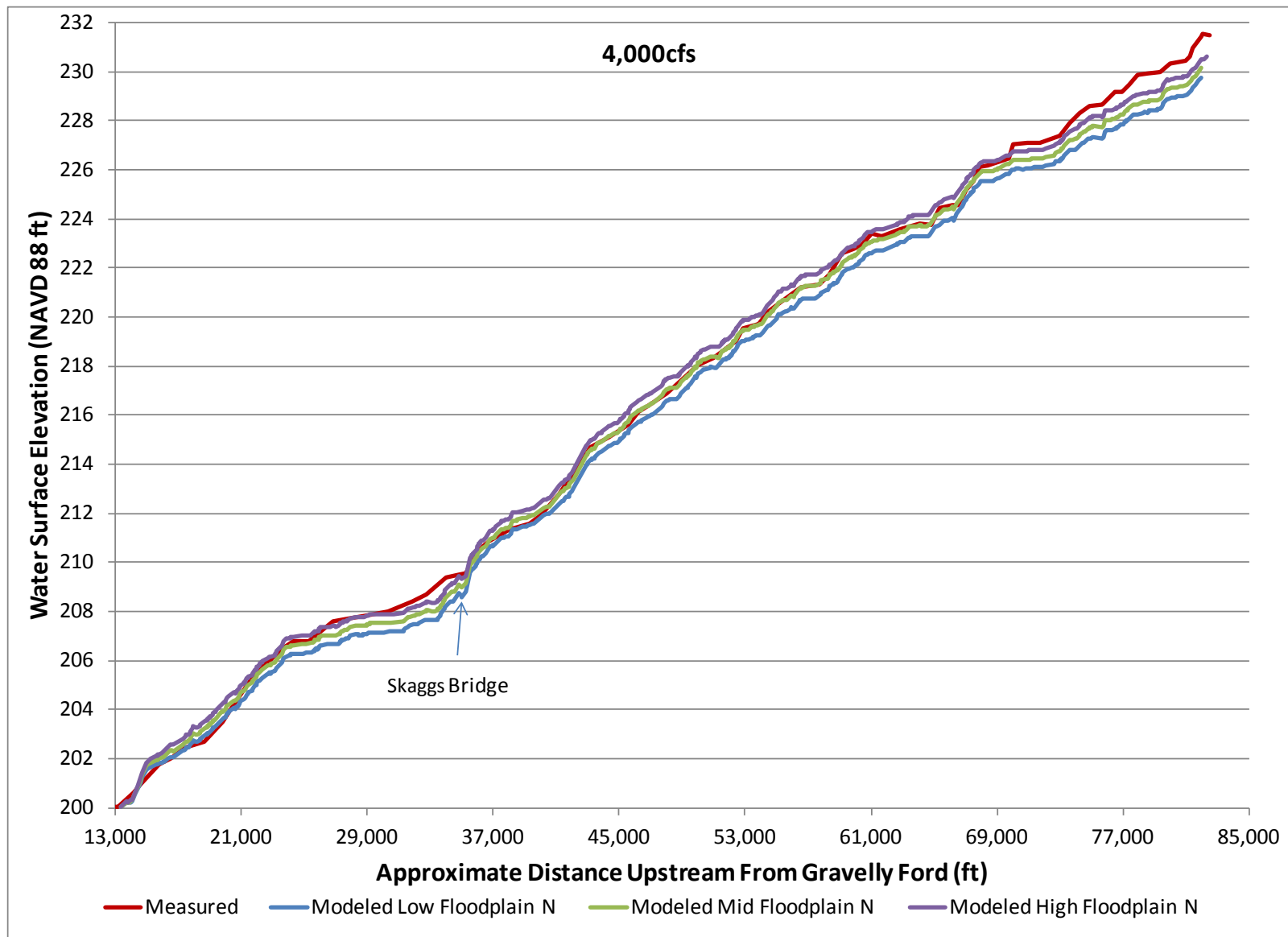


Figure 3-5. Measured and simulated water surface elevations for 4,000 cfs. The measured water surface elevation and simulated water surface elevation for three in-channel Manning's  $n$  values are plotted as a function of distance from the Gravelly Ford station.

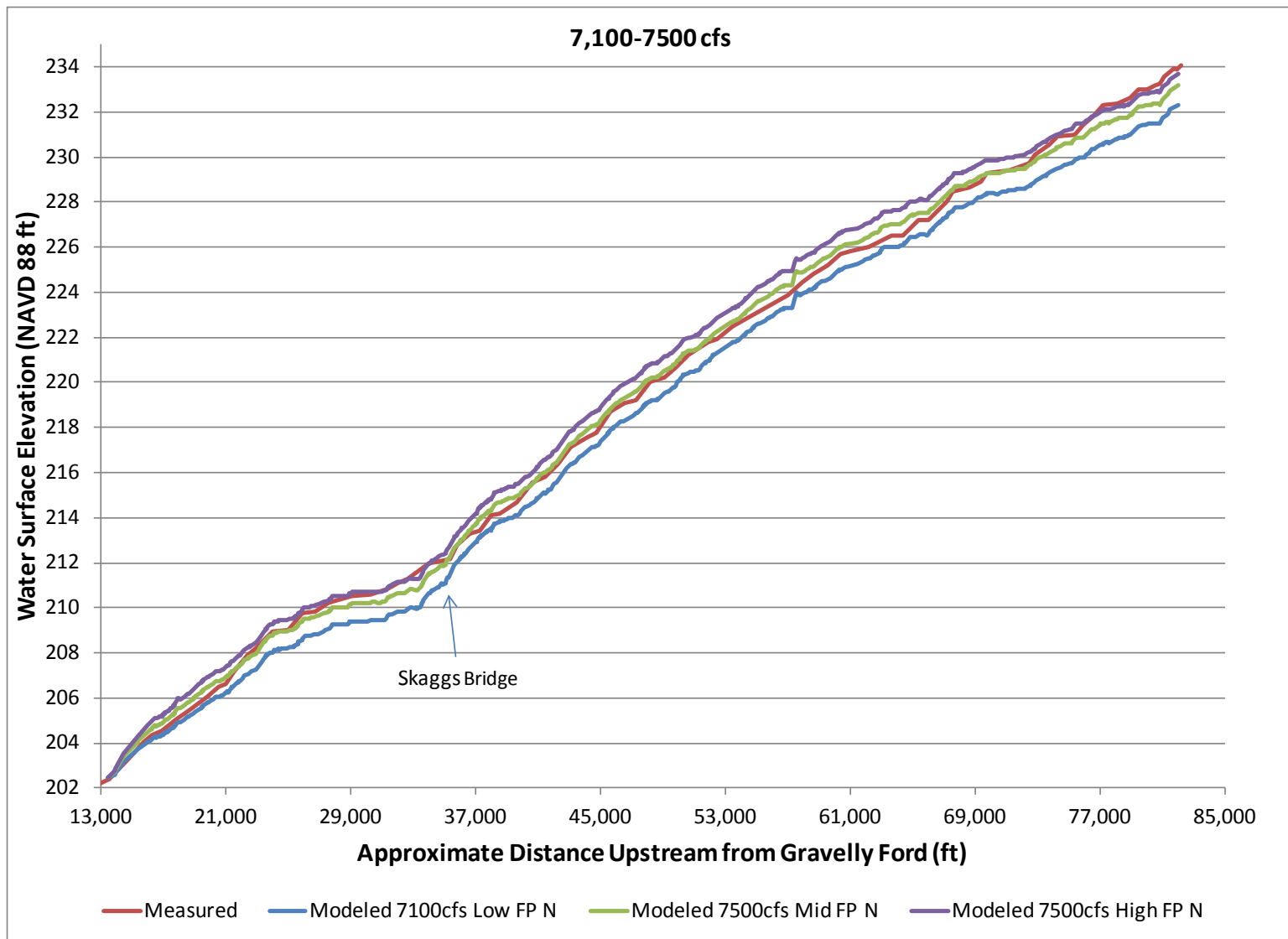


Figure 3-6. Measured and simulated water surface elevations for 7,100 to 7,500 cfs. The measured water surface elevation and simulated water surface elevation for three in-channel Manning's  $n$  values are plotted as a function of distance from the Gravelly Ford station. Note that the low floodplain  $n$  values were only used at the 7,100 cfs flow.

## 3.2 Reach 2A

### 3.2.1 Boundary Conditions

Reach 2A extends from Gravelly Ford (MP 229) to the Chowchilla Bifurcation Structure (MP 216). The input (upstream) boundary condition for the Reach 2A SRH-2D model, specified as a volumetric flow rate, is located approximately 3 miles upstream of Gravelly Ford (overlapping with Reach 1B). The exit (downstream) boundary condition is conditional on the operation of the Chowchilla Bifurcation Structure (CBS). The CBS consists of two distinct hydraulic control structures: the Chowchilla Bypass Control Structure (CBCS) controls flow from the San Joaquin River into the Chowchilla Bypass, and the Chowchilla Diversion Structure (CDS) diverts flow from the San Joaquin River channel (Figure 3-7). Simulating the hydraulics within Reach 2A depends on an operational model for the CBS and specification of boundary conditions at the CDS and CBCS. Under flood conditions, the design operation of the CBS is such that flows up to 1500 cfs are routed through the CDS down the San Joaquin River; the differential flow above 1500 cfs is routed through the CBCS down the Chowchilla Bypass. This operational model was used to assign the exit boundary conditions for the 2D hydraulic simulations described in this report. Simulations with a flow rate greater than 1500 cfs were assigned two downstream boundary conditions: The CDS was assigned an outflow of 1500 cfs, and the CBCS was assigned a discharge water surface elevation based on the rating curve for the structure. The rating curve (Figure 3-8) was developed from one-dimensional HEC-RAS modeling of Reach 2A through each of the CDS and the CBCS, respectively. For simulations with a flow rate less than 1500 cfs, it is assumed that the flow is routed entirely through the CDS and the discharge water surface condition is based on the CDS rating curve.

The Reach 2A simulated flows ranged from 400 cfs to 7400 cfs. The boundary conditions used for each simulated flow are given in Table 3-6.



Figure 3-7. Aerial view of the Chowchilla Bifurcation Structure (CBS).

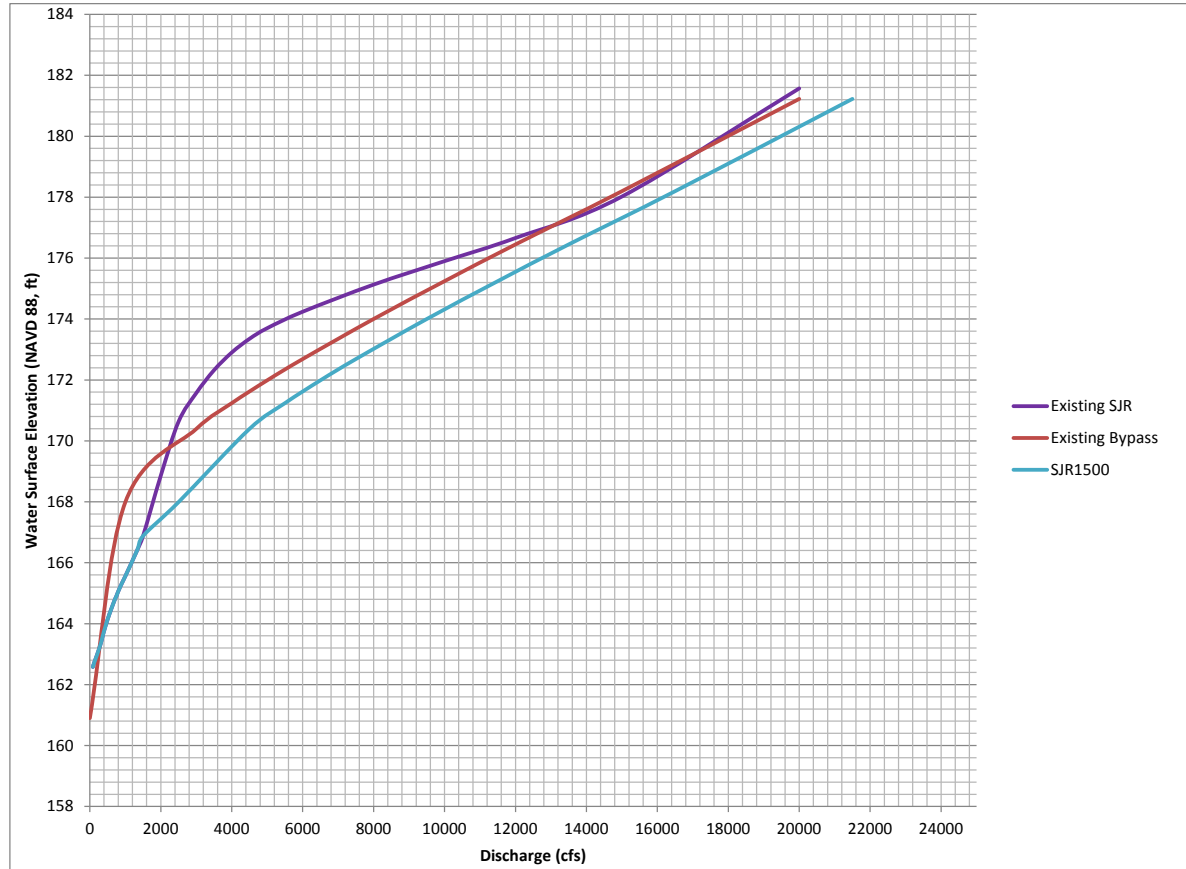


Figure 3-8. Rating curve for the CBS calculated from results of 1D HEC-RAS modeling. Water surface elevation (y-axis) is plotted as a function of discharge (x-axis). Two 1D models were developed: The first model included flow only through the CDS (Existing SJR), and the second model included flow only through the CBCS (Existing Bypass). The CBCS creates a greater backwater influence and therefore is assumed to determine the water surface elevation for total flows greater than 1500 cfs (SJR1500).

Table 3-4. Summary of boundary conditions applied for each Reach 2A SRH-2D simulation. Orthometric height H is specified in the NAVD 88 datum.

Reach 2a Flow (cfs)	CBS Boundary Conditions	
	CDS	CBCS
400	H = 163.5 ft	N/A
700	H = 164.0 ft	N/A
1000	H = 164.5 ft	N/A
1375	H = 165.4 ft	N/A
2355	Q = 1500 cfs	H = 167.3 ft
2500	Q = 1500 cfs	H = 167.5 ft
4500	Q = 1500 cfs	H = 169.5 ft
7400	Q = 1500 cfs	H = 170.0 ft

### 3.2.2 Calibration

Model calibration was performed by comparing simulated water surface elevation to measured water surface elevation at comparable discharges. The water surface elevation from the simulation results is taken at the approximate thalweg of the channel. The exit water surface elevation boundary condition and the Manning's *n* roughness were used as calibration parameters for the model.

The survey data used as a basis of comparison for model calibration was acquired during a 2005 field survey by Reclamation. Data was collected in May and June at approximate discharges of 7,400 and 1,000 cfs, respectively. Field notes indicate some unsteadiness in discharge during data acquisition; the approximate average flow was used for the calibration.

Figure 3-9 and Figure 3-10 show the water surface elevation comparison between survey data and simulation results for discharges of 7400 cfs and 1000 cfs, respectively. The exit boundary condition height and the Manning's *n* values in the models were adjusted in order to calibrate to the survey data. Calibrated roughness can show flow dependence; in this case, however, there was not enough calibration data to resolve this trend. Therefore, the roughness values calibrated at 7400 cfs were used for all the simulations, and the exit boundary condition height was adjusted commensurate with the flow. The water surface elevation measurements for the 7400 cfs flow contained some nonphysical irregularities near Gravelly Ford and upstream of CBS. These measurements were disregarded in the calibration process, although they do affect the calculated average difference and standard deviation between calibration and measurements. Table 3-5 contains the calibration data and boundary conditions applied for the calibration flows at 1000 cfs and 7400 cfs. Table 3-6 shows the calibrated Manning's *n* roughness values for the ground types simulated in the model.



Specification of the exit water surface elevation as a downstream boundary condition is somewhat complicated by the local hydraulics in the vicinity of the CBS. The acceleration of the simulated flow through the CBS and CBCS structures causes a localized water surface elevation drop below the backwater elevation in the pool. However, the rating curve for the CBCS and CDS are based on water surface elevation in the backwater. This creates an inconsistency between the specification of the exit water surface elevation boundary condition and the predicted water surface elevation in the rating curve. For the higher flows simulated, this elevation drop is approximately 1 ft, and is accounted for in the calibration process by reducing the exit boundary condition below what would be predicted by the rating curve. Variation in the downstream exit boundary condition of approximately 1 ft causes a backwater change in the water surface elevation over a distance of about 1 mile.

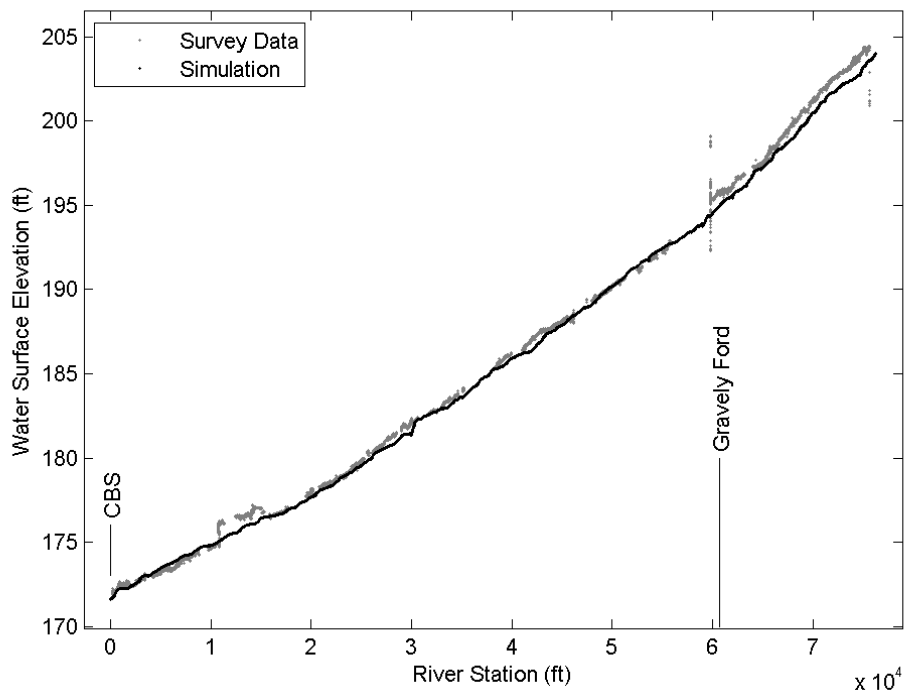


Figure 3-9. Model calibration for 7400 cfs simulated flow. Water surface elevation is plotted from survey data (gray) and simulation results (black) as a function of distance upstream from the Chowchilla Bifurcation Structure (CBS). Also shown for reference is the location of Gravelly Ford. Nonphysical measurement anomalies are apparent at a few locations and are due to survey error.

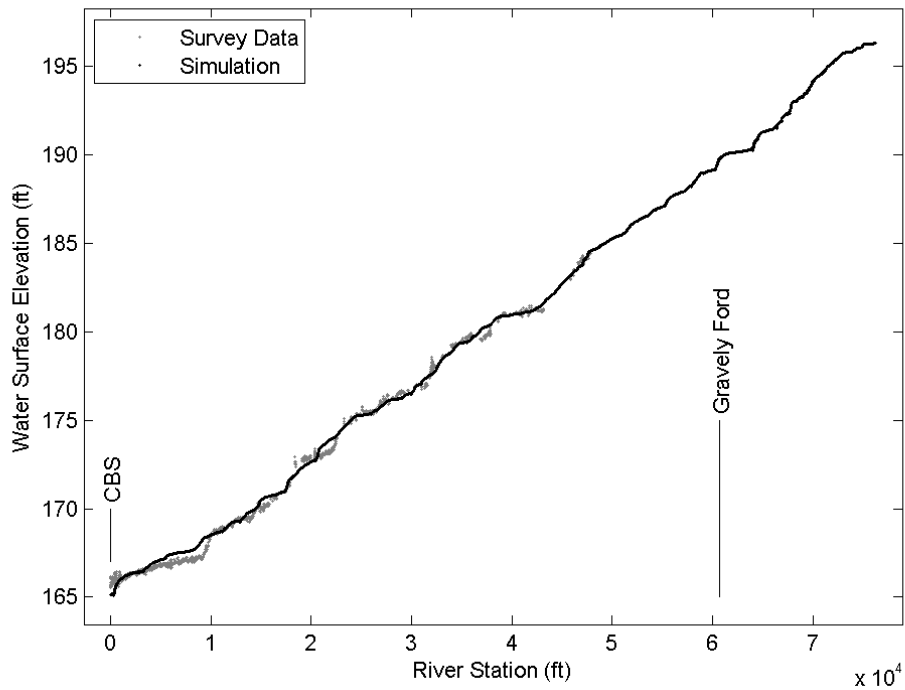


Figure 3-10. Model calibration 1000 cfs simulated flow. Water surface elevation is plotted from survey data (gray) and simulation results (black) as a function of distance upstream from the Chowchilla Bifurcation Structure (CBS). Also shown for reference is the location of Gravelly Ford.

Table 3-5. Measured flows and calibration data for Reach 2A model. Also shown are the average difference and calculated standard deviation of the variation between measured and simulated water surface elevation after calibration. The columns labeled CBCS and CDS contain the boundary conditions applied at the CBS structures, respectively. Consistent with the CBS operational model, only differential flows above 1500 cfs are routed through the CBCS.

Survey Date	Discharge (cfs)	CBS Boundary Conditions		Avg Diff Mag (ft)	Std Dev (ft)
		CDS	CBCS		
June, 2005	1000	H = 164.5 ft	N/A	0.28	0.36
May, 2005	7400	Q = 1500 cfs	H = 170 ft	0.38	0.52

Table 3-6. Calibrated Manning's  $n$  values for land use type in the Reach 2A SRH-2D model.

Land Use Type	Manning's $n$
Channel	0.039
Agriculture	0.045
Bare Ground	0.045
Scattered Trees & Light Brush	0.066
Medium Density Trees & Brush	0.10
Dense Trees & Brush	0.12
Urban & Industrial	0.08

### 3.3 Reach 2b

Reach 2B extends from the Chowchilla Bifurcation Structure at the upstream end (MP 216) to Mendota Dam (MP 205) at the downstream end. An existing conditions model was developed as well as two additional models for the purpose of evaluating potential changes related to levee setback conditions.

#### 3.3.1 Boundary Conditions

Downstream boundary conditions for Reach 2B were derived from the assumption that the water surface elevation of Mendota Pool is operated at a constant water surface elevation of 154.3 ft (NAVD 88). This is not always true due to operational changes when flashboards are removed. However, records of when this occurs were not available at the time of this study. For the calibration discharge of 1,100 cfs, the pool was set at the measured elevation nearest to Mendota Dam of 154.1 ft. For all other discharges modeled using the existing conditions model, a water surface elevation of 154.3 ft was used as the downstream boundary condition.

#### 3.3.2 Calibration

Two measured water surface profiles were collected by DWR in November 2009 and April 2010 with discharges in Reach 2B of approximately 161 cfs and 1,030 cfs, respectively (SJRRP 2010, 2011b). During the collection of water surface profile data for the 161 cfs discharge, no measurements were collected downstream from San Mateo Road at approximate MP 212. It is uncertain whether flow was steady state in Reach 2B during the water surface profile measurements at 161 cfs. Both flows were used for comparisons with model results and for determination of the best Manning's  $n$  roughness values to match the measured profiles.

Preliminary modeling of Reach 2B was conducted in 2008 based upon terrain data from 1997-1999 and calibrated using various high water marks collected in 2005 (Reclamation, 2008). For this initial model, four classifications of roughness were defined, including (1) unvegetated channel, (2) light vegetation, (3) heavy vegetation, and (4) levee. Within the extents of the mesh, roughness zones were spatially delineated using the 1998 aerial photographs and the topography data from the model surface. Multiple roughness values and combinations were examined to calibrate the 2008 model to match available 2005 high water mark data and also to evaluate model sensitivity to changes in roughness. Results from this modeling effort suggested that the best Manning's  $n$  values to represent channel hydraulics were 0.035 in the channel, 0.06 for light vegetation, 0.2 for heavy vegetation, and 0.035 for the levee.

For this current study, the existing conditions mesh used in the 2008 study was extended downstream to the Mendota Dam boundary, updated with topography collected in 2008 and 2009 and recalibrated with updated water surface profiles.

In addition, a roughness category for agricultural area was included. Various sets of Manning’s  $n$  values were evaluated to understand which channel and floodplain roughness combinations applied to the updated model most closely matched the measured water surface profiles collected in November 2009 and April 2010 (Table 3-7).

Table 3-7. Combinations of roughness values used in model calibration. The 2008 model used 2005 highwater marks and 1997-99 topography.

Manning's Roughness Values					
Land Use	2008 model best fit to 2005 HWM	Mid Floodplain $n$	Low Floodplain $n$	Mid Channel $n$	Low Channel $n$
Channel	0.035	0.035	0.035	0.03	0.025
Heavy Vegetation	0.2	0.1	0.07	0.2	0.2
Light Vegetation	0.06	0.06	0.05	0.06	0.06
Top of Levee	0.035	0.035	0.035	0.035	0.035
Agricultural Field	0.045	0.045	0.045	0.045	0.045

Model results for 161 cfs and 1,130 cfs were compared with the measured water surface profiles collected in 2009 and 2010 to determine the best fit roughness values for the updated Reach 2B model (Figure 3-11 to Figure 3-13). Initially, three combinations of floodplain roughness were modeled while maintaining a constant in-channel Manning’s  $n$  value of 0.035. Comparison of the floodplain roughness differences for the 1,130 cfs discharge illustrates that all combinations of floodplain roughness overpredict the water surface elevations along the measured profile. However, the values for floodplain roughness (light and heavy vegetation) from the 2008 model appear to best capture trends and significant changes in the measured water surface profile. This is especially notable at the upstream extent of Mendota Pool (just downstream from San Mateo Road) where heavy vegetation is present within the main portion of the channel.

To more closely match the elevation of the measured water surface profiles, the in-channel Manning’s  $n$  values were adjusted to 0.03 and 0.025. Comparing the simulations with lower in-channel values to the measured profiles at 161 cfs and 1,130 cfs, model results suggest that the “low” channel roughness values (shown in Table 3-7) matches most closely with the measured water surface profiles. Using this combination, the modeled water surface profile remains slightly higher than the measured water surface profile throughout the reach. However, possible changes in the vegetation over time due to consistent flows entering the reach will likely result in higher roughness values, particularly upstream from San Mateo Road. For this reason and for consistency with upstream and downstream reaches, the low channel  $n$  values were selected for use in all existing conditions model runs for the floodplain rearing study.

### 3.3.3 Alternative Levee Alignment Models

In addition to existing conditions geometry, 2D models were developed by TetraTech to represent the levee setbacks IAFP2 and IAFP4 associated with the compact Mendota Pool Bypass alignment as described in SJRRP (2011). Reclamation ran the levee setback models for flows ranging from 50 cfs to 4,500 cfs to evaluate effects of increased floodplain areas. Model inputs for these analyses are described in detail in SJRRP (2011). Manning's  $n$  values used for the models are shown in Table 3-8. The downstream boundary for these models is located at the proposed bifurcation of the Mendota Pool Bypass for the compact alignment, which is located at approximate MP 206. The downstream boundary conditions used in the models are shown in Table 3-9.

Table 3-8. Manning's  $n$  values applied in the alternative levee alignment IAFP2 and IAFP4 hydraulic models.

$n$ -value	Land Use	Discharge Range
0.035	Main channel	0 to 350 cfs
0.2	Very thick vegetation	350 to 1,100 cfs
0.1	Mature vegetation	1,100 to 1,500 cfs
0.085	Floodplain	Generally >1,500 cfs

Table 3-9. Downstream Boundary Conditions used in the Reach 2B models to evaluate effects of alternative levee alignments.

Discharge (cfs)	Water Surface Elevation (NAVD88ft)
50	150.98
175	150.98
285	151.56
475	152.19
1000	153.33
1225	153.70
2180	155.02
3655	156.60
4500	157.41

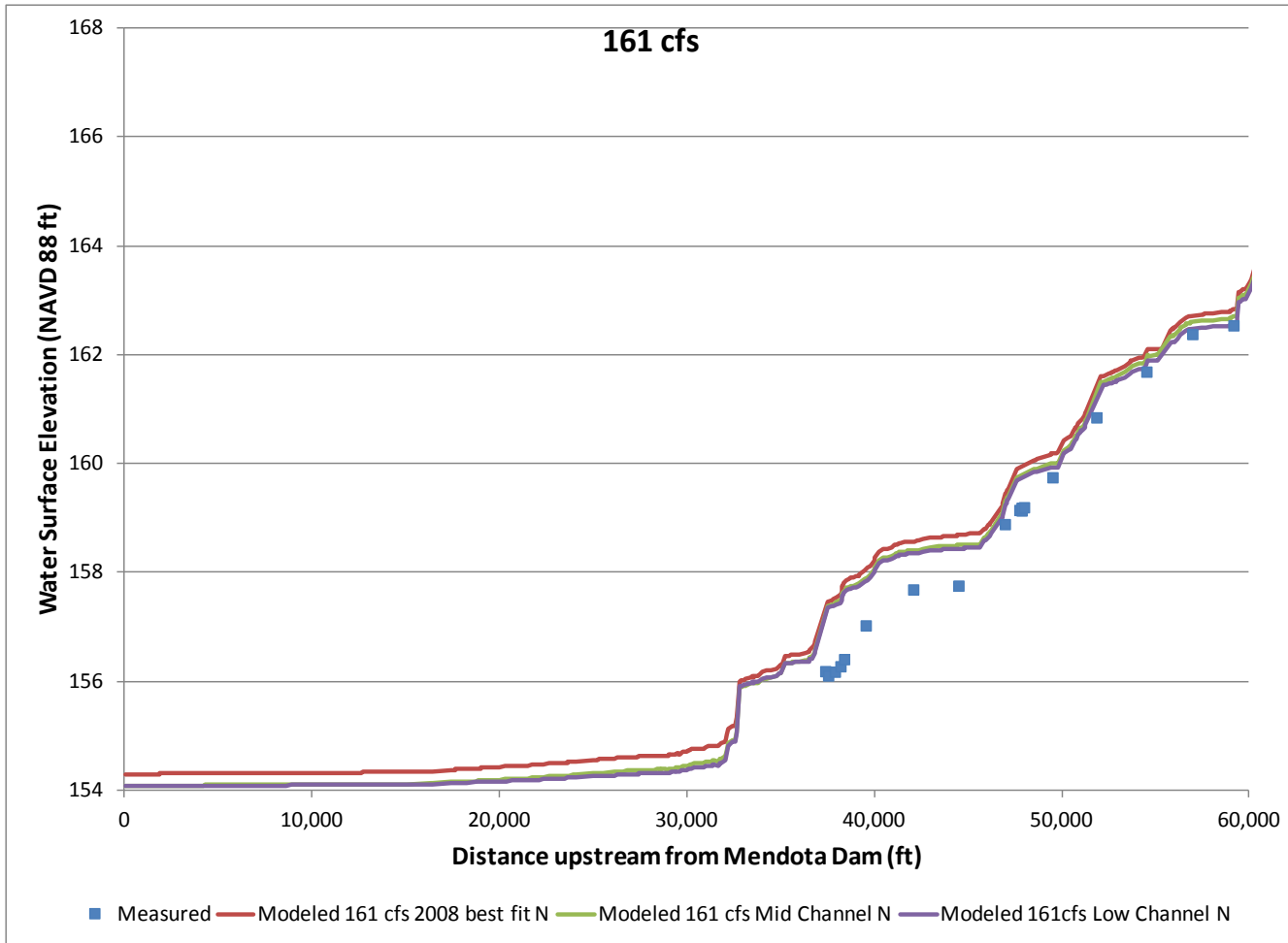


Figure 3-11. Measured and modeled results for 161cfs. No floodplain areas are accessed at this discharge and therefore these results illustrate the differences in the channel roughness values of 0.035, 0.03 and 0.025 applied.

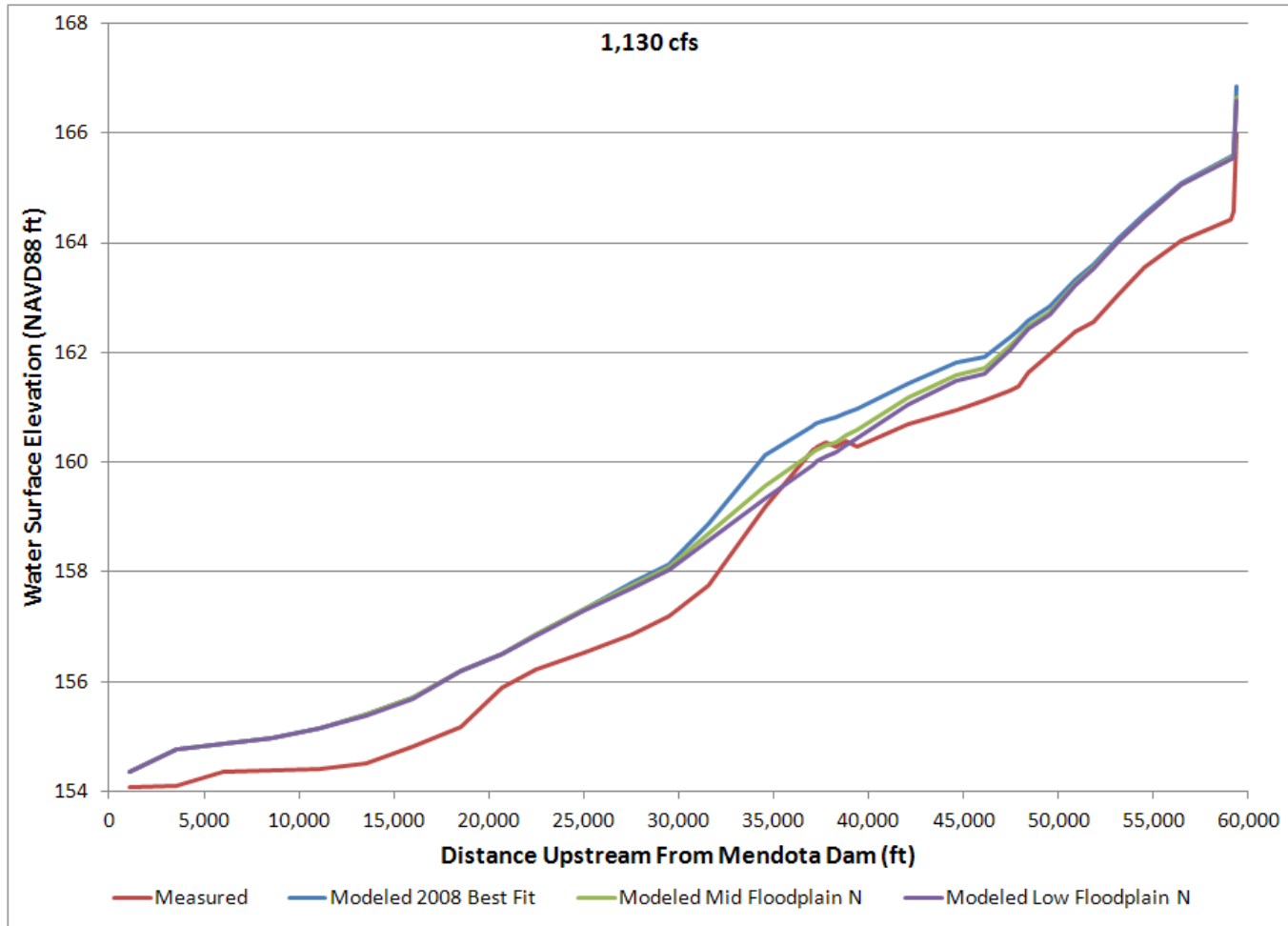


Figure 3-12. Measured and modeled results at 1,130 cfs showing variation in floodplain roughness combinations in Table 3-5 with all in-channel roughness values constant at 0.035.



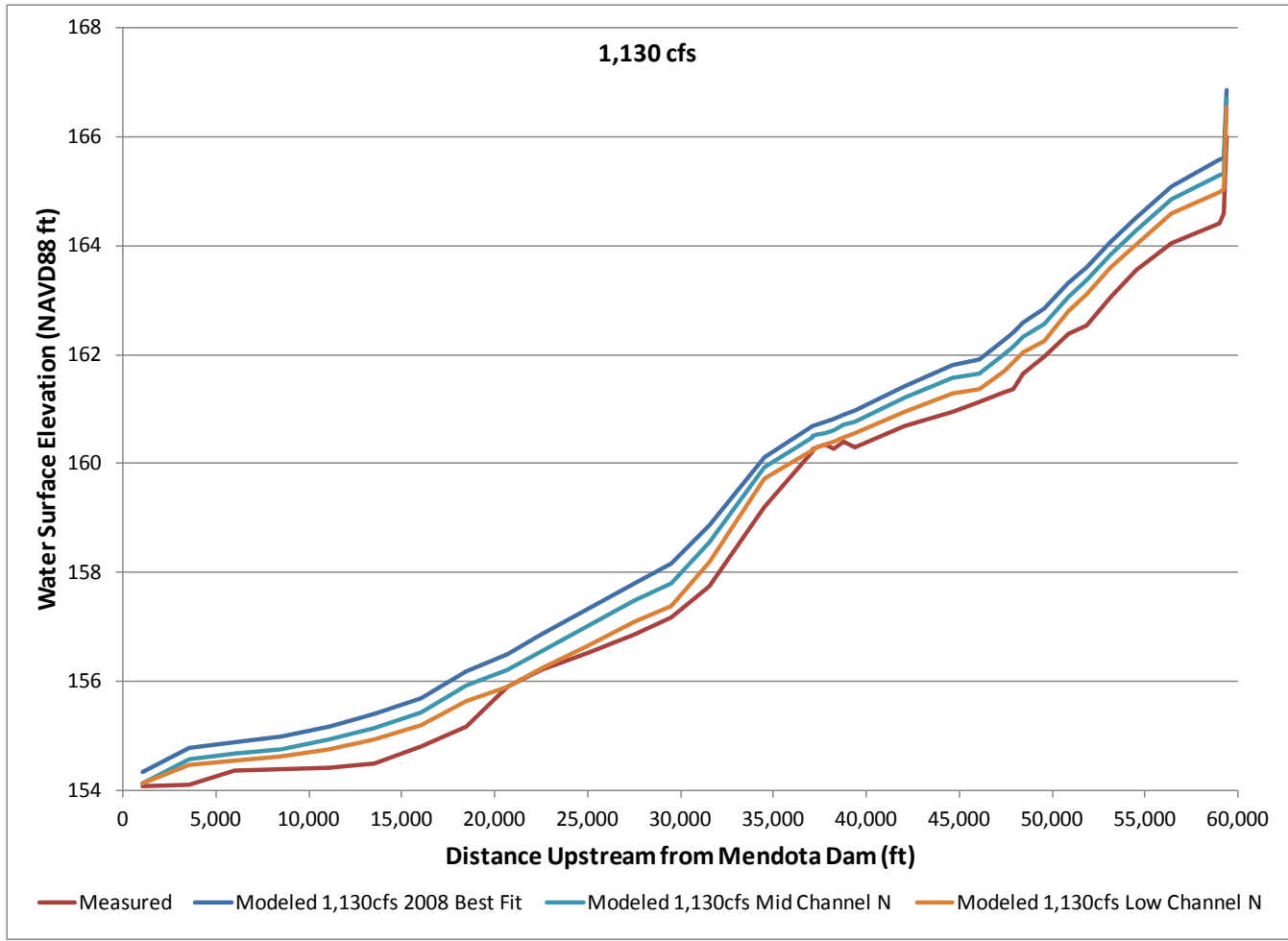


Figure 3-13. Measured and modeled results showing variation in channel roughness combinations at 1,130 cfs. The floodplain roughness values for each run were held constant while the channel roughness values were varied at 0.035, 0.03, and 0.025.

### 3.4 Reach 3

#### 3.4.1 Boundary Conditions

Reach 3 extends from Mendota Dam (MP 205) to Sack Dam (MP182). The SRH-2D model boundary conditions consist of an input flow rate, an exit water surface elevation at Sack Dam, and an outflow to Arroyo Canal. The outflow to Arroyo Canal was set at 57 cfs in all of the simulations for consistency with the measured flows when hydrographic surveys were performed. Table 3-10 summarizes the flows simulated in Reach 3 with corresponding water surface elevations at Sack Dam.

Table 3-10. Summary of flows simulated in Reach 3 with corresponding water surface elevation boundary condition applied at Sack Dam. An additional outflow boundary condition of 57 cfs to Arroyo Canal was applied for all simulations.

Flow Rate (cfs)	Sack Dam water surface elevation (NAVD 88, ft)
800	118.5
875	118.5
1225	119.8
1800	121.0
2180	121.5
3500	123.0
3655	123.1
4500	123.7

#### 3.4.2 Calibration

The calibration of the Reach 3 model was performed using measured water surface elevation data collected during three different surveys. The flow rates during each of the surveys are estimates due to gage uncertainty and temporal variation of the actual flow during the survey. Table 3-11 contains a summary of the measured water surface elevation source data, boundary conditions applied at Sack Dam, and calibration results. Figure 3-14 to Figure 3-16 show comparisons of measured and simulated water surface elevation at calibration flows of 875 cfs, 3500 cfs, and 1800 cfs, respectively. The Manning's  $n$  values were used as tuning parameters in the calibration process (Table 3-12). The results of the calibration process were used to develop a rating curve (Figure 3-17), from which boundary conditions were derived for the remaining flow simulations (Table 3-10).

Table 3-11. Summary of surveyed flows in Reach 3 used for model calibration.

Survey Date	Discharge (cfs)	Sack Dam WSE (NAVD 88, ft)	Avg Diff Mag (ft)	Std Dev (ft)
USBR; April 9-10, 2010	875	118.5	0.22	0.26
DWR; Jan 10-11, 2011	1800	120.8	0.27	0.31
DWR; April 4-5, 2011	3500	123	0.31	0.37

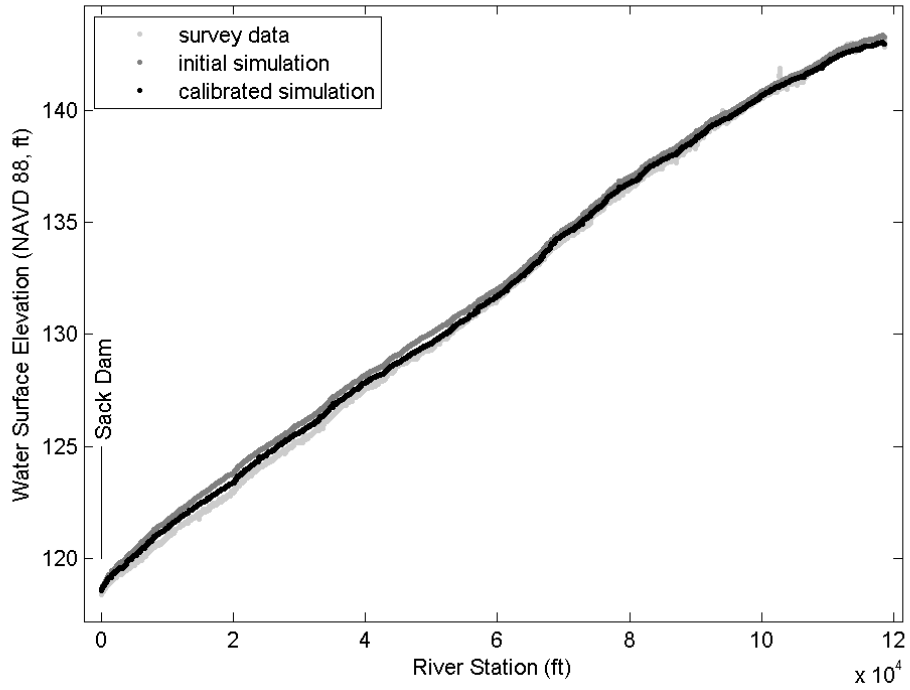


Figure 3-14. Water surface elevation plotted as a function of distance upstream from Sack Dam for 875 cfs simulated flow. Survey data (light gray) are plotted in comparison to simulation results before (gray) and after (black) calibration.

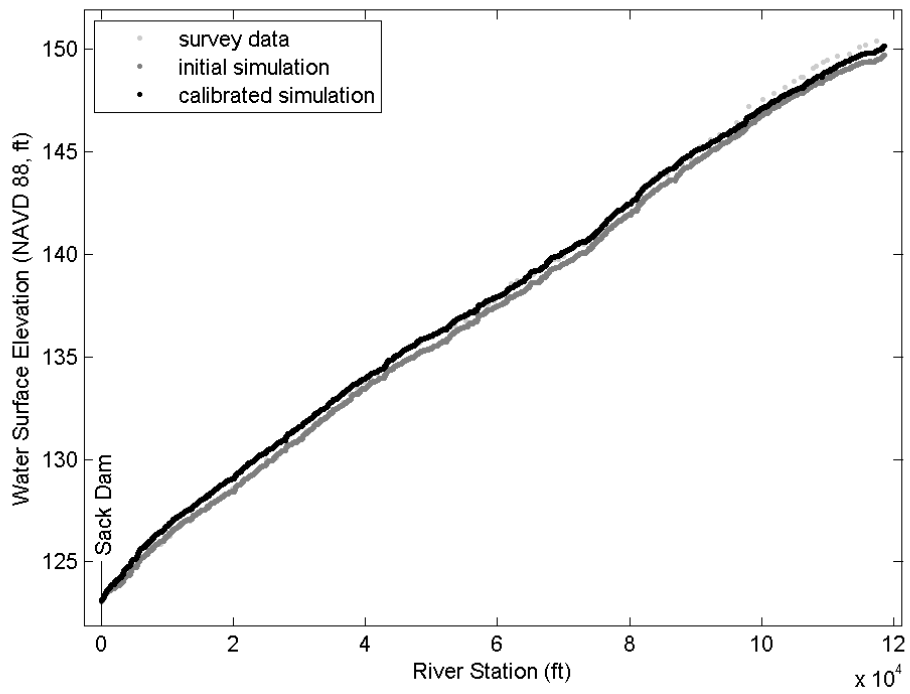


Figure 3-15. Water surface elevation plotted as a function of distance upstream from Sack Dam for 3500 cfs simulated flow. Survey data (light gray) are plotted in comparison to simulation results before (gray) and after (black) calibration.

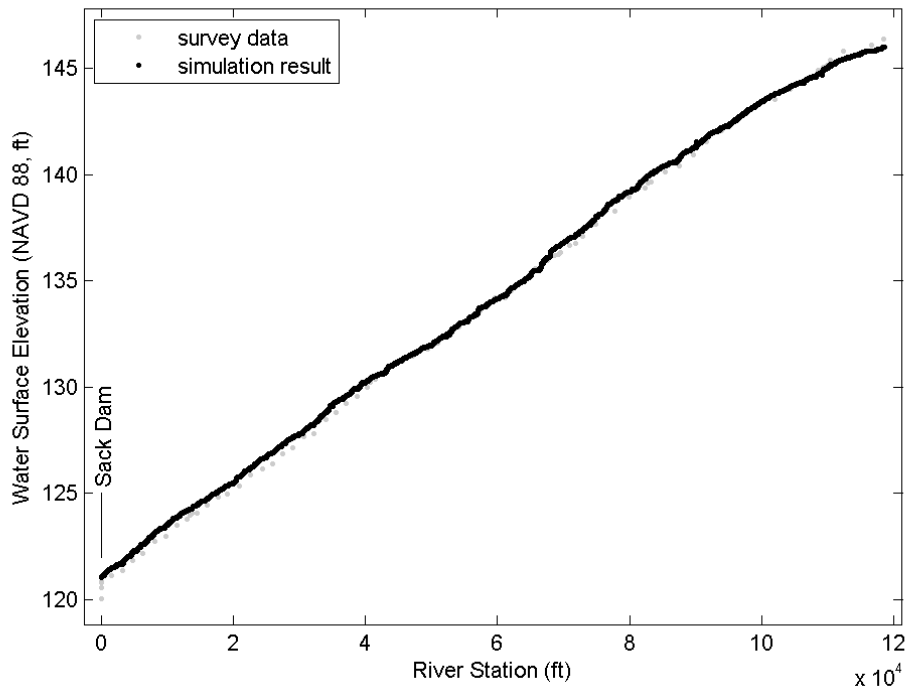


Figure 3-16. Water surface elevation plotted as a function of distance upstream from Sack Dam for 1800 cfs simulated flow. Survey data (gray) are plotted in comparison to simulation results (black).

Table 3-12. Calibrated Manning's  $n$  values for land use type in the Reach 3 SRH-2D model.

Land Use Type	Manning's $n$
Channel	0.035
Agriculture	0.065
Bare Ground	0.045
Scattered Trees & Light Brush	0.080
Medium Density Trees & Brush	0.10
Dense Trees & Brush	0.120
Urban & Industrial	0.08

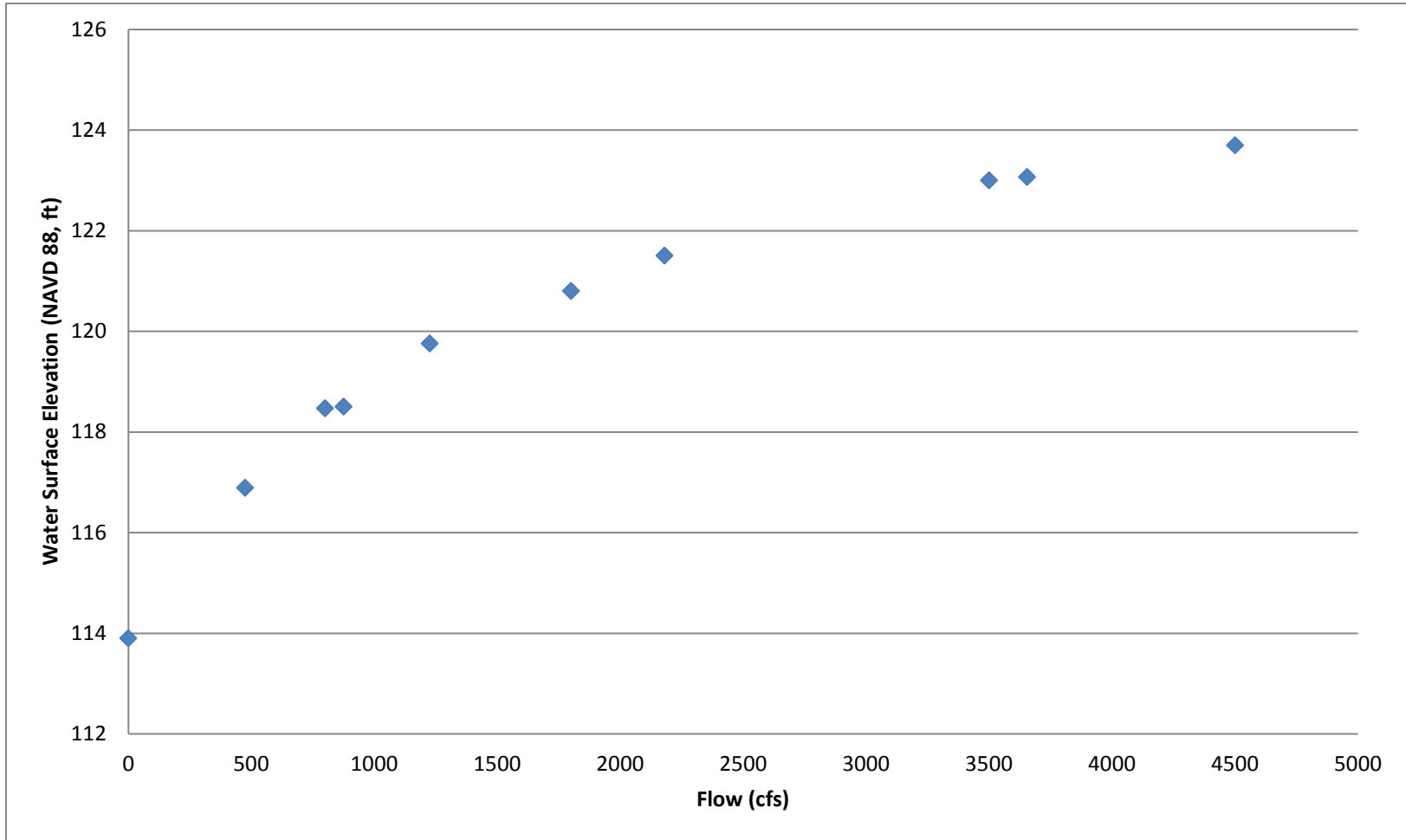


Figure 3-17. Rating curve developed from simulation calibration data for Reach 3. Water surface elevation (downstream boundary condition, NAVD88 ft) at Sack Dam is plotted as a function of flow through the reach.

## 3.5 Reach 4A

### 3.5.1 Boundary Conditions

Reach 4A extends from Sack Dam (MP 182) to the Sand Slough Control Structure (SSCS; near MP 168), at which point flow is diverted from the historical San Joaquin River channel (Reach 4B1) into the Eastside Bypass. The Reach 4A SRH-2D model has an input boundary condition specified as a volumetric flow rate. The downstream boundary condition is specified as an exit water surface elevation applied in the vicinity of SSCS. A third boundary condition could be applied as an output into the historical San Joaquin River channel; however, for the purposes of these simulations that outflow was assumed negligible. A rating curve for specification of the downstream exit water surface elevation was developed using 1D HEC-RAS modeling (Figure 3-18).

Table 3-13 summarizes the flows simulated using the Reach 4A SRH-2D model with corresponding downstream boundary conditions.

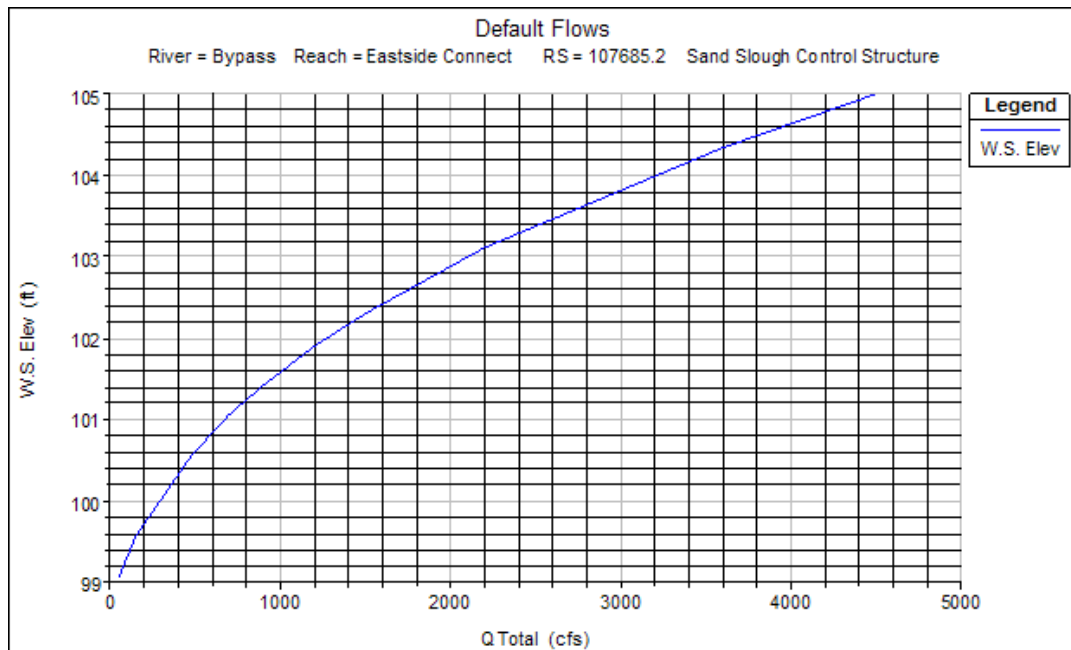


Figure 3-18. Rating curve for Reach 4A model developed from HEC-RAS modeling. Water surface elevation (NAVD 88, ft) is plotted as a function of simulated flow (cfs).

Table 3-13. Summary of flows simulated in Reach 4A with corresponding water surface elevation boundary condition applied in the vicinity of SSCS. Flows into Reach 4B1 were assumed negligible.

Flow Rate (cfs)	SSCS water surface elevation (NAVD 88, ft)
475	100.55
700	101.05
900	101.43
1200	101.9
1500	102.3
2200	103.1
3600	104.35
4500	105.0

### 3.5.2 Calibration

The calibration of the Reach 3 model was performed using measured water surface elevation data collected during two surveys. The flow rates during each of the surveys are estimates due to gage uncertainty and temporal variation of the actual flow during the survey.

Table 3-14 contains a summary of the measured water surface elevation data source, boundary conditions applied near SSCS, and calibration results. Figure 3-19 and Figure 3-20 show comparisons of measured and simulated water surface elevation at calibration flows of 730 cfs and 3300 cfs, respectively. Table 3-15 contains a table with the Manning’s *n* roughness values derived during the calibration process and applied in the simulations.

The model calibration for the 730 cfs flow shows marked discrepancy between the measured and simulated water surface elevation in the lower portion of the model reach (Figure 3-19). It was not possible to calibrate the model in that portion of the model reach without using physically unrealistic roughness values. This discrepancy is attributed to unresolved differences in the vegetative cover conditions. It is likely that the conditions at the time of the survey were such that dense vegetation or accumulated sediment was creating an elevated water surface elevation above what would be predicted based on the bathymetry data and modeled hydraulics. This hypothesis is supported by visual inspection of varying conditions in that portion of Reach 4A. As a result, the calibration process was focused on matching the water surface elevation conditions above this portion of the reach where conditions are more favorable for consistent comparison. It is likely that the vegetation obstructions or sediment accumulations present in the



lower part of the channel will not remain there once full SJRRP flows are in place.

Table 3-14. Summary of surveyed flows in Reach 4A used for model calibration

Survey Date	Flow Rate (cfs)	SSCS WSE (NAVD 88, ft)	Avg Diff Mag (ft)	Std Dev (ft)
USBR; April 9-10, 2010	730	101.8	0.59	0.77
DWR; April 12, 2011	3300	106.5	0.48	0.57

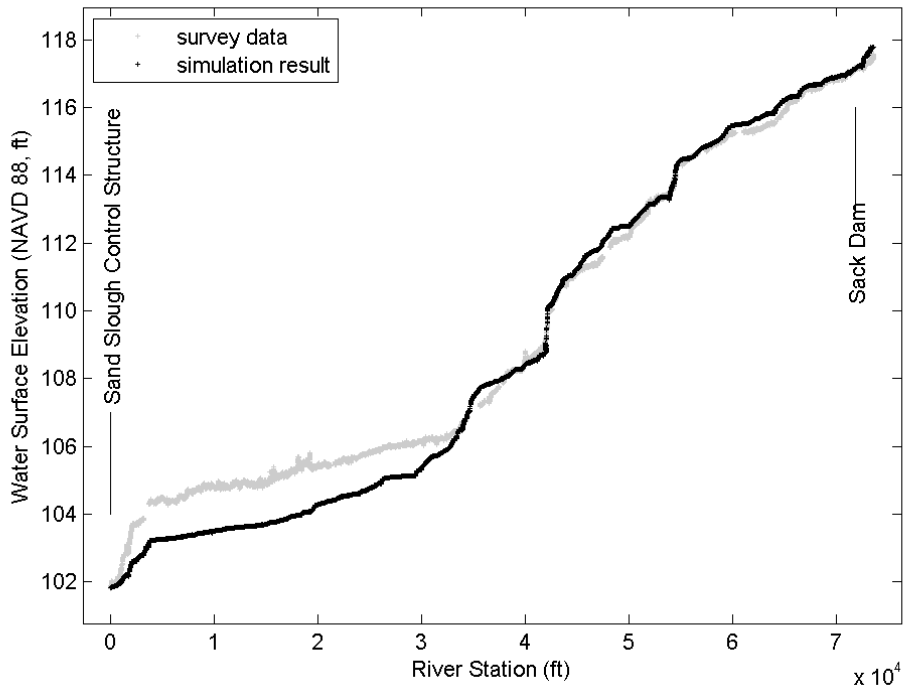


Figure 3-19. Water surface elevation as a function of distance upstream from SSCS. Shown is survey data (gray) and the model calibration result (black) for a simulated flow of 730 cfs.

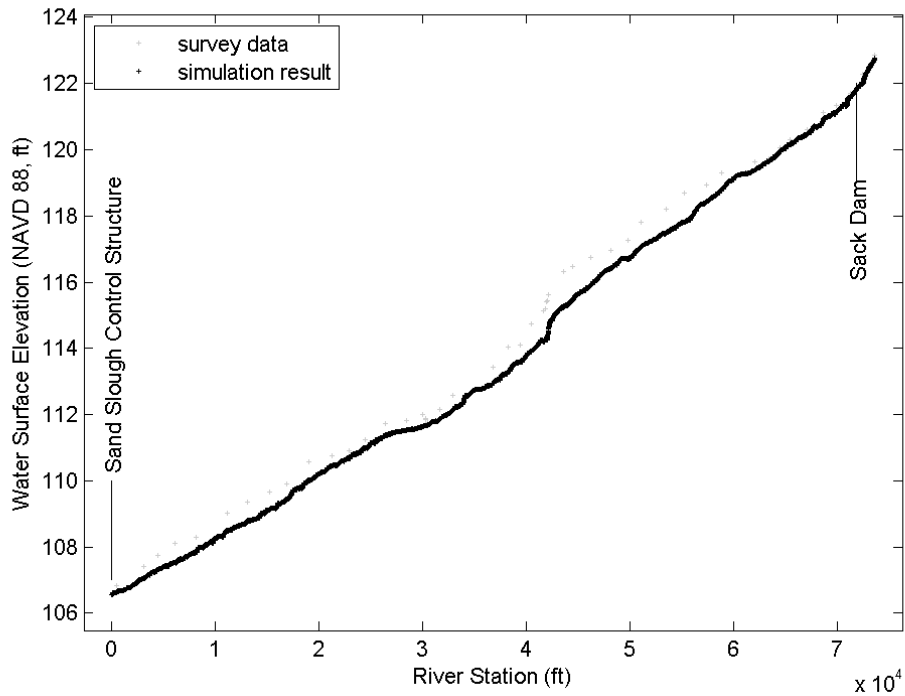


Figure 3-20. Water surface elevation as a function of distance upstream from SSCS. Shown is survey data (gray) and the model calibration result (black) for a simulated flow of 3300 cfs.

Table 3-15. Calibrated Manning's  $n$  values for land use type in the Reach 4A SRH-2D model.

Land Use Type	Manning's $n$
Channel	0.035
Agriculture	0.045
Bare Ground	0.045
Scattered Trees & Light Brush	0.080
Medium Density Trees & Brush	0.10
Dense Trees & Brush	0.120
Urban & Industrial	0.08

## 3.6 Reach 4B1

### 3.6.1 Calibration

There has been no flow in Reach 4B1 since the construction of the head gates at the top of the reach in the 1960s. Therefore, there is no calibration possible within the reach.

### 3.6.2 Alternative Levee Alignments

As part of the SJRRP, there will be levee improvements and/or levee setbacks within Reach 4B1. Four different levee options are considered in this report: A, B, C, and D. The same main channel alignment was used for all the options. Following the existing river alignment, the total channel length of Reach 4B1 is 21 miles and the bed elevation drops from approximately 95 to 75 feet.

The levee alignments are given in Figure 3-21 and a description of the alignments is given below. The area enclosed by each alignment is given in Table 3-16.

**Option A:** Existing Levee alignment with improvements to contain the design flow. Based on the original design capacity of this reach when the bypass system was constructed in the 1960s, the maximum flow capacity with this alignment is 1500 cfs. Levee improvements would also be necessary to convey 475 cfs because the existing levees are not continuous and several road crossings would have to be reconstructed to pass flow. The levees are typically 250 to 400 ft apart in this option, but there are several sections with large channel curvature where the levee width is much wider.

**Option B:** This is considered the minimum levee setback necessary to convey 4500 cfs and maintain a minimum level of riparian habitat. The levees are setback a minimum of 250 ft from the edge of the channel so that levee maintenance will be minimized. Some side channels would be constructed, but on a limited basis. The channel would be primarily a single thread channel. The levees are typically 1300 to 2000 ft apart.

**Option C:** Option C is considered an intermediate levee setback between Option B and D that would contain a minimum of 4500 cfs. The levees are typically 3500 to 5500 ft wide, though the width decreases to about 2500 ft at the downstream end of the reach.

**Option D:** Option D is considered a maximum levee setback that would reconnect historical side channels and restore a significant portion of the complex channel network of the San Joaquin that existed prior to the advent of intensive agricultural production. The levees are typically 5000 to 11000 ft wide, though the width decreases to about 2500 ft at the downstream end of the reach.

For each levee option, a considerable amount of earthwork will be required in Reach 4B1 to restore channel conveyance, floodplain connectivity, and prevent fish stranding. At this stage of alternative development, two example areas (designated as Area 1 and Area 2) were chosen to design these features and the location of these areas is shown in Figure 3-21. These two example areas were chosen as representative portions of Reach 4B1. These areas represent about 1/3 of the total area of Reach 4B1.

Separate boundary conditions were applied to each of the example areas based upon the results of 1D hydraulic modeling.

For options B, C, and D, it was assumed that the existing levees would be removed to approximately the surrounding floodplain elevations. This material would be used to grade the floodplain so that the floodplain slopes away from the levees and towards side channel or the main channel. The cut and fill was balanced in each alternative to minimize material being imported or exported from the reach. However, it is unlikely that a significant portion of the existing levee material could be used to construct new levees. This is because most of the material would be needed as fill in the floodplain. Furthermore, the existing material is not necessarily appropriate for fill in constructing new levees.

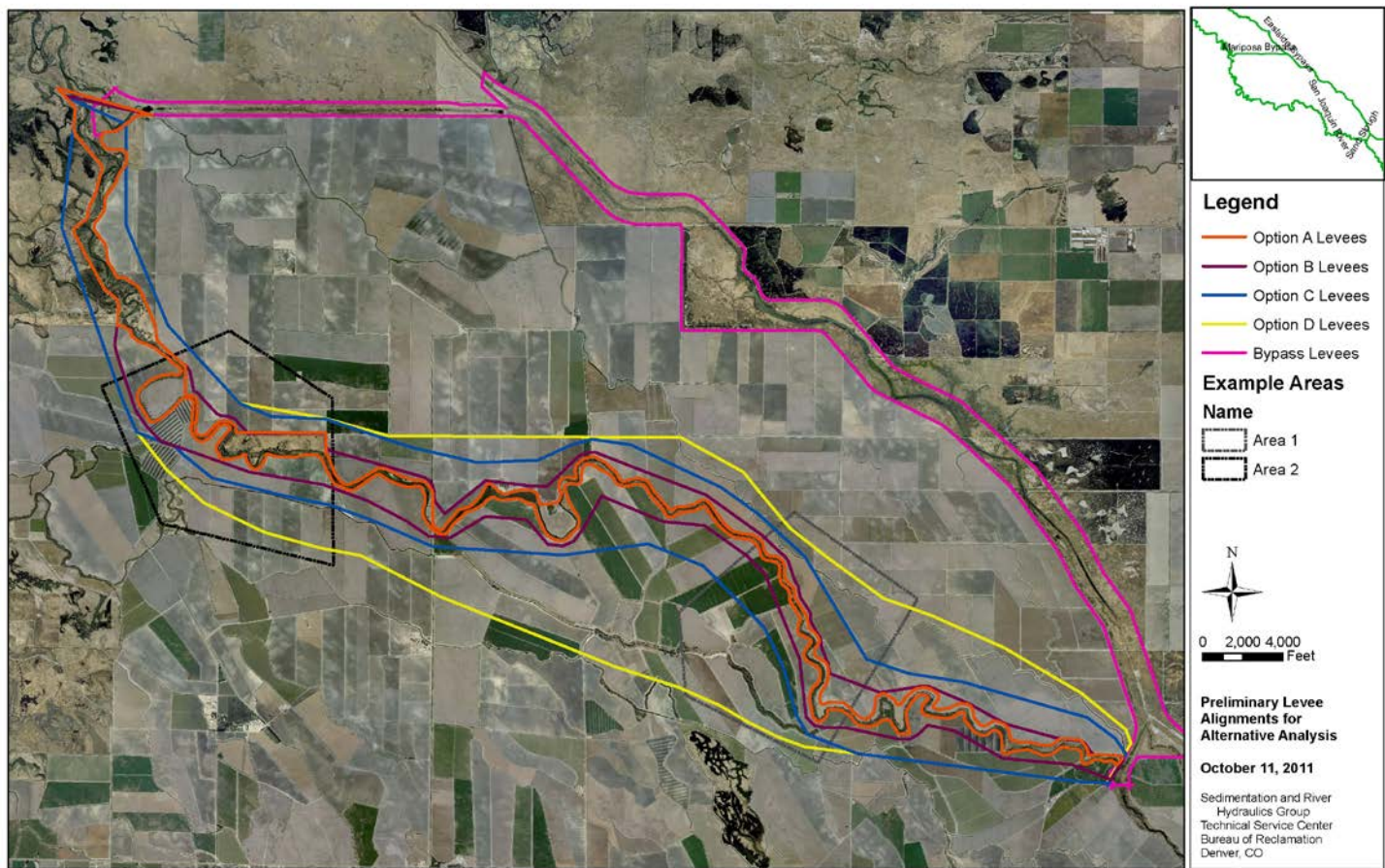
To analyze the flow hydraulics in the reach, it was necessary to modify the existing terrain to incorporate these features. The location of the side channels and levee removal is shown in Figure 3-22 for example Area 1 and Figure 3-23 for example Area 2.

The side channels for Option D are shown in Figure 3-22 and Figure 3-23. Side channels are also incorporated into the other levee options, but only if they are fully encompassed within the levees. The side channels are intended to have approximately 1 ft of water at a flow of 150 cfs. In the final design, the side channel may be varied so that some become active at different discharges. Example cross sections for Option D are shown in

Figure 3-24 and Figure 3-25.

Table 3-16. Area enclosed by Levee Alignments A, B, C, and D.

Levee Alignment Option (A-D)	Total Area Enclosed (acres)
Option A	1,265
Option B	2,985
Option C	6,195
Option D	10,150



1

Content Subject to Change; For Discussion Purposes Only

Figure 3-21. Levee options for Reach 4B1.

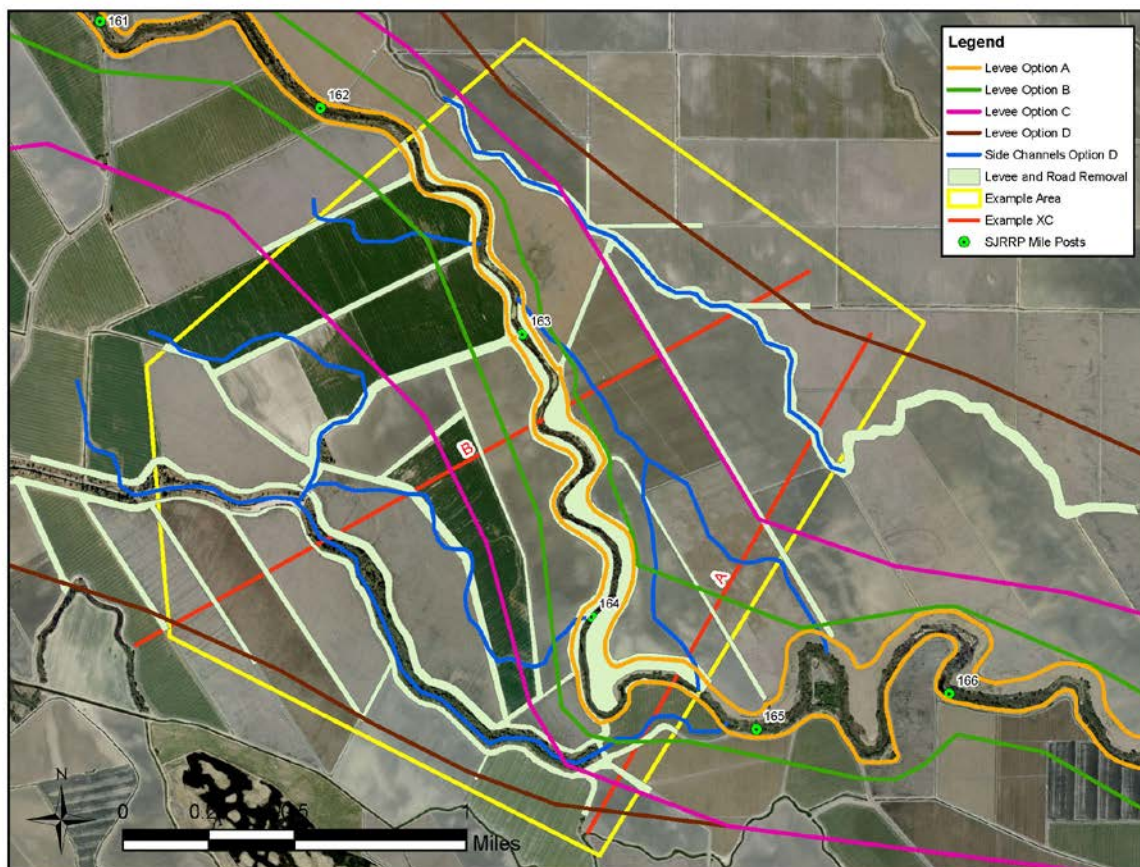


Figure 3-22. Design Features in Example Area 1 in Reach 4B1. Cross sections A and B are shown in

Figure 3-24.

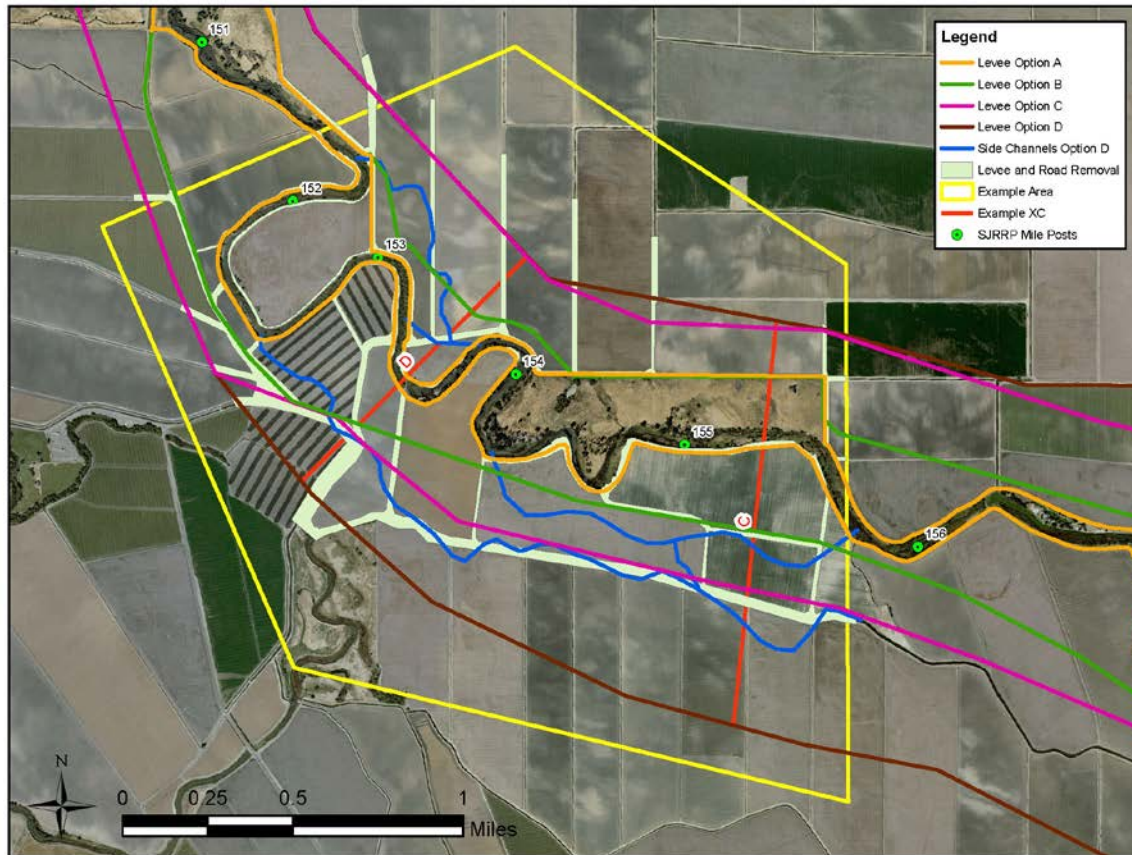


Figure 3-23. Design Features in Example Area 2 in Reach 4B1. Cross sections C and D are shown in Figure 3-25.



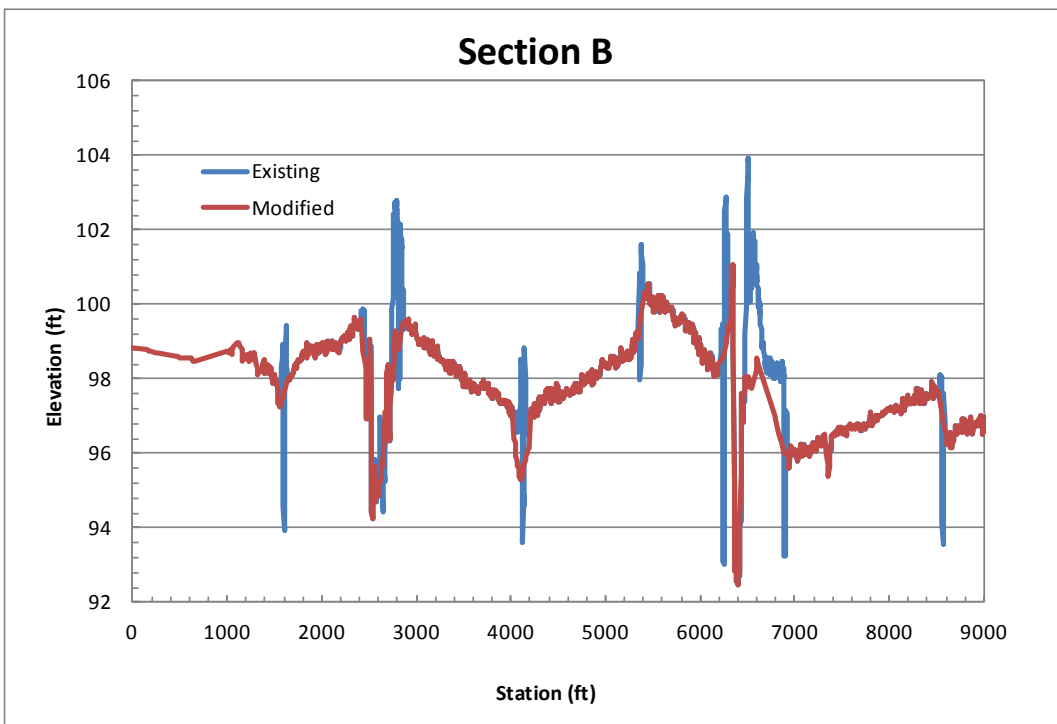
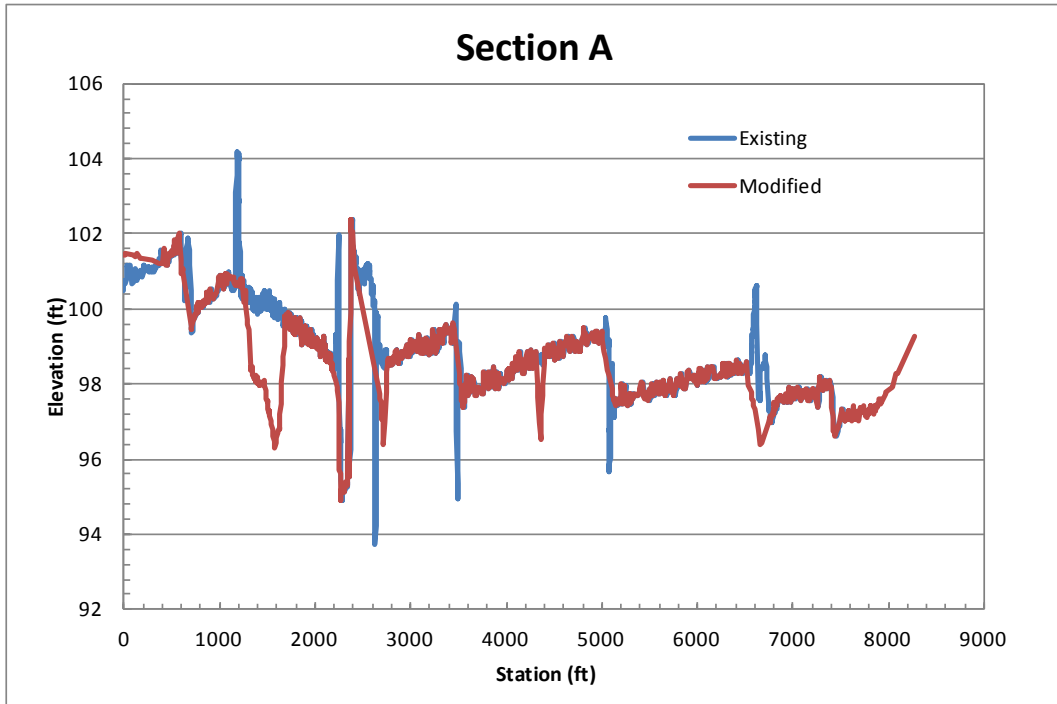


Figure 3-24. Existing and modified cross sections A and B for Levee Option D.

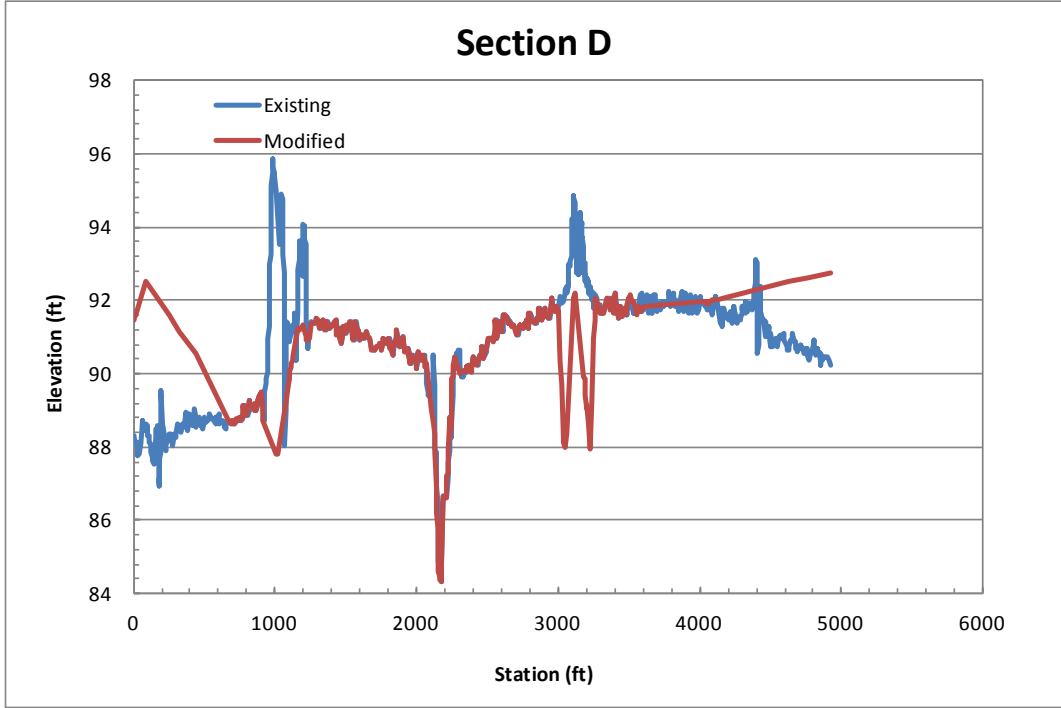
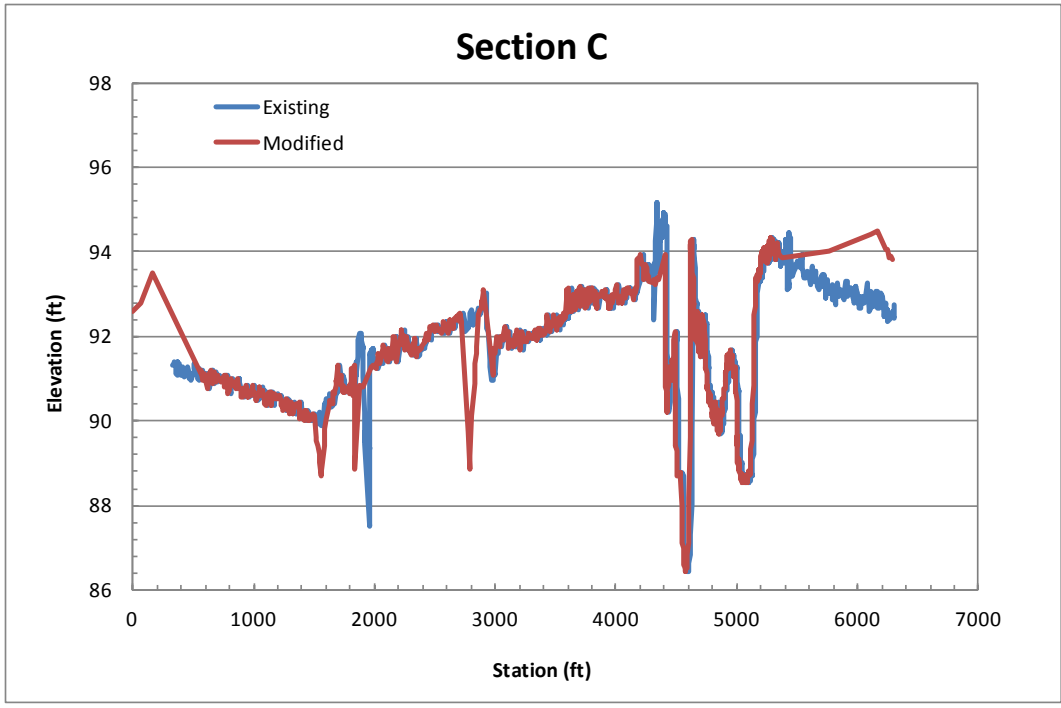


Figure 3-25. Existing and modified cross sections C and D for Levee Option D.

## 3.7 Reach 4B2

### 3.7.1 Boundary Conditions

Boundary conditions in the model consist of water surface elevations at the downstream end of the model for each simulated inflow. Water surface elevations were based primarily upon flows surveyed in 2010 and 2011; for flow rates higher than those surveyed, the MEI (2008) study was referenced. The rating curve at the downstream boundary is shown with measured values in Figure 3-26. The flows at the upstream end of Reach 5 were computed using the difference between USGS gages 11261500 (“San Joaquin River at Fremont Ford Bridge, CA”) and 11261100 (and “Salt Slough at HW 165 near Stevinson”).

### 3.7.2 Calibration

Hydrographic surveys of the water surface elevations were performed in April 8, 2011 from Mariposa Drop Control Structure to downstream of the confluence with the Eastside Bypass (SJRRP, 2011b). The flow rate in Reach 4B2 on that day was estimated by taking the difference between the CDEC gage at Eastside Bypass near El Nido (ELN) and the CDEC gage at Eastside Bypass below Mariposa (EBM). The flow at ELN varied between 9,825 and 9,883 cfs and the flow at EBM varied between 5,540 and 5,917. This gives an average flow in Reach 4B2 of approximately 4,120 cfs on April 7, 2011.

The initial floodplain Manning’s  $n$  roughness values were taken from the MEI (2008) study in which hydraulic roughness is based on vegetation density in the floodplain. The initial and calibrated Manning’s  $n$  values for each vegetation type category is listed in Table 3-17. The initial roughness values were increased by a factor of 1.25 so that the model results were consistent with the measured water surface elevation data. Table 3-18 contains a tabular comparison between measured and simulated water surface elevations for the data collected on April 7, 2011. Figure 3-27 shows a plot of the water surface elevation comparison as a function of distance upstream.

Table 3-17. Hydraulic Roughness Values used in Reach 4B2.

Description	Initial $n$ Values	Calibrated $n$ Values
Channel	0.035	0.044
Bare soil	0.045	0.056
Scatter Trees and Light Brush	0.060	0.075
Medium Density Trees and Brush	0.080	0.100
Dense Trees and Brush	0.100	0.125

Table 3-18. Comparison between Measured and Simulated Water Surface Elevations for the data collected on April 7, 2011 in Reach 4B2.

Date	Flow (cfs)	Average Difference (ft)	Standard Deviation (ft)
April 7, 2011	4120	-0.03	0.165

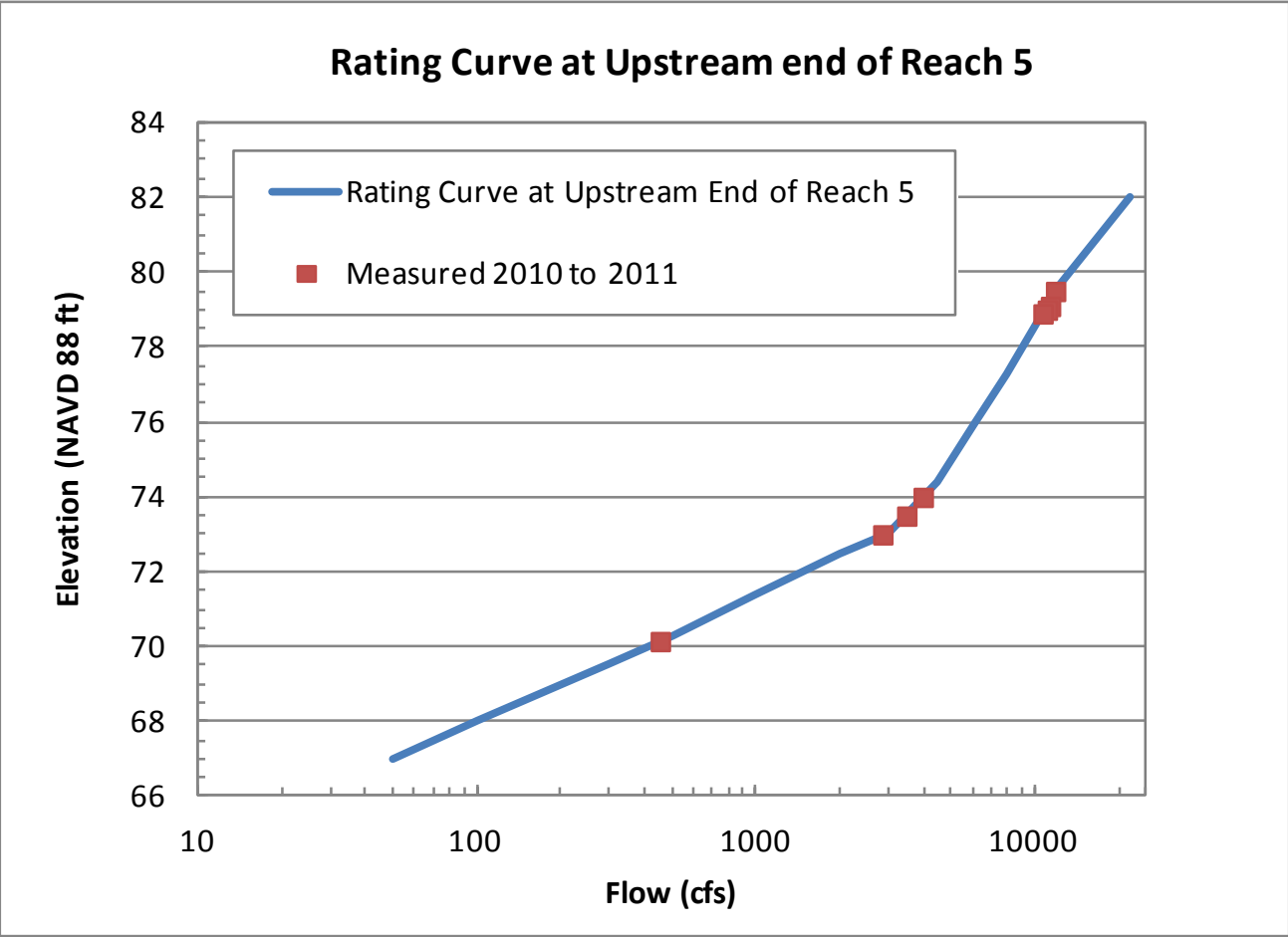


Figure 3-26. Rating curve used for Reach 4B2 downstream boundary condition at XC 55382, which is just downstream of Eastside Bypass Control Structure.

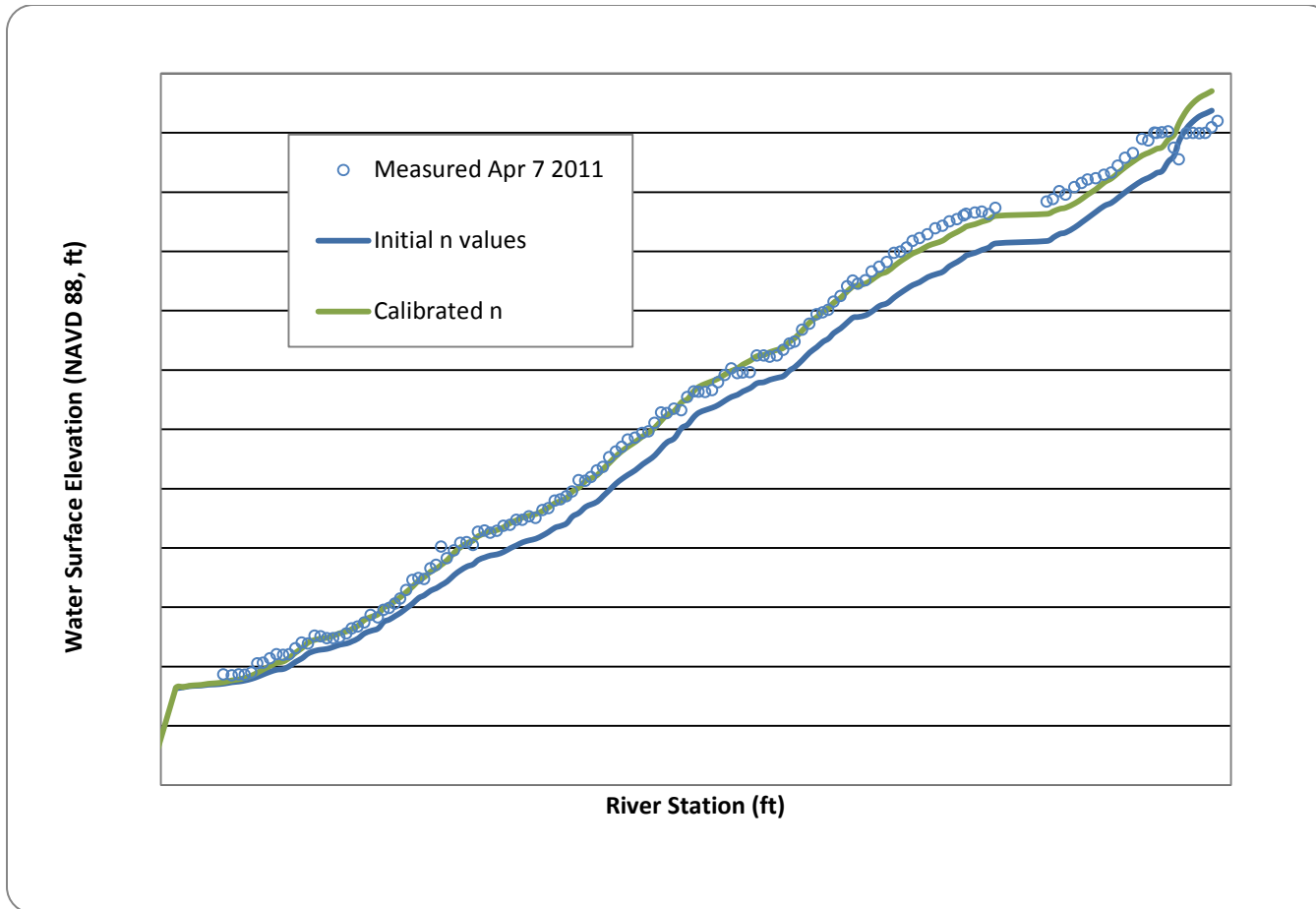


Figure 3-27. Comparison between calibrated and measured water surface elevations for the flow occurring on April 7, 2011 in Reach 4B2.

### 3.8 Reach 5

Inundation mapping was conducted for Reach 5 from results of 1D HEC-RAS modeling. The existing conditions model titled SJRRP07, documented in Mussetter Engineering, Inc (MEI, 2008) was used in order to represent the existing levels of floodplain available along the San Joaquin River. Steady-state releases from Friant Dam of 50, 100, 200, 400, 600, 800, 1000, 1250, 1500, 1750, 2000, 2250, 2500, 2750, 3000, 3500, 4000, and 4500 cfs were modeled. Table 3-19 shows the corresponding flows in different sections of Reach 5, including flow loss assumptions and tributary inflows. MEI used equal exceedance frequencies to historical releases of these Friant flows to determine downstream tributary inflow at Mud and Salt Sloughs as well as Bear Creek.

Water surface elevations were interpolated between the HEC-RAS cross-sections to develop a 3D surface of elevations. This surface was then compared to 3D terrain surfaces that the SJRRP developed from a combination of 1998 Ayers / COE photogrammetry and 2008 LIDAR. Mussetter Engineering, Inc. used these same datasets to develop the HEC-RAS cross-sectional geometry. The difference between water surface elevation and terrain elevation created a depth map. The inundation map of MEI was edited to better represent existing inundated areas that could provide habitat along the San Joaquin River. Areas removed include off-channel pools with no surface connection (an artifact of the 1D HEC-RAS modeling), and floodplain associated with tributary watersheds. At each Friant release flow modeled by MEI, the area of inundation was then calculated.

Table 3-19. Flows used in Reach 5 corresponding to Friant Release.

Location	Station (ft)	Friant Release (cfs)																	
		50	100	200	400	600	800	1000	1250	1500	1750	2000	2250	2500	2750	3000	3500	4000	4500
Salt Slough	59245	71	163	328	555	775	990	1202	1463	1729	2000	2277	2566	2852	3129	3403	3935	4476	5052
Mud Slough	17180	88	228	478	743	978	1203	1424	1694	1973	2254	2543	2849	3149	3438	3723	4273	4835	5441
Merced River	17181	134	408	900	1416	1760	2084	2399	2779	3201	3620	4081	4635	5147	5546	5929	6615	7339	8184



## 4 Habitat Analysis

Results from hydraulic simulations of prescribed river restoration flows through Reaches 1B, 2A, 3, 4A, 4B2, and 5 were used to inform a habitat estimation model for predicting available suitable salmon rearing habitat. The following sections describe criteria for determining suitable depths, velocities, and cover, and methodology for combining suitability indices to estimate area of available suitable habitat.

### 4.1 Hydraulic Suitability

Two-dimensional SRH-2D hydraulic models were developed for each of the Reaches 1B-4B2. For each 2D hydraulic simulation performed, the model computes depth and velocity of flow at every grid point within the computational mesh. Distributions of simulated water depth were used to compute the *total inundated area* (TIA) for each reach and flow. The results of 1D HEC-RAS hydraulic modeling for Reach 5 were used to estimate the area of inundation for each flow through the reach.

To compute the available *area of suitable habitat* (available ASH), habitat suitability relationships were applied to depth, velocity, and cover variables on 5 ft by 5 ft grid cells distributed over a subportion of each reach. Habitat suitability indices (HSI) are correlative relationships developed from field observations of species numbers and habitat conditions. The indices provide a simple and efficient way of mapping habitat quality over large expanses of a river system. Subportions of each reach were selected for the purpose of reducing the computational overhead of habitat calculations. The subportion habitat results were extrapolated to the entirety of each reach using TIA as a scaling factor.

Fish observations from the Stanislaus River, a tributary of the San Joaquin River, were used as the basis for depth and velocity hydraulic habitat suitability (Figure 4-1; Aceituno 1990). Hydraulic suitability relationships exist from other river systems such as the Trinity River (Hampton 1997); however, the Stanislaus River data had several benefits over the other data sets: Stanislaus River habitat suitability curves are from within the San Joaquin Basin, are based on data collected from actual fish observations over multiple years, and generally fit in the mean area of the range of curves from multiple river systems considered. It should be noted that Stanislaus River fish observations are based on habitat preferences within the channel, as there was no available data on fry or juvenile habitat preferences on floodplains within the San Joaquin Basin.

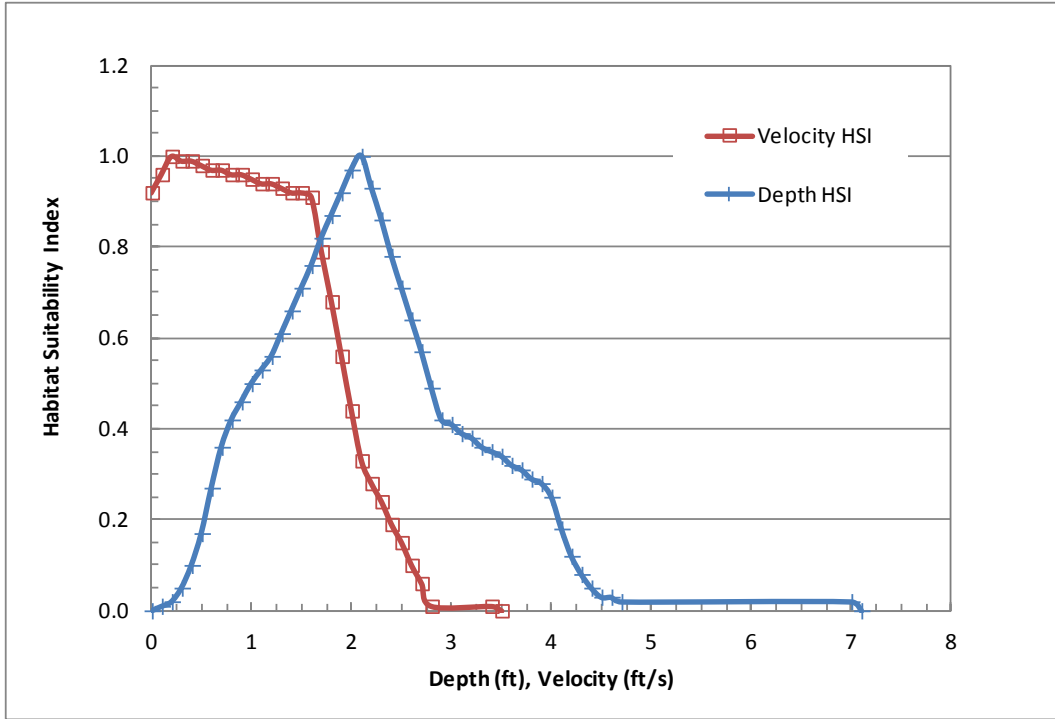


Figure 4-1. Habitat Suitability Index values as a function of depth and velocity from Stanislaus River (Aceituno, 1990).

## 4.2 Cover Suitability

Cover is an important component of overall habitat quality, and has a direct effect on the density of juvenile salmonids observed (McMahon and Hartman, 1989). Cover suitability was analyzed in addition to depth and velocity to determine suitable habitat.

### 4.2.1 Vegetation Mapping

To compute cover suitability under existing conditions in each reach, a review of the literature values for cover types was first conducted. Table 4-1 contains the categories and values from four different studies of cover: Raleigh (1986), Sutton (2006), Washington Department of Fish and Wildlife (WDFW 2004), and Hampton (1988). The average cover suitability value is also given in the table. This data was then correlated to the two datasets primarily used to determine cover types: 1) the vegetation mapping data documented in Moise and Hendrickson (2002) and 2) 2007 aerial photography that has a pixel density of 0.5 ft to delineate edge habitat.

The vegetation mapping data did not contain the same cover categories as Table 4-1 and therefore some adjustment of the categories was necessary. Eleven basic vegetation communities were found along the San Joaquin in Moise and Hendrickson (2002). The percentage area within each category and within each reach is given in Figure 4-2 to Figure 4-7. This vegetation mapping did not identify overhanging vegetation, aquatic vegetation, root wads, or woody debris. Conversely, the cover categories for which literature values are available (Table 4-1) did not contain values for cottonwood and many other riparian tree species.

Therefore, a modified set of categories was used in this study as specified in Table 4-2. In this study, average literature values were applied for No Cover, River Wash, Gravel, Grasses, Wetland, and Willow categories. Gravel and Cobble/Boulder categories were not used because there are not significant areas of these features in Reaches 1B through 5. To provide a value for tree species missing from the literature, a new category called “Edge Habitat” was defined as high value ( $HSI_C = 1$ ) habitat adjacent to features that provide cover for juvenile salmon.

Table 4-1. Cover habitat categories considered in development of cover methodology.

Cover Type	HSI <sub>c</sub> score for each cover type				Average HSI Value
	Raleigh 1986	Sutton 2006	WDFW 2004	Hampton 1988	
No Cover	0.01	N/A	0.1	0.1	0.07
Woody Debris	0.9	0.6	N/A	0.7	0.73
Cobble/Boulder	0.2	0.5	N/A	0.18	0.29
Grass	N/A	0.5	0.48	N/A	0.49
Gravel	0.25	0.3	N/A	N/A	0.28
Willow	N/A	0.8	N/A	N/A	0.80
Undercut Bank	1	1	1	1	1.00
Aquatic Vegetation	0.3	0.6	1	0.5	0.60
Overhanging Vegetation	0.38	0.8	1	0.1	0.57
Root Wad	N/A	0.7	1	0.7	0.80

Table 4-2. Cover HSI scores from literature and those assumed for this study.

Cover Type	HSI <sub>c</sub> score for each cover type				Assumed HSI Value
	Raleigh 1986	Sutton 2006	WDFW 2004	Hampton 1988	
No Cover, River Wash	0.01	N/A	0.1	0.1	<b>0.07</b>
Gravel Bars	0.25	0.3	N/A	N/A	<b>0.28</b>
Grass, Herbaceous	N/A	0.5	0.48	N/A	<b>0.49</b>
Willow Riparian and Willow Scrub	N/A	0.8	N/A	N/A	<b>0.80</b>
Wetland/Marsh	0.3	0.6	1	0.5	<b>0.60</b>
Edge Habitat	N/A	N/A	N/A	N/A	<b>1.00</b>

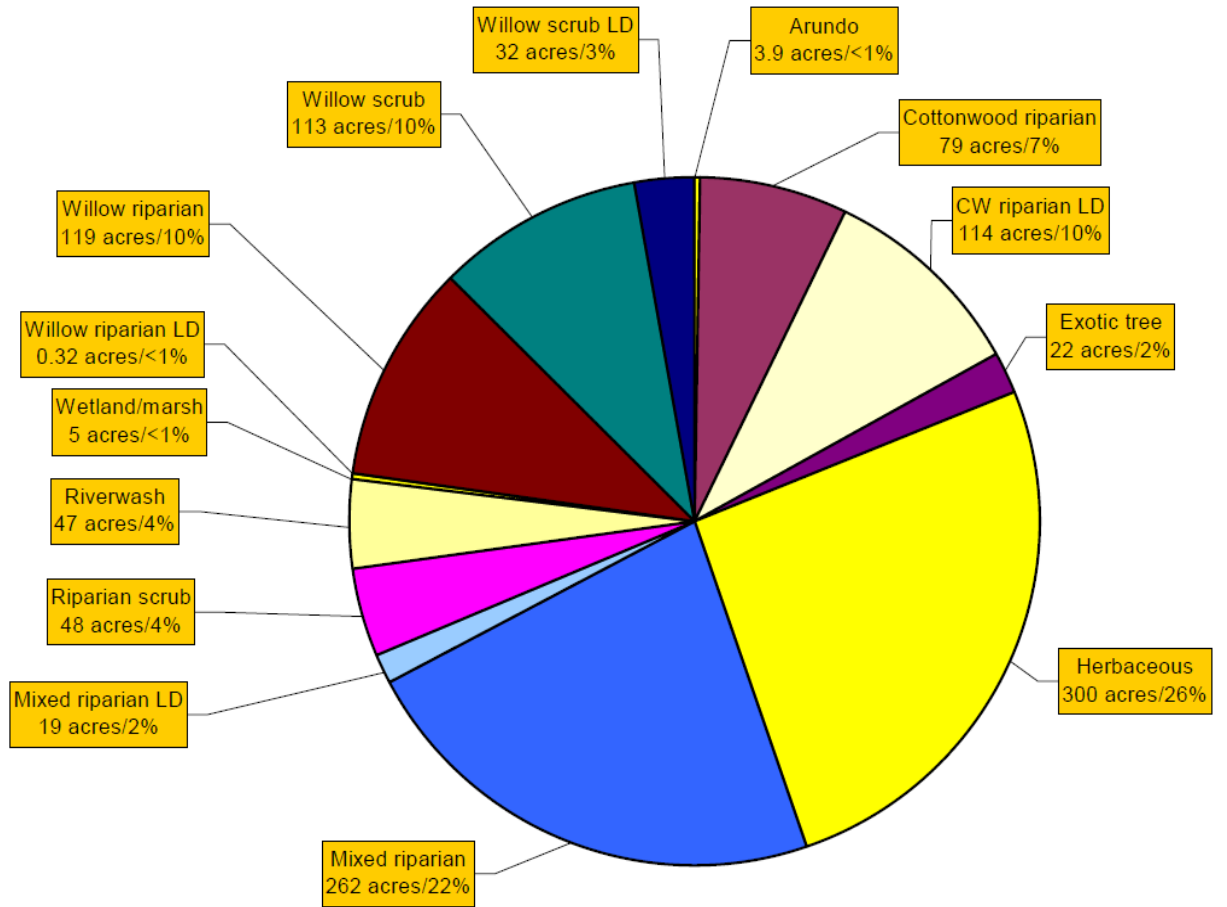


Figure 4-2. Percentage within each vegetation category for Reach 1B from Moise and Hendrickson (2002).

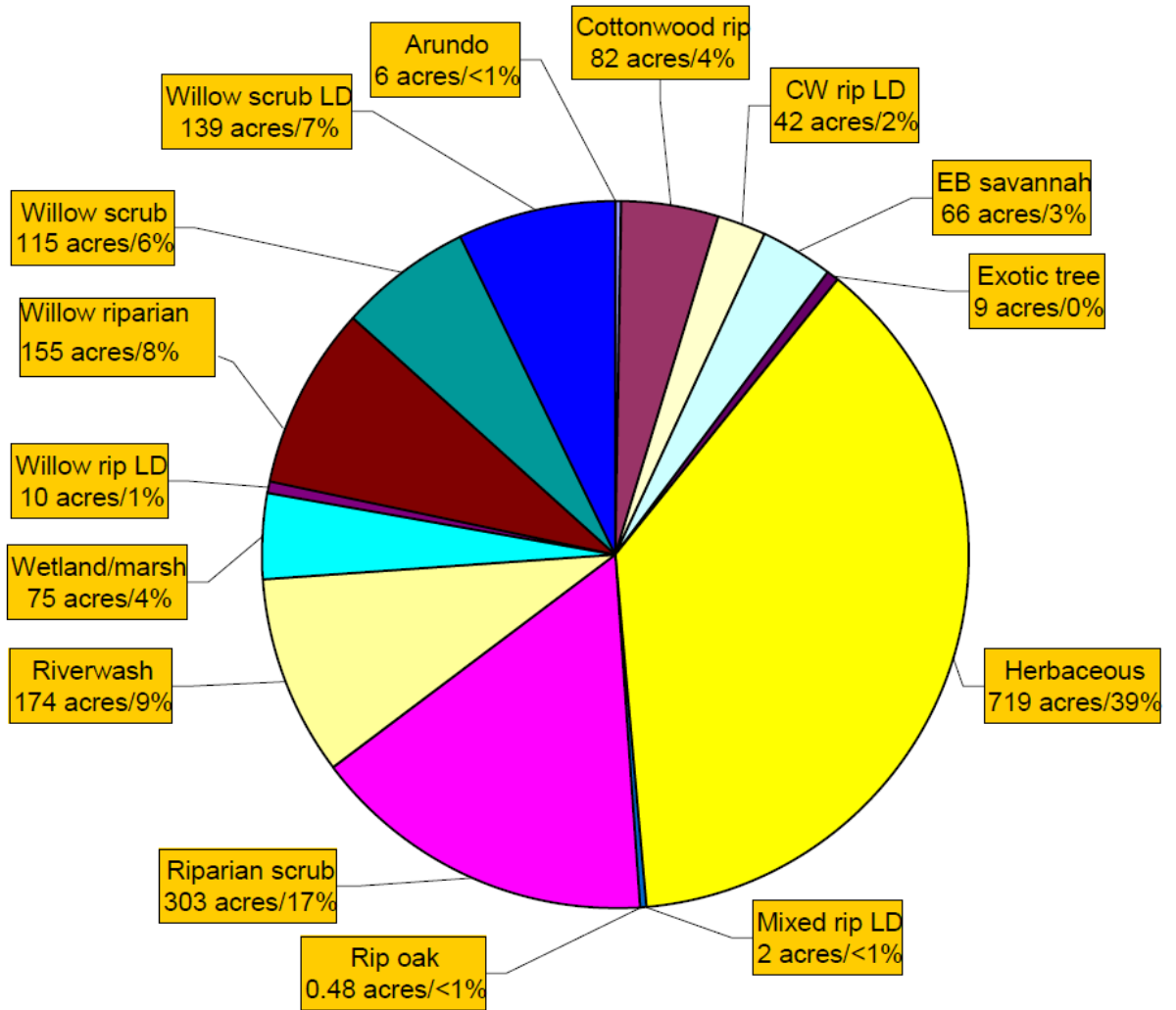


Figure 4-3. Percentage within each vegetation category for Reach 2 from Moise and Hendrickson (2002).

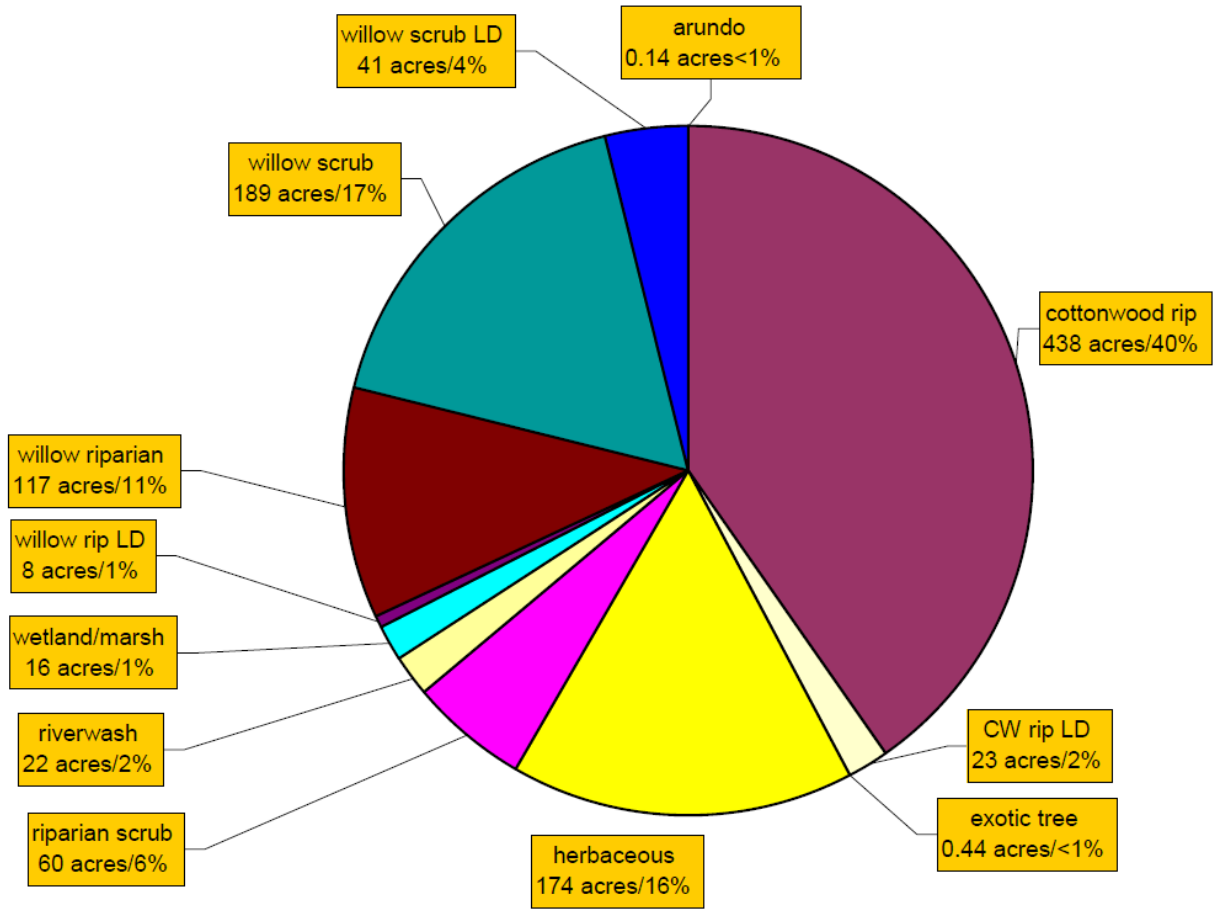


Figure 4-4. Percentage within each vegetation category for Reach 3 from Moise and Hendrickson (2002).

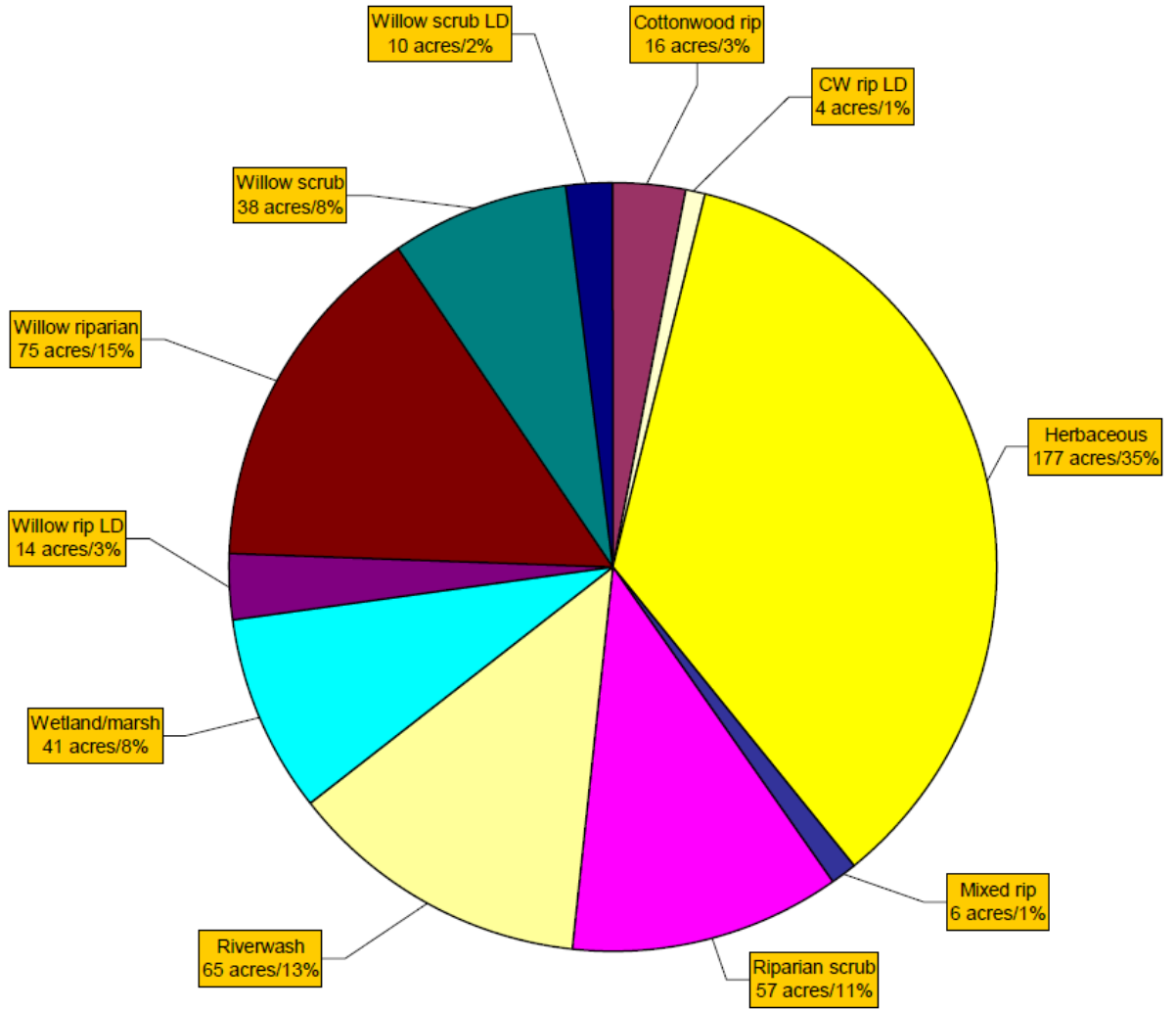


Figure 4-5. Percentage within each vegetation category for Reach 4A from Moise and Hendrickson (2002).



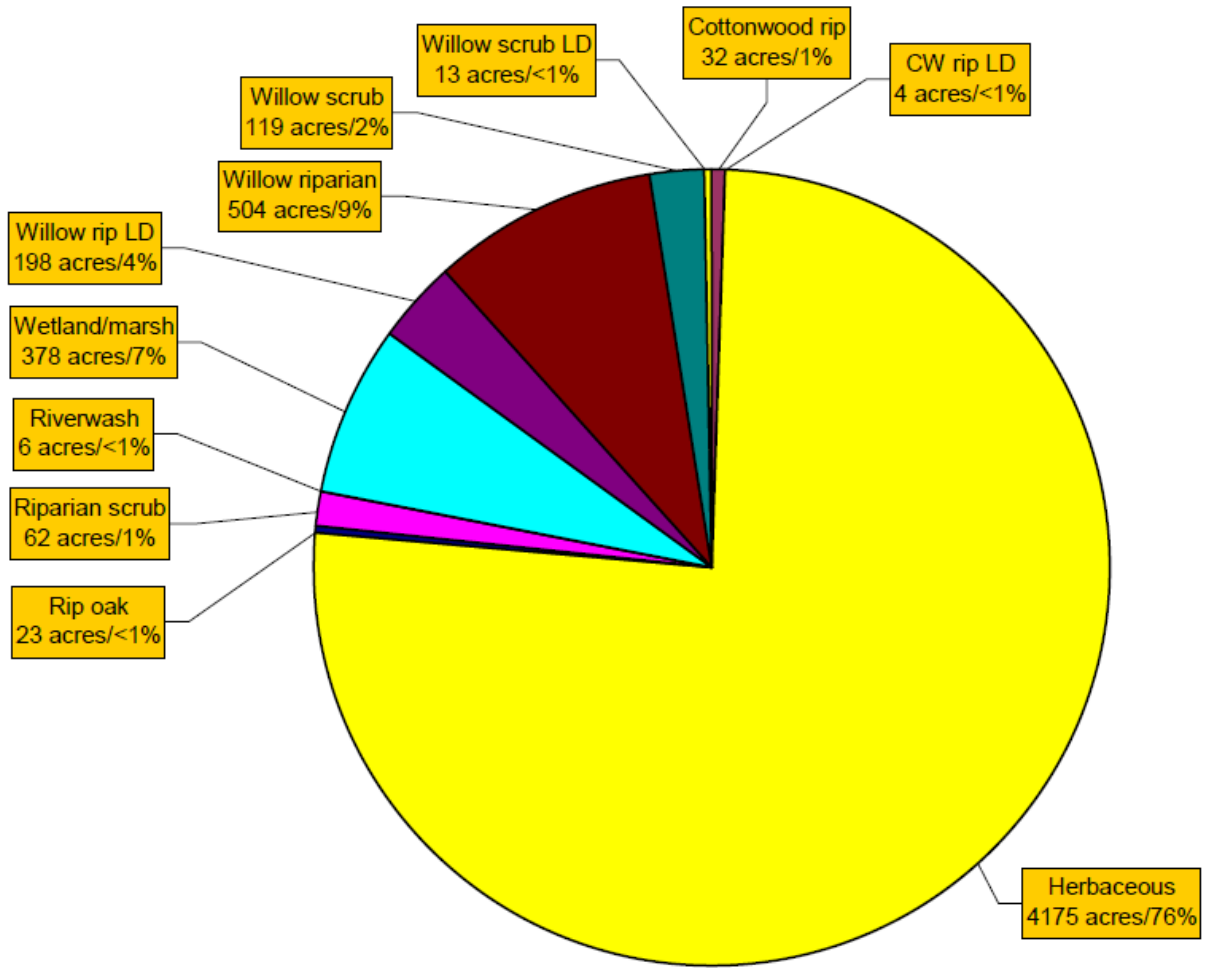


Figure 4-6. Percentage within each vegetation category for Reach 4B from Moise and Hendrickson (2002).

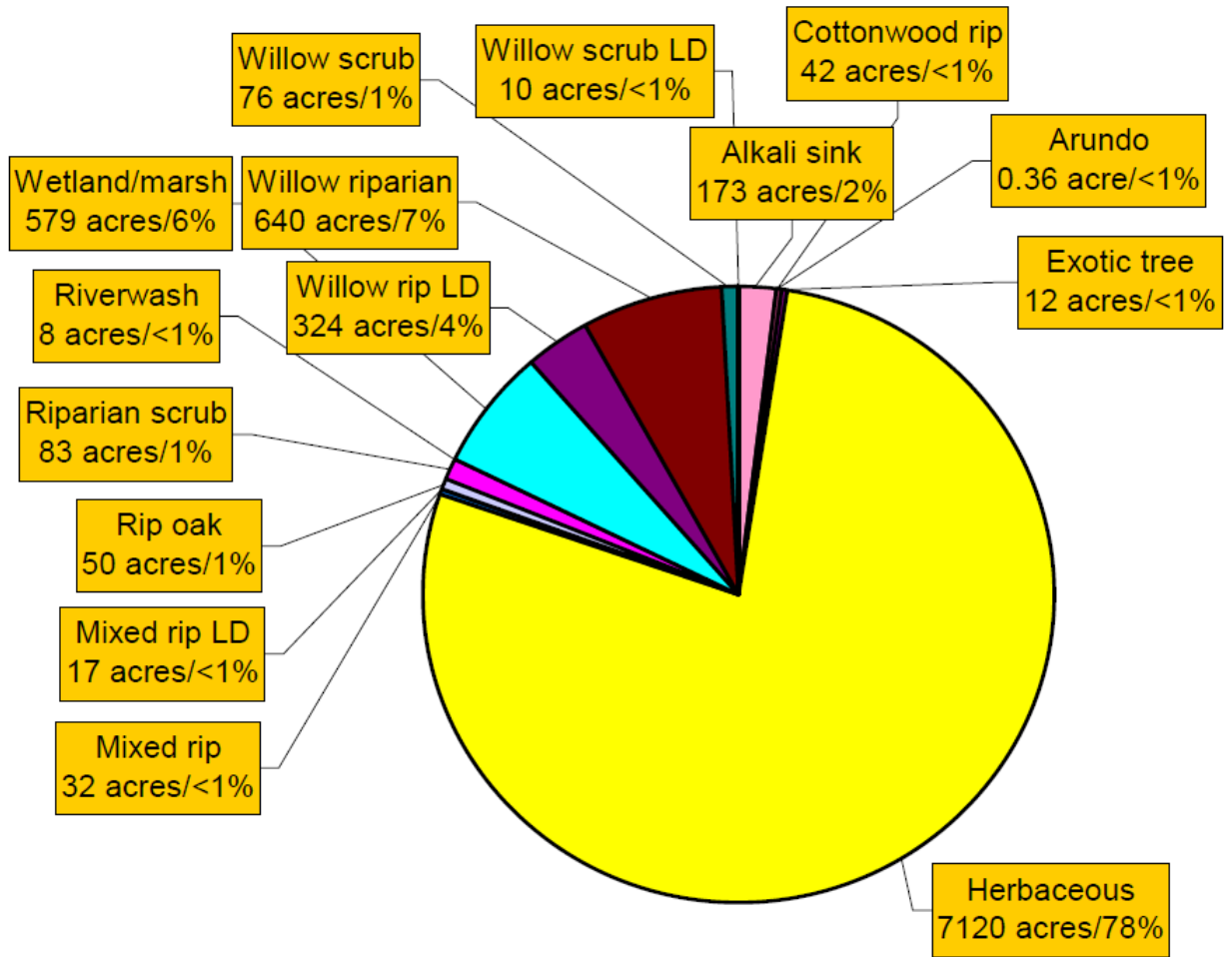


Figure 4-7. Percentage within each vegetation category for Reach 5 from Moise and Hendrickson (2002).

#### 4.2.2 Edge Habitat Classification

The basic concept of edge habitat is that juvenile salmonids set up territories around cover features. The cover features act as current breaks and provide safety from potential predators and competitors, but they also serve as feeding stations. Therefore, cover features must be within close proximity to a food source to be used by juvenile salmonids. In most stream systems, optimal cover features are close to open water, which acts as a transport mechanism bringing food to juvenile salmonids stationed near the features. The distance juveniles are willing to move from cover to open water to feed and the distance of the cover feature to open water determines its overall utility. A cover feature with an HSI value of 1.0 (e.g., undercut bank above) may have a high cover value, but if it is not located within close proximity to open water, juvenile salmonids will abandon the feature in favor of other, more bioenergetically favorable features. This represents a trade-off between “safety” and optimal foraging strategy, and inherently means

that habitats with high heterogeneity and edge features are more useful to juvenile salmonids than habitats with low heterogeneity and no edge features (Figure 4-8).

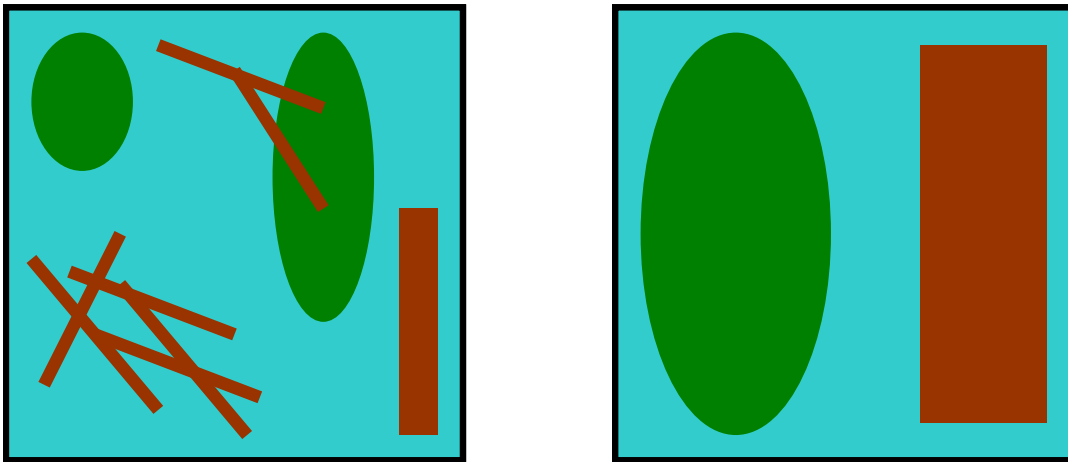


Figure 4-8. Example high (left) and low (right) heterogeneity habitats. Green and brown areas represent cover. Blue areas represent open water. Juvenile salmonids generally station themselves on the edges of cover features, so a greater number of smaller cover features generally provides more suitable “edge” habitat than a limited number of larger cover features even though the larger cover features may provide more overall cover area.

Juvenile salmonid burst speeds are one useful way to define areas surrounding cover features that are suitable for occupation. Burst speeds typically determine how far into open water juvenile salmonids will move from cover to forage (i.e., maximum range of taking prey if a prey item is detected). This tradeoff represents a combination of “safety” and optimal foraging strategy, and can be used to quantify habitat based on fish size and corresponding burst speed. A position that allows juveniles to remain near cover and dart into open water to forage is considered optimal and can be defined in terms of darting time. Bell (1991) suggested that a maximum darting time of 7.5 sec should be used for fish, because after this period fish are unable to pass water over their gills at a rate necessary to obtain the increased oxygen levels required for additional energy expenditure. The distance from optimal holding positions that juveniles can travel in 7.5 sec (out and back to holding position) becomes the optimal foraging distance (3.75 sec). Therefore, suitable habitat can be considered open water habitat that meets depth and velocity criteria within 3.75 sec of cover. Based on NMFS fish passage criteria, this distance is 0.90 m ( $3.75 \text{ sec} * 0.24 \text{ m/sec}$ ) for juvenile size fish (>50 mm). Therefore, a rough approximation of usable rearing habitat area is the area which meets depth and velocity suitability criteria within ~1.0 m of cover. These values are similar to those reported by Hardin et al. (2005) in an observational study of juvenile Chinook salmon in the Klamath River, California (~0–3 ft).

This approach assumes cover features themselves are not important habitat; however, cover features influence the quality of open water habitat near their perimeter. For GIS-based modeling, this concept is relatively easy to apply by (1) creating a 1 meter buffer around edge features, (2) cropping the original cover feature from the resulting buffered polygon, and (3) overlaying vegetation-based cover polygons on the resulting edge habitat polygons. The cover suitability (HSIc) distribution used in this study was ultimately produced through a union of the buffered edge habitat and the mapping classifications.

To compute the amount of edge habitat available, features within the 2007 aerial photographs were digitized by hand. Because of the time required for the digitization, cover features were digitized only within subportions of each reach; locations are given in Figure 4-9. Representative cover habitat areas used to determine cover habitat available in each reach. A feature was digitized as edge habitat if it was a tree, large woody debris, steep bank line, irregular bank line, large bush, or other flow obstruction visible in the aerial photographs. If there was a dense stand of woody vegetation, only the outer edge of the dense stand was digitized. There was no digitization of edge habitat features in Reaches 2B and 4B1 since these reaches will be subject to significant re-vegetation efforts; the current vegetative conditions are not necessarily representative of future conditions. An example of the edge habitat features overlaying the vegetation classification of Moise and Hendrickson (2002) is shown in Figure 4-10.

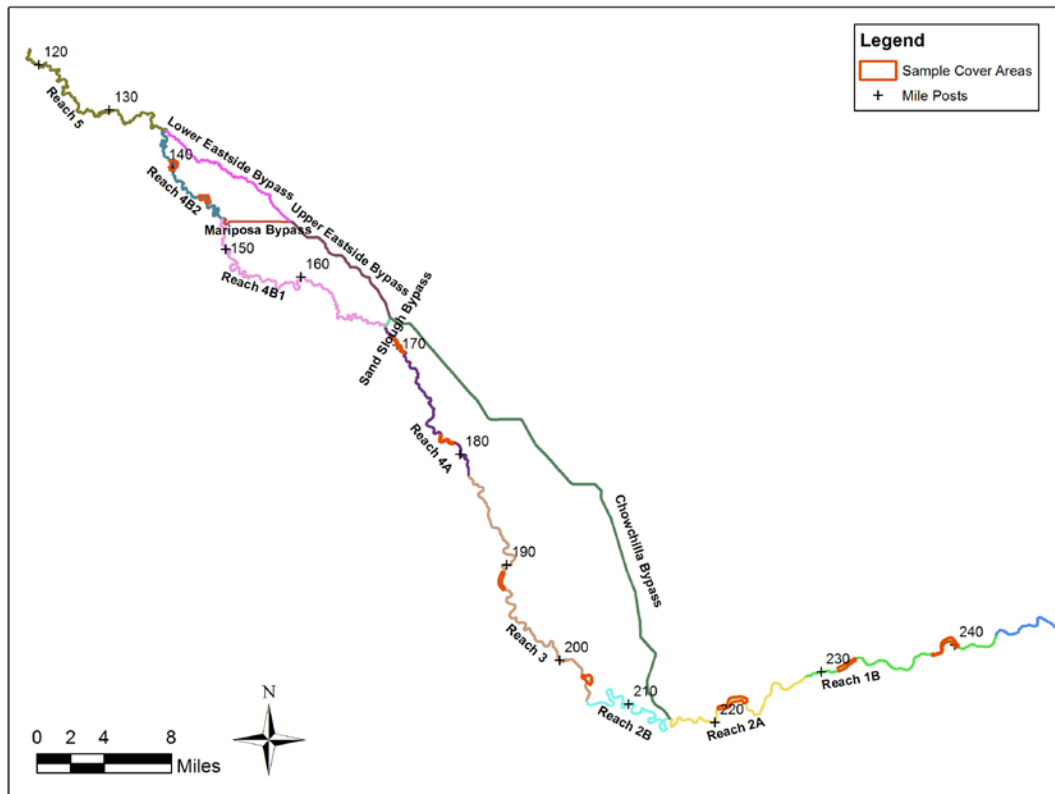


Figure 4-9. Representative cover habitat areas used to determine cover habitat available in each reach.

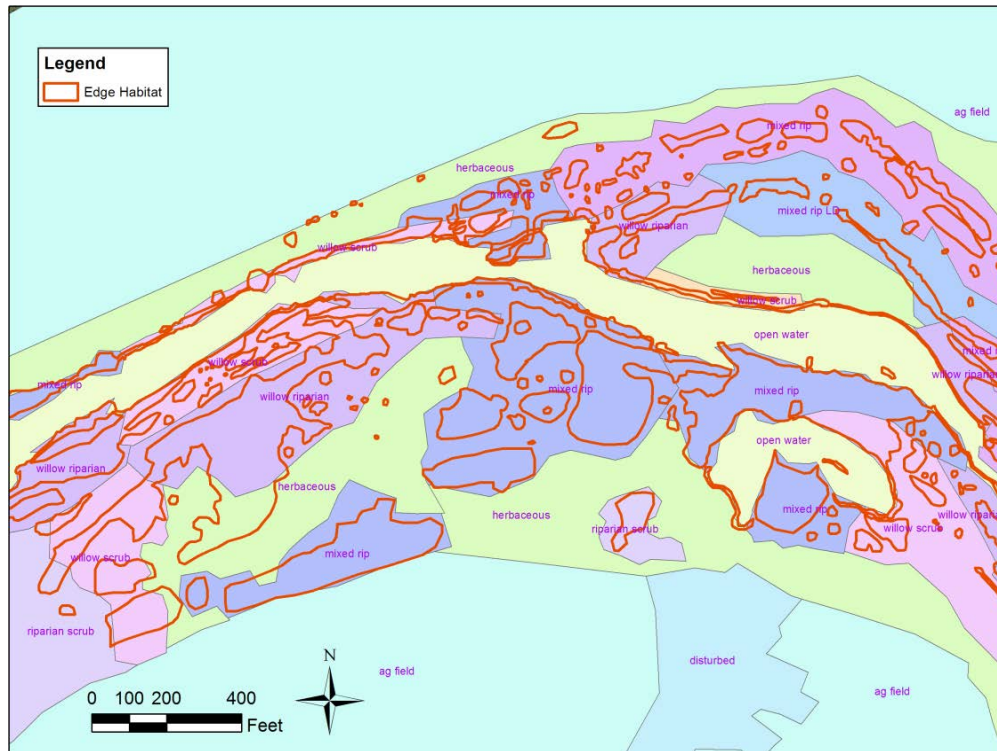


Figure 4-10. Example of the vegetation types overlaid with the Edge Habitat in Reach 1B.

### 4.3 Habitat Modeling

The method for estimating available ASH relies on distributions of both hydraulic suitability and cover suitability. At each grid cell within the selected subportions of each reach and for each flow, an HSI ranging from 0 to 1 was assigned to each variable (depth, velocity, and cover), from which a total HSI was computed at each grid cell. The total habitat suitability index ( $HSI_T$ ) of each grid cell was computed as the minimum of the individual HSI values:

$$HSI_T = \min(HSI_D, HSI_V, HSI_C) \quad (13)$$

where  $HSI_T$  = total habitat suitability of the grid cell  
 $HSI_D$  = depth habitat suitability of the grid cell  
 $HSI_V$  = velocity habitat suitability of the grid cell  
 $HSI_C$  = cover habitat suitability of the grid cell

The above equation assumes that each variable can be a limiting factor to the habitat suitability. Total HSI is also commonly computed as the geometric mean or simply as the product of the three individual HSI values. However, using the geometric mean or the product does not consider that certain habitat factors may limit the suitability of a particular area. For example, if  $HSI_C = 0.1$  and  $HSI_D = HSI_V = 0.6$ , the minimum method gives  $HSI_T = 0.1$ , whereas the product method would give  $HSI_T = 0.036$ , and the geometric mean would give  $HSI_T = 0.47$ . For

this analysis, it is assumed that the product method could underestimate habitat quality, and the geometric mean could overestimate habitat quality, particularly in cases where an individual factor is limiting.

Available ASH was calculated as the sum over all the grid cells of the inundated cell area multiplied by  $HSI_T$  for that grid cell:

$$ASH = \sum_{i=1}^N TIA_i \cdot HSI_{T,i} \quad (14)$$

where ASH = area of suitable habitat

$TIA_i$  = inundated area within the grid cell  $i$

$HSI_{T,i}$  = total habitat suitability of the grid cell  $i$

$N$  = number of grid cells within simulation domain

In practice, the available area of suitable habitat was computed for the selected subportions of each reach and then scaled by the reach TIA in order to estimate available ASH for the entire reach. The procedure was as follows: (1) calculate the depth, velocity, and cover HSI at every 5 ft by 5 ft grid cell within the subportion areas. (2) Compute the total HSI at every grid cell within the subportion area by taking the minimum of the three HSI components (see Figure 4-11). (3) Compute the fractional available ASH of total inundated area by evaluating Equation 14 within the subportion area and dividing by the total inundated subportion area. (4) The fractional available ASH of each subportion area was then scaled by the reach TIA to estimate the total available ASH for that reach. An illustrative flowchart of the computational procedure to compute area of suitable habitat is shown in Figure 4-11. The computational procedure is conceptually similar to that used in PHABSIM (Milhous 2012) and RIVER2D (Steffler and Blackburn 2002) computer programs. For Reach 5, the fractional available ASH values from Reach 4B2 were used to extrapolate to the available ASH for the entire reach.

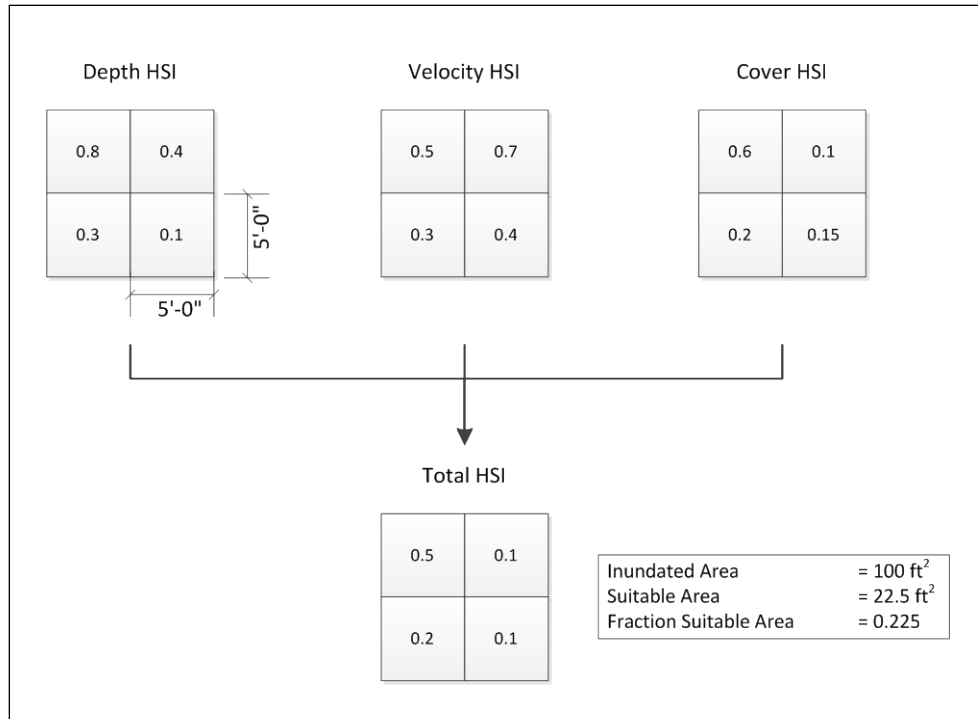


Figure 4-11. Graphical representation of an example HSI and suitable area calculation.



# 5 Results

## 5.1 Available Suitable Habitat

The Settlement specifies maximum two-week periods of flow for various water year types. These benchmarks define the flow available and the corresponding flows simulated in the hydraulic models for the purpose of habitat estimation. Due to variation in inputs and outputs from reach to reach, the flow rate corresponding to water year type is reach-dependent. Table 5-1 gives the simulated flows for each reach and water year type used in the habitat analysis.

Table 5-1. Maximum two-week Restoration flows in Settlement for various year types used in the analysis.

Water Year Classification	Maximum 2-week flow (cfs)		
	Reach 1B	Reach 2A	Reach 2B to 5
Dry	1500	1375	1225
Normal	2500	2355	2180
Wet	4000	3855	3655

Three critical flows were simulated in each reach, corresponding to the maximum expected flow rate during a “dry” year, “normal” year, and “wet” year, respectively. For each simulated reach and flow scenario, the total inundated area (TIA) was computed. The available area of suitable habitat (ASH) was then computed for Reaches 1B, 2A, 3, 4A, and 4B2 as a fraction of TIA based on the habitat suitability framework presented in Section 4. Figure 5-1 through

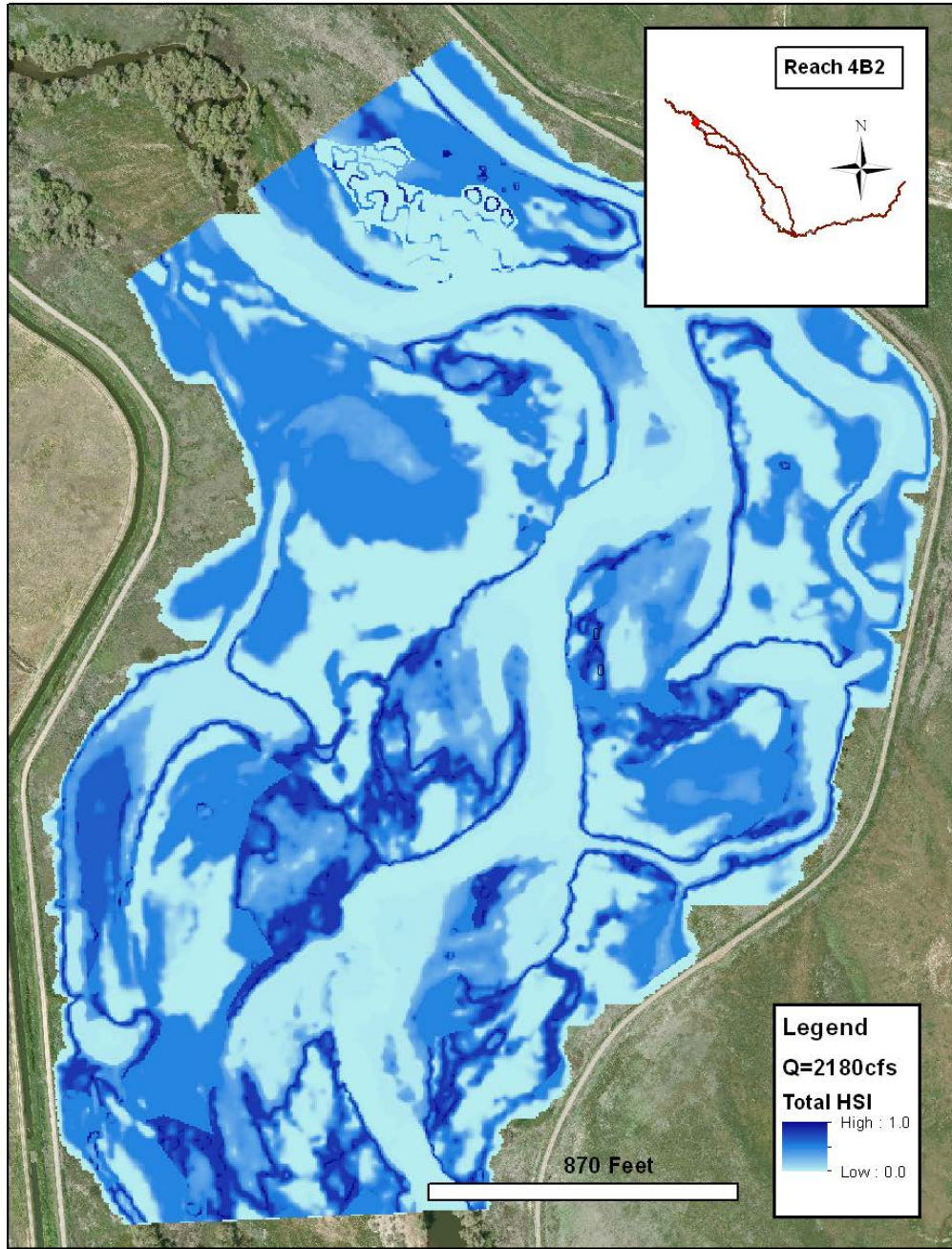


Figure 5-5 illustrate representative distributions of total HSI computed for a normal water year type simulated in Reaches 1B, 2A, 3, 4A, and 4B2, respectively. Table 5-2, Table 5-3 and Table 5-4 present the computed TIA, available ASH, and fractional ASH values for Reaches 1B, 2A, 3, 4A, and 4B2 for the dry, normal, and wet water year types, respectively. The standard deviation of the available ASH values was also calculated for each reach and presented in Table 5-2, Table 5-3, and Table 5-4. Habitat suitability estimates in Reach 5 were generated by assuming the same fractional available ASH as in Reach 4B2.

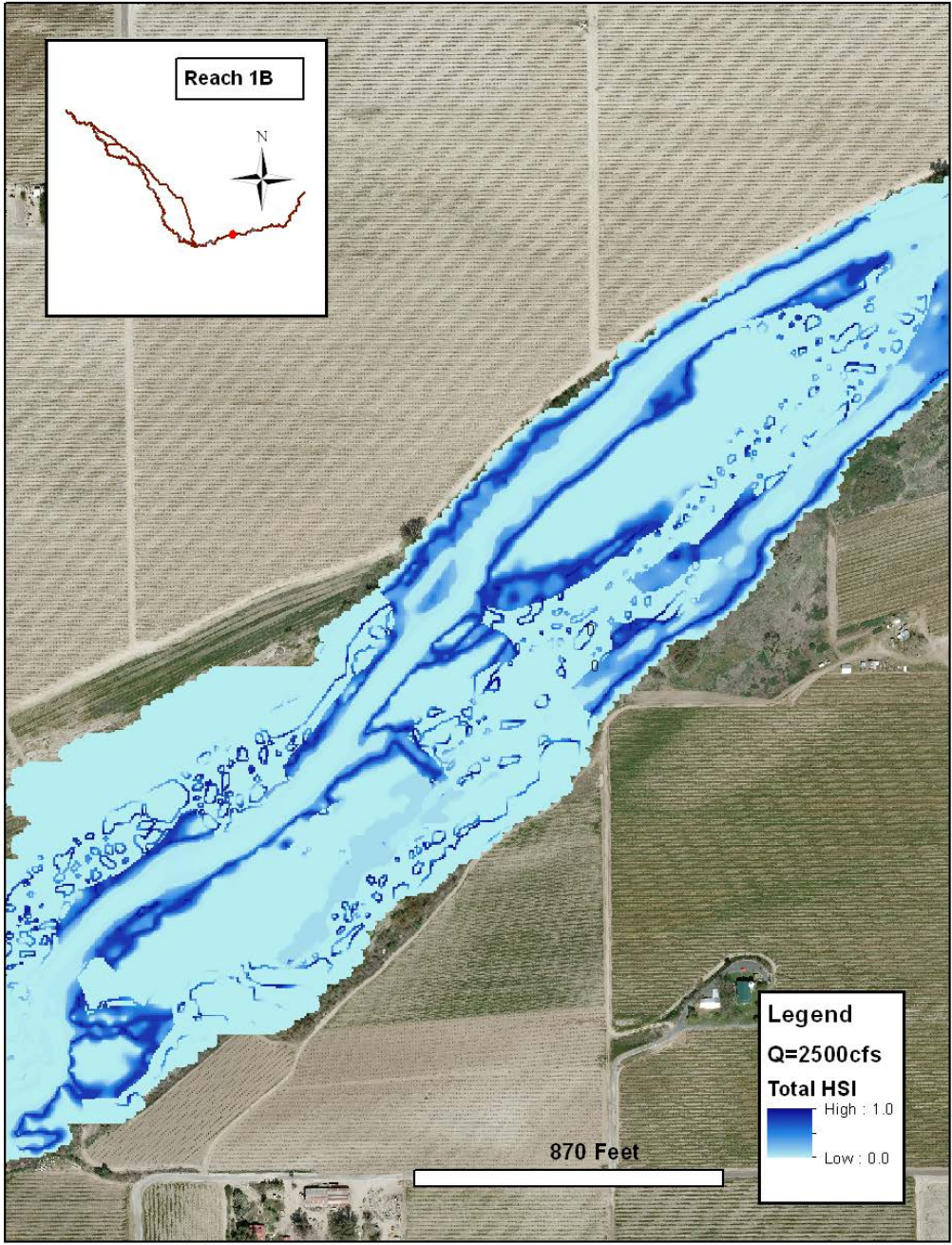


Figure 5-1. Combined HSI for portion of Reach 1B for normal year conditions.

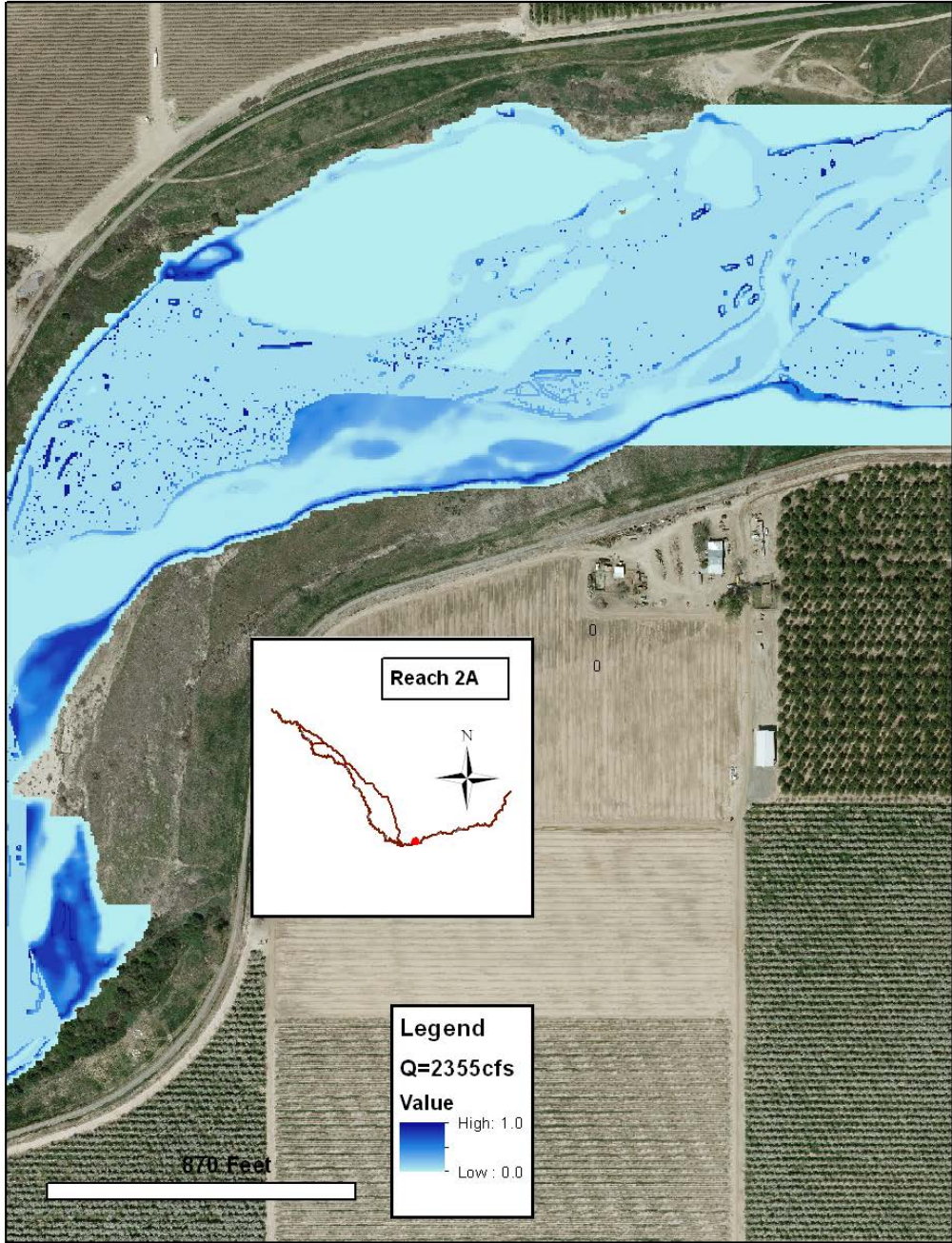


Figure 5-2. Combined HSI for portion of Reach 2A for normal year conditions.

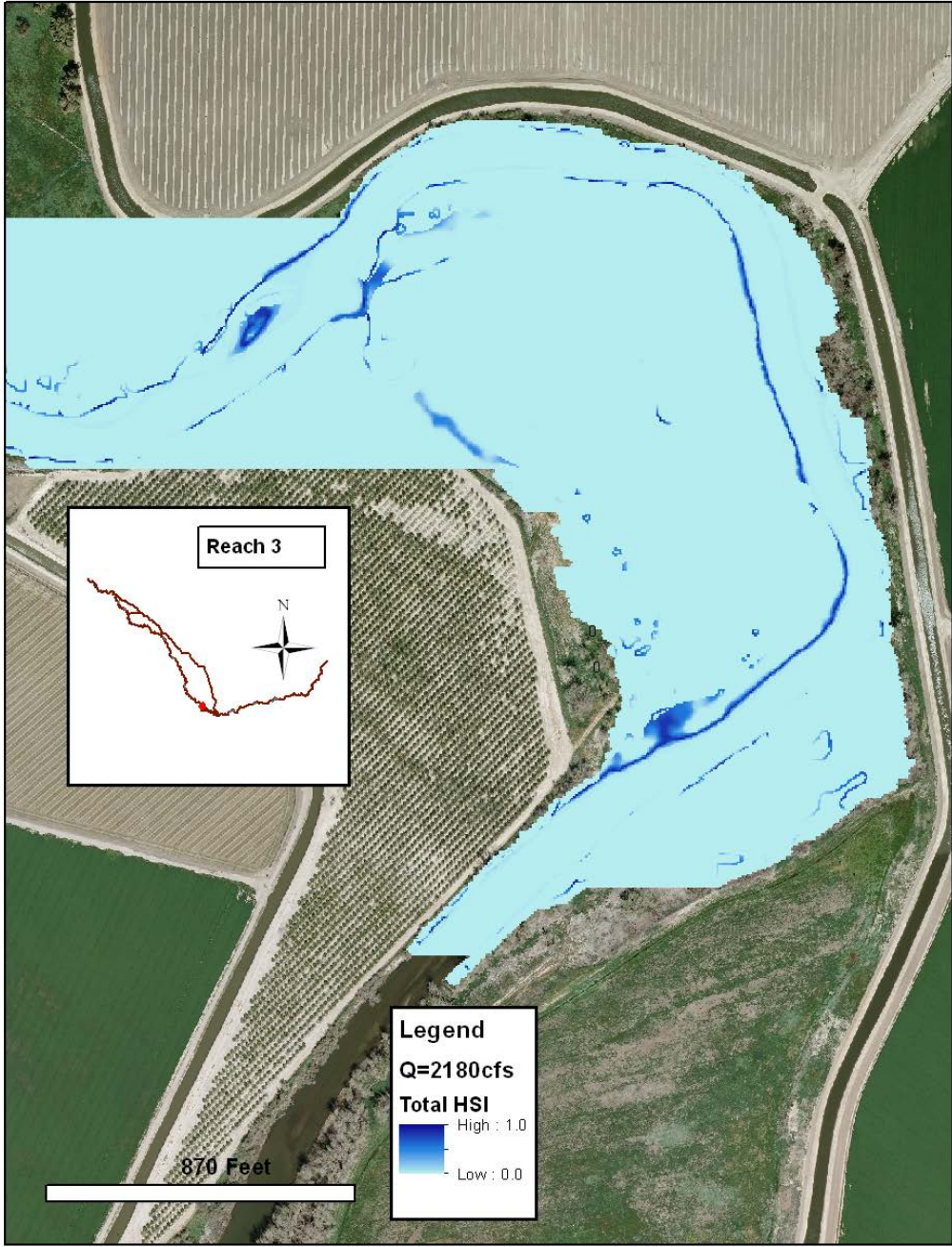


Figure 5-3. Combined HSI for portion of Reach 3 for normal year conditions.

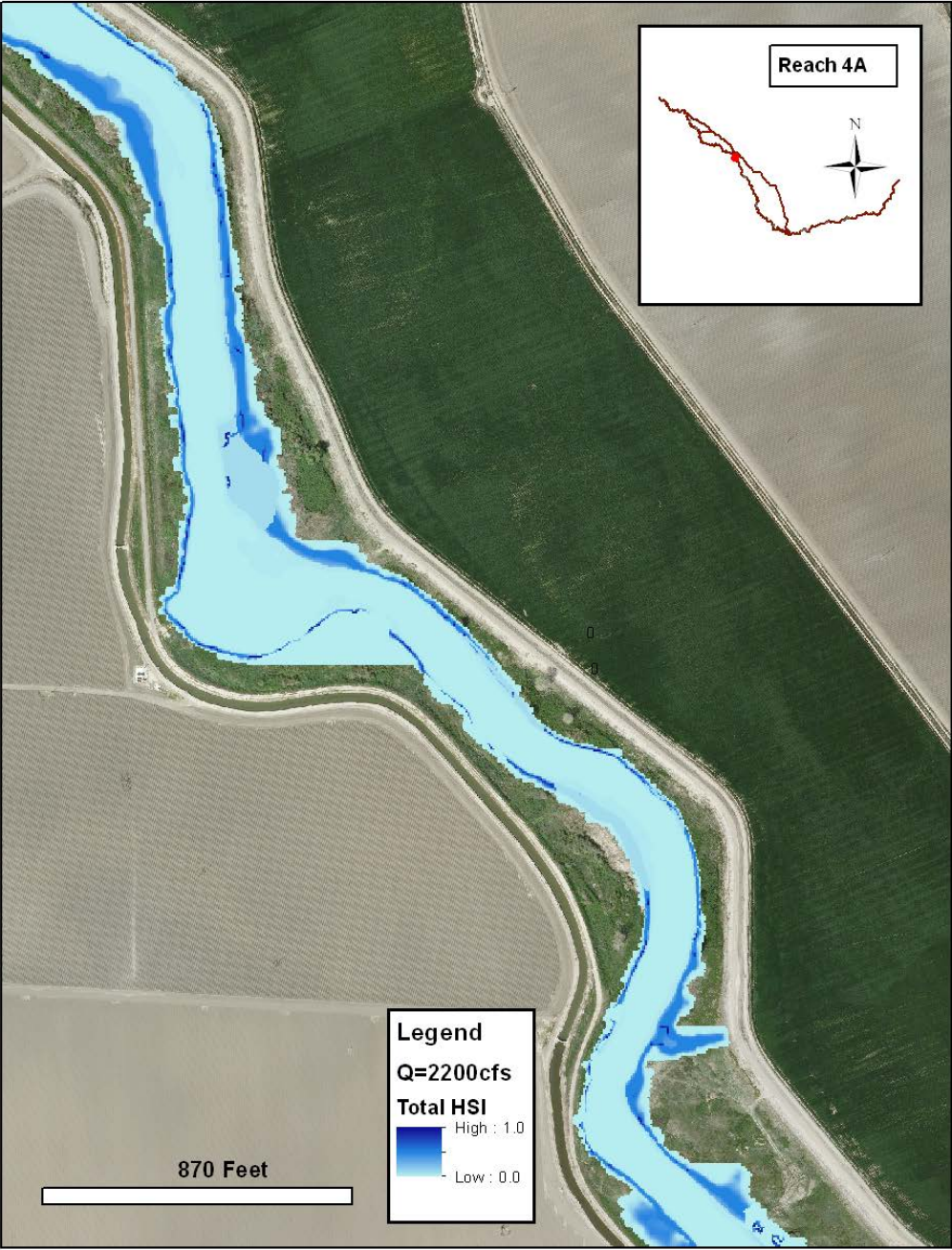


Figure 5-4. Combined HSI for portion of Reach 4A for normal year conditions

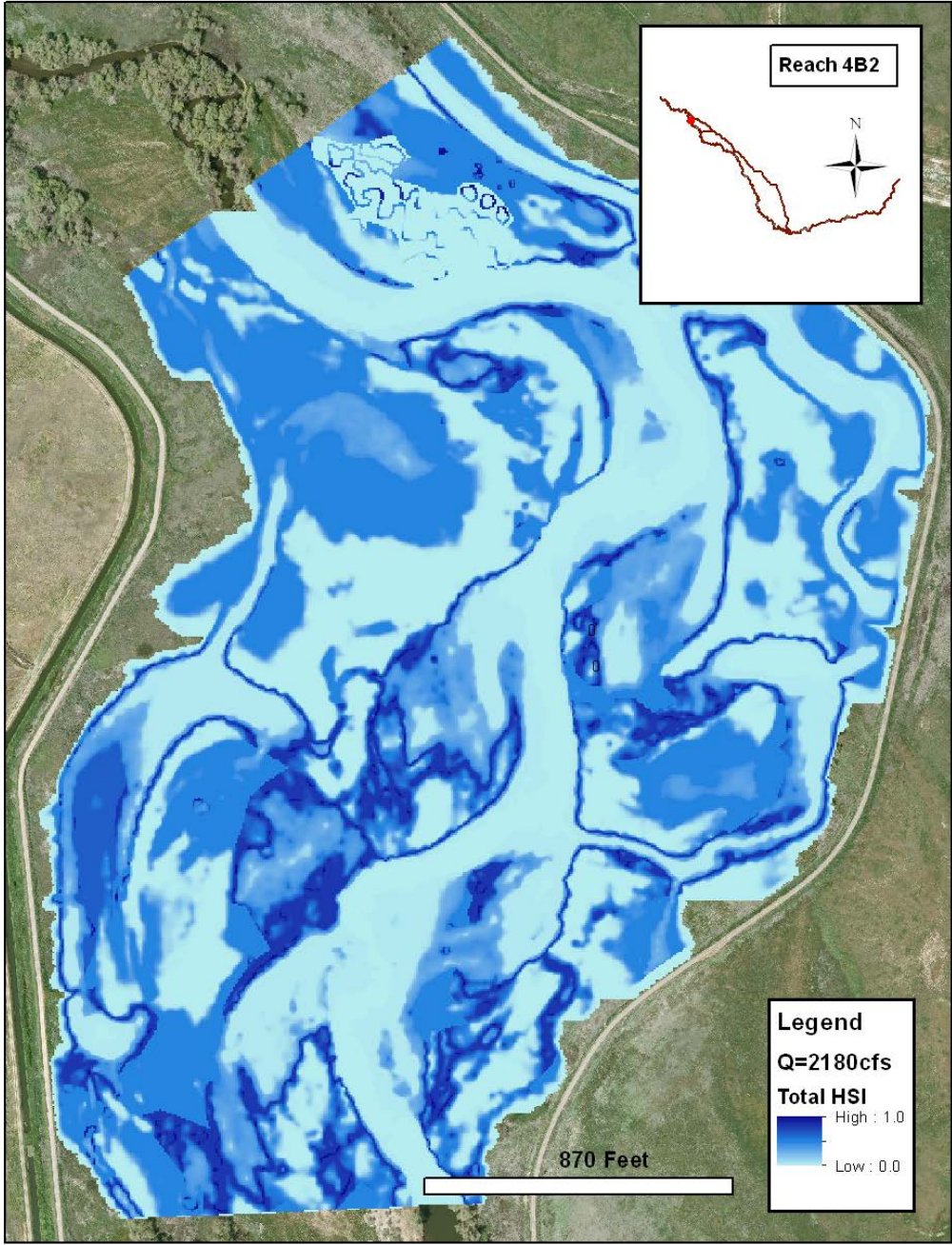


Figure 5-5. Combined HSI for portion of Reach 4B2 for normal year conditions.

Table 5-2. Summary of habitat analysis results for “dry” water year type. The columns from left to right indicate the river reach, total inundated area (*TIA*), and available area of suitable habitat (*ASH*). Available *ASH* is given as fraction of *TIA* and as acres; the standard deviation of the available *ASH* calculation is also given. Habitat computations were not performed for Reaches 2B and 4B1 because future vegetative conditions are unknown.

Reach	TIA (acres)	Available ASH		
		Fraction	Acres	HSI <sub>T</sub> Std. Dev.
1B	668	0.10	67	0.31
2A	625	0.15	94	0.21
3	495	0.09	45	0.20
4A	359	0.14	50	0.24
4B2	713	0.28	200	0.32
5*	823	0.28	230	0.32

\*Reach 5 assumes Reach 4B2 fractional suitability

Table 5-3. Summary of habitat analysis results for “normal” water year type. The columns from left to right indicate the river reach, total inundated area (*TIA*), and available area of suitable habitat (*ASH*). Available *ASH* is given as fraction of *TIA* and as acres; the standard deviation of the available *ASH* calculation is also given. Habitat computations were not performed for Reaches 2B and 4B1 because future vegetative conditions are unknown.

Reach	TIA (acres)	Available ASH		
		Fraction	Acres	HSI <sub>T</sub> Std. Dev.
1B	798	0.07	56	0.29
2A	743	0.14	104	0.21
3	770	0.08	62	0.26
4A	427	0.13	56	0.23
4B2	1041	0.27	281	0.30
5*	1373	0.27	371	0.30

\*Reach 5 assumes Reach 4B2 fractional suitability



Table 5-4. Summary of habitat analysis results for “wet” water year type. The columns from left to right indicate the river reach, total inundated area (TIA), and available area of suitable habitat (ASH). Available ASH is given as fraction of TIA and as acres; the standard deviation of the available ASH calculation is also given. Habitat computations were not performed for Reaches 2B and 4B1 because future vegetative conditions are unknown.

Reach	TIA (acres)	Available ASH		
		Fraction	Acres	HSI <sub>T</sub> Std. Dev.
1B	982	0.06	59	0.29
2A	876	0.13	114	0.21
3	1015	0.07	71	0.25
4A	525	0.13	68	0.24
4B2	1432	0.24	344	0.30
5*	2192	0.24	526	0.30

\*Reach 5 assumes Reach 4B2 fractional suitability

Table 5-5. Summary of total inundated area (TIA) calculations for the levee options in Reaches 2B and 4B1 for each water year type. The columns from left to right indicate the river reach, levee option, and TIA in acres for each of the water year types.

Reach	Levee Option	TIA (acres)		
		Dry	Normal	Wet
2B	FP2	494	1176	1572
	FP4	549	1496	1983
	Existing	558	752	-
4B1	A	981	-	-
	B	2228	2756	2847
	C	3555	5306	5966
	D	5473	7309	9173

Table 5-6. Available ASH (acres) organized by reach and water year type. Also shown is the average ASH for each Reach, weighted by the estimated time percentage of each water type.

Reach	Water Year Type			Weighted Average Available Suitable Habitat (acres)
	Dry 1000-1500 cfs (20% of years)	Normal 2180-2500 cfs (60% of years)	Wet 3600-4500 cfs (20% of years)	
1B	67	56	59	<b>59</b>
2A	94	104	114	<b>104</b>
3	45	65	71	<b>60</b>
4A	50	56	68	<b>57</b>
4B2	200	281	344	<b>277</b>
5	230	371	526	<b>374</b>

## 5.2 Sensitivity Tests

### 5.2.1 Grid Sensitivity

A grid sensitivity test was performed to evaluate dependence of the habitat analysis results on resolution of the computational mesh used in the SRH-2D model. The Reach 2A hydraulic model was used as a test case for the evaluation; a secondary Reach 2A computational grid was created with resolution twice that of the original.

It is generally expected that the resolution of quadrilateral elements within a hybrid 2D mesh is most important in accurately predicting details of the local hydraulics, since quadrilateral elements are used in the primary flow channel through the mesh. However, the habitat analysis presented herein is based on gross hydraulic metrics over an entire river reach and adjacent floodplain (as opposed to details of the local hydraulics), and is therefore predicted to be relatively insensitive to grid resolution. This hypothesis was tested by computing Reach 2A SRH-2D hydraulic simulations (1375 cfs, 2355 cfs, and 3855 cfs) on grids with resolution  $L_{EQ} = 16$  and  $L_{EQ} = 8$ . The habitat analysis was then performed using the results from both sets of hydraulic simulations. The total HSI was computed using the geometric mean of the individual HSI variables as opposed to the minimum of the HSI variables. Table 5-7 summarizes the results from the Reach 2A sensitivity analysis. The results of the analysis suggests that the habitat analysis is fairly insensitive to the resolution of the computational grid used in the SRH-2D hydraulic simulations. There is a small difference in calculated total inundated area (about 5%); the higher resolution computational grid results in smaller estimates of TIA. This is to be expected given the greater area of averaging over the wetted cells of a lower resolution grid. The fraction of TIA that represents hydraulically-suitable habitat (only considering depth and velocity) and available suitable habitat, respectively, does not show dependency on the resolution of the computational grid. Thus, any difference in computed habitat area due to change in resolution of the computational grid is due purely to the difference in total inundated area.

Table 5-7. Summary of results from sensitivity test of habitat analysis to change in resolution of the SRH-2D computational mesh.

Area	1375 cfs		2355cfs		3855cfs	
	$L_{E4Q} = 16$	$L_{E4Q} = 8$	$L_{E4Q} = 16$	$L_{E4Q} = 8$	$L_{E4Q} = 16$	$L_{E4Q} = 8$
TIA (ac)	625	592	743	713	875	836
HSH (frac)	0.46	0.46	0.41	0.41	0.35	0.35
ASH (frac)	0.35	0.35	0.33	0.33	0.29	0.29

### **5.2.2 Sensitivity to Method of Total HSI Calculation**

The sensitivity of available ASH to the method of total HSI calculation was tested by calculating available ASH using (a) the geometric mean of the individual HSI components and (b) the minimum of the individual HSI components. The available ASH was significantly larger if total HSI was calculated as a geometric mean instead of as a minimum value. For example, the available ASH estimate in a normal water year for Reach 2A is approximately 250% larger when calculating total HSI using the geometric mean versus minimum value. For the purposes of this study, calculating total HSI as a geometric mean would likely overestimate available ASH. Physical conditions (e.g., hydraulics, vegetation, etc.) that act as limiting factors on the quality of the habitat are more appropriately accounted for through calculation of total HSI as a minimum value.

## 6 References

- Aceituno, M.E. 1990. Habitat preference criteria for chinook salmon of the Stanislaus River, California. USDI Fish & Wildlife Service, Sacramento, California.
- Bell, M.C. 1991. Fisheries handbook of engineering requirements and biological criteria. Third edition. U.S. Army Corps of Engineers, Office of the Chief Engineers, Fish Passage Development and Evaluation Program, North Pacific Division, Portland, OR.
- Hampton, M. 1988. *Development of habitat preference criteria for anadromous salmonids of the Trinity River*. U.S. Fish and Wildlife Service, Sacramento, California. 93 pp
- Hampton, M. 1997, *Microhabitat Suitability Criteria for Anadromous Salmonids of the Trinity River*, U.S. Fish and Wildlife Service, Sacramento, California. 252 pp
- Lai, Y. 2008. *SRH-2D version 2: Theory and User's Manual, Sedimentation and River Hydraulics – Two-dimensional River Flow Modeling*, US Bureau of Reclamation, Technical Service Center, Denver, CO.
- McMahon, T. and Hartman, G.F. 1989. "Influence of Cover Complexity and Current Velocity on Winter Habitat Use by Juvenile Coho Salmon," *Canadian Journal of Fisheries and Aquatic Sciences*, 46(9): 1551-1557, 10.1139/f89-197.
- Moise, G.W. and Hendrickson, B., 2002. "Riparian Vegetation of the San Joaquin River," State of California Department of Water Resources, Technical Information Record SJD-02-1.
- Mussetter Engineering, Inc., 2008. San Joaquin HEC-RAS Model Documentation Technical Memorandum prepared for California Dept. of Water Resources, Fresno, California, June 2.
- Raleigh, R.F., W.F. Miller, and P.C. Nelson. 1986. *Habitat suitability index models and instream flow suitability curves: Chinook salmon*. U.S. Fish Wildlife Service Biological Report 82(10.122). 64 p.
- Reclamation, 2008. Draft two-dimensional modeling of the San Joaquin River: Reach 2B, prepared by the Technical Service Center, Sedimentation and River Hydraulics Group, Denver, CO.
- Steffler P., and Blackburn, J. (2002). "River2D, Two-Dimensional Depth Averaged Model of River Hydrodynamics and Fish Habitat," University of Alberta, September, 2002.
- SJRRP, 2010. Annual Technical Report, Appendix G "Surveys"
- SJRRP, 2011a. Annual Technical Report, Appendix B "Reports"

- SJRRP, 2011b. Annual Technical Report, Appendix G “Surveys”
- SJRRP, 2011c, San Joaquin River Restoration Program. *First Administrative Draft Mendota Pool Bypass and Reach 2B Project, Project Description Technical Memorandum*. May.
- SJRRP, 2011d. Draft Program Environmental Impact Statement/Environmental Impact Report (PEIS). April 2011.
- USACE, 2010. *HEC-RAS River Analysis System, Hydraulic User’s Manual, Version 4.1*, Hydrologic Engineering Center, Davis, CA, January 2010.
- United States Geological Survey 2001. “PHABSIM for Windows,” User’s Manual and Exercises, Mid Ecological Science Center, November 2001, Open File Report 01-340.
- Washington Department of Fish and Wildlife, 2004. Instream Flowstudy Guidelines Technical and Habitat Suitability Issues including fish preference curves,